UNCLASSIFIED

AD 297 373

Reproduced
by the

ARMED SERVICES TECHNICAL INFORMATION AGENCY
ARLINGTON HALL STATION
ARLINGTON 12, VIRGINIA

UNCLASSIFIED

NOTICE: When government or other drawings, specifications or other data are used for any purpose other than in connection with a definitely related government procurement operation, the U. S. Government thereby incurs no responsibility, nor any obligation whatsoever; and the fact that the Government may have formulated, furnished, or in any way supplied the said drawings, specifications, or other data is not to be regarded by implication or otherwise as in any manner licensing the holder or any other person or corporation, or conveying any rights or permission to manufacture, use or sell any patented invention that may in any way be related thereto.

CATALOGED BY ASTIA
AS AD No. 297373

63-2-5

RADC-TDR-62-629

297 373

EQUIRIPPLE TRANSMISSION LINE NETWORKS

by

Werner Kohler and Herbert J. Carlin

Report No. PIBMRI-1089-62

for

Rome Air Development Center
Air Force Systems Command
Rome, New York

Contract No. AF-30(602)-2213

24 January 1963

MAR 4 1963

POLYTECHNIC INSTITUTE OF BROOKLYN
MICROWAVE RESEARCH INSTITUTE

ELECTROPHYSICS DEPARTMENT

Best Available Copy

"Qualified requestors may obtain copies of this report from ASTIA Document Service Center, Arlington Hall Station, Arlington 12, Virginia. ASTIA Services for the Department of Defense contractors are available through the 'Field of Interest Register' on a 'need-to-know' certified by the cognizant military agency of their project or contract."

"This report has been released to the Office of Technical Services, U.S. Department of Commerce, Washington 25, D.C., for sale to the general public."

RADC-TDR-62-629

Report No. PIBMRI-1089-62
Contract No. AF-30(602)-2213

EQUIRIPPLE TRANSMISSION LINE NETWORKS

by

Werner Kohler and Herbert J. Carlin

Polytechnic Institute of Brooklyn
Microwave Research Institute
55 Johnson Street
Brooklyn 1, New York

Report No. PIBMRI-1089-62
Contract No. AF-30(602)-2213

24 January 1963

Title Page
Foreword
Abstract
Table of Contents
69 Pages of Text
15 Pages of Figures
Distribution List

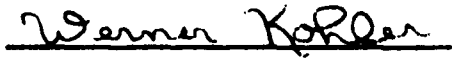

Werner Kohler

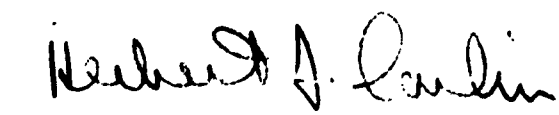

Herbert J. Carlin, Head
Department of Electrophysics

Prepared for
Rome Air Development Center
Air Force Systems Command
Rome, New York

FOREWORD

The author wishes to express his gratitude to Professor H. J. Carlin, whose guidance and encouragement made this thesis possible.

The author is further indebted to George Zysman for his help during the development of the work.

The work reported herein was sponsored by the National Science Foundation and the Rome Air Development Center under Contract No. AF-30(602)-2213.

ABSTRACT

The synthesis of microwave broadband equalizers, comprised solely of a cascade of lossless equilength transmission lines operating between a resistive generator and a resistive load, has been thoroughly established in the literature.[1] For this class of network, equiripple response specification is accomplished through recourse to techniques employed in the analogous lowpass lumped-parameter case. The d.c. point, at which the lines become transparent, enables one to readily prescribe the value of the load resistance.

This thesis considers the case in which the aforementioned cascade configuration is augmented by the presence of lossless transmission line stubs, having lengths commensurate with those of the lines. Tchebycheff-type response specification is developed for specific types of this generic class, which, because of the stubs, possess finite ω-frequency zeros of transmission.

One specific type of particular interest is the single shunt short-circuited stub bandpass filter. This network is explicitly considered in the following section of the thesis. A means for the a priori determination of load resistance and stub characteristic impedance, with the stub at a given end of the cascade, is developed. A technique is then evolved whereby one may, by altering the stub position, systematically adjust the value of the terminating resistance.

The last segment of the thesis is devoted to the design of a reflection-type tunnel diode amplifier, utilizing a transmission line equalizer. The diode parasitics are approximated in the frequency band of interest by transmission line stubs. This approximation circumvents the problem of transcendental functions inherent in lumped reactance-transmission line mixtures and enables the adaptation of the above-mentioned equiripple response functions by an extension of the Fano theory of broadbanding.

TABLE OF CONTENTS

LIST OF FIGURES

LIST OF FIGURES
(continued)

I. INTRODUCTION

The general network structure to be herein considered is that of a lossless reciprocal two-port, comprised of a cascade of equilength transmission lines augmented by transmission line stubs, operating between a resistive generator and a resistive load. The initial problem to be treated is the prescription of an equiripple response characteristic, which may be physically realized by particular types of the above general structure.

The network approach which will be used is that of the scattering formalism, the subject of papers by Carlin[2] and Youla.[3] Consider the basic system, as shown in Figure 1.

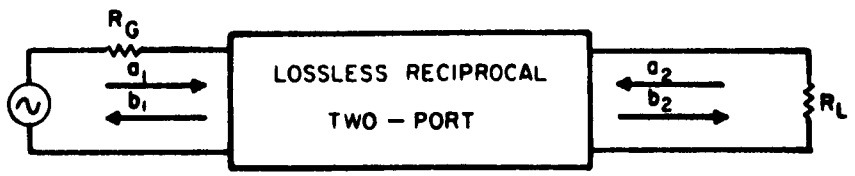

Figure 1 - System Representation

This system is described by the following scattering matrix representation:

$$\begin{bmatrix} b_1 \\ b_2 \end{bmatrix} = \begin{bmatrix} s_{11}(p) & s_{12}(p) \\ s_{12}(p) & s_{22}(p) \end{bmatrix} \begin{bmatrix} a_1 \\ a_2 \end{bmatrix} \tag{1}$$

where a_1, a_2 are the incident "voltage" waves; b_1, b_2 are the reflected "voltage" waves; p is the complex frequency variable, equal to $\sigma + j\omega$.

The choice of the scattering formalism is motivated by its particular adaptability to the problem at hand. Consider the following properties, which are delineated in reference 2:

a) The constraint of losslessness upon the two-port equalizer necessitates that:

$$\left[S'(-p)\right]\left[S(p)\right] = 1_2, \text{ a 2 x 2 unit matrix. (the prime denotes transpose)} \tag{2a}$$

Furthermore, because of reciprocity, $s_{21} = s_{12}$. (2b)

b) If the port normalization numbers are chosen as equal to the respective port terminations, R_G and R_L, $|s_{21}(j\omega)|^2 = |s_{12}(j\omega)|^2$ becomes identical to the power transfer ratio, referred to generator available power. Thus, $|s_{12}(j\omega)|^2$ becomes a direct measure of the available gain of the network between the prescribed terminations.

c) If port 2 is normalized to its termination, R_L, (upon which $a_2 = 0$),

$$s_{11} = s_{in} = \frac{b_1}{a_1} \tag{3}$$

That is, the s_{11} coefficient of the lossless two-port becomes equal to the input scattering coefficient of the one-port, comprised of the lossless equalizer terminated in R_L.

These properties, in essence, outline the synthesis procedure. The specification of an equiripple power transfer characteristic is tantamount to the prescription of $|s_{12}|^2$, subject to the above normalization constraints. Since, from the unitary condition (2a);

$$|s_{11}|^2 = 1 - |s_{12}|^2 , \tag{4}$$

$|s_{11}|^2$ is thereby also prescribed. The proper factorization will then yield $s_{11} = s_{in}$, from which the input immittance function can be readily ascertained.

Thus, the problem of equiripple response specification becomes that of prescribing an analytic form for $|s_{12}|^2$ which will both produce the desired shape and be physically realizable as the desired network. The type of network to be herein considered is, as was previously stated, the cascade of transmission lines augmented by stubs. Therefore, let us initiate the investigation of this problem by considering a transmission line of length ℓ and characteristic impedance Z_o.

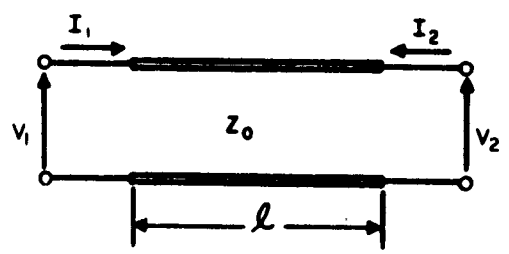

Figure 2 - Transmission Line

Its impedance matrix is:

$$[Z] = Z_o \begin{bmatrix} \coth \frac{\ell}{v} p & \operatorname{csch} \frac{\ell}{v} p \\ \operatorname{csch} \frac{\ell}{v} p & \coth \frac{\ell}{v} p \end{bmatrix} \tag{5}$$

where

v = velocity of propagation

$p = \sigma + j\omega$

The corresponding scattering matrix of this two-port (normalized arbitrarily to 1 ohm at each port) is readily determined by the relation:

$$[S] = \left[[Z] - 1_2\right]\left[[Z] + 1_2\right]^{-1} \tag{6}$$

where the minus one exponent denotes inverse.

The resultant matrix is:

$$[S] = \frac{1}{(\tanh \frac{\ell}{v} p)(Z_o^2 + 1) + 2 Z_o} \begin{bmatrix} (\tanh \frac{\ell}{v} p)(Z_o^2 - 1) & 2 Z_o \operatorname{sech} \frac{\ell}{v} p \\ 2 Z_o \operatorname{sech} \frac{\ell}{v} p & (\tanh \frac{\ell}{v} p)(Z_o^2 - 1) \end{bmatrix} \tag{7}$$

It is evident from these considerations that the dependence of the pertinent parameters upon the frequency variable, p, is transcendental. At real frequencies ($\sigma = 0$; $p = j\omega$) their behavior is periodic, with the first period being

$$-\frac{\pi}{2} \leq \frac{\ell}{v} \omega \leq \frac{\pi}{2} \tag{8}$$

It is this transcendental dependence of the functions upon p which makes further consideration of the problem in the p-domain unfeasible.

It has been shown by Richards[4] that the complex frequency transformation:

$$\lambda = \tanh \eta = \sum + j\Omega \tag{9a}$$

with

$$\eta = p \frac{\ell}{v} = \alpha \ell + j\beta \ell \tag{9b}$$

removes this difficulty. That is, an input immittance function or reflection factor of an arbitrary configuration of lossless transmission lines and resistors, which is a transcendental function in the p-plane, becomes a rational function in the λ-plane.

This p-to-λ plane mapping is not a unique, or one-to-one, mapping. On the contrary, since its primary purpose is to transform the transcendental p-plane functions into polynomial-type λ functions, it must, among other things, transform each $j\omega$-axis period into an infinite interval.

Thus, strips of the $j\omega$ axis of length $j\pi \frac{v}{l}$, the first extending from $-j\frac{\pi}{2}\frac{v}{l}$ to $+j\frac{\pi}{2}\frac{v}{l}$, each map onto the entire $j\Omega$ axis. The positive σ-axis maps onto the positive Σ-axis between 0 and 1; the negative σ-axis maps onto the Σ-axis between 0 and -1. The line $p = j\frac{\pi}{2}\frac{v}{l}$ maps onto the Σ-axis between ∞ and +1 for $\sigma > 0$ and between $-\infty$ and -1 for $\sigma < 0$. The mapping of the upper portion of the first right-half p-plane strip onto the λ-plane is shown in Figure 3.

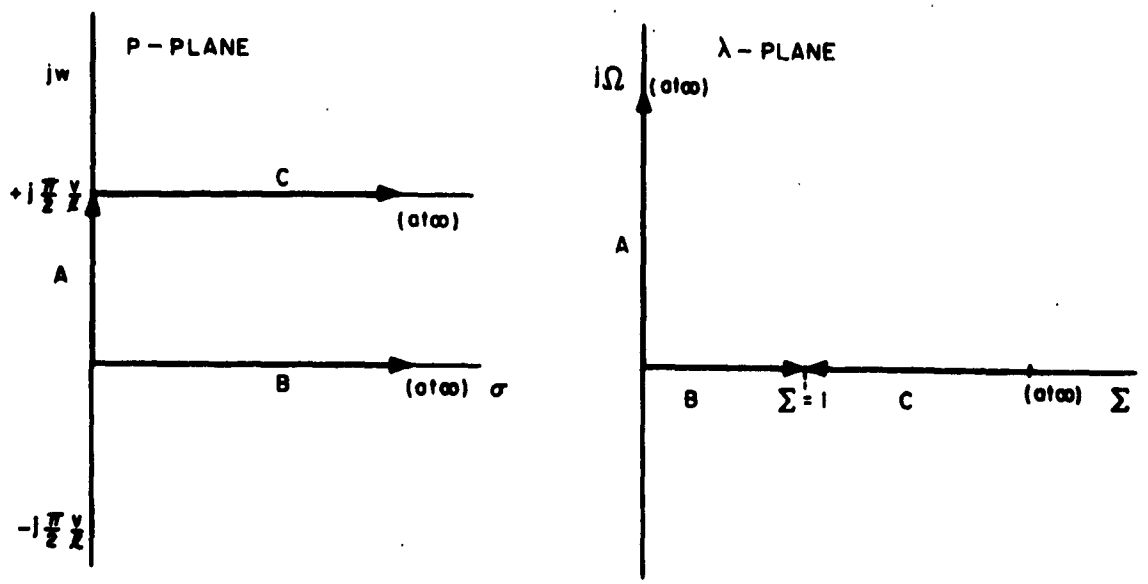

Figure 3 - Richards Frequency Transformation

A realizable reflection factor s(p) of the type encountered in transmission line networks must be a "bounded-real" p-plane function. That is,

$$\begin{aligned} &\text{a)}\ \ s(p^*) = s^*(p) \quad \text{(the asterik denotes complex conjugate)} \\ &\text{b)}\ \ s(p) \text{ is analytic in } \sigma > 0 \\ &\text{c)}\ \ 0 \leq |s(j\omega)| \leq 1 \ . \end{aligned} \tag{10}$$

Thus, an essential property of the Richards transformation is its mapping of the right-half p-plane into the right half λ -plane and its mapping of the $j\omega$-axis onto the $j\Omega$ axis. This causes the above properties of $s(p)$ to be carried over into $s(\lambda)$.

In terms of the new frequency variable λ , the scattering matrix of the transmission line becomes:

$$[S] = \frac{1}{\lambda(Z_o^2 + 1) + 2Z_o} \begin{bmatrix} \lambda(Z_o^2 - 1) & 2Z_o\sqrt{1-\lambda^2} \\ 2Z_o\sqrt{1-\lambda^2} & \lambda(Z_o^2 - 1) \end{bmatrix} \quad (11)$$

The ultimate network of interest is the cascade of lines and stubs. A generic form for the $s_{12}(\lambda)$ of this network is desired since, as previously noted, the square of its magnitude along the $j\Omega$ axis can be equated to a power transfer ratio. This general form may be implied if one considers the following:

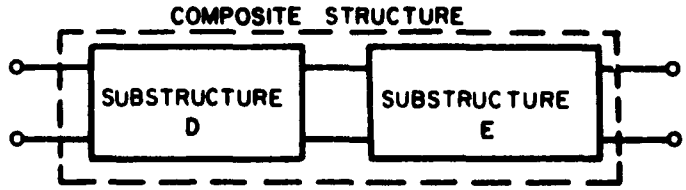

Figure 4 - Cascade Connection of Two Substructures

In Figure 4, D and E represent two networks connected in tandem. Let [D] and [E] represent the respective scattering matrices of these networks. Then, if [S] represents the scattering matrix of the composite network, it may be shown that:

$$s_{12}(\lambda) = \frac{d_{12}(\lambda)\, e_{12}(\lambda)}{1 - d_{22}(\lambda)\, e_{11}(\lambda)} \quad (12)$$

The important aspect of equation 12 is the fact that $s_{12}(\lambda)$ involves the product of $d_{12}(\lambda)$ and $e_{12}(\lambda)$ in the numerator and a rational denominator. If, then, equation 12 is successively applied to a cascade of n equilength transmission lines, having different characteristic impedances, the resultant form of $s_{12}(\lambda)$ will,

from equation 11, be:

$$s_{12}(\lambda) = \frac{(1 - \lambda^2)^{\frac{n}{2}}}{P_n(\lambda)} \tag{13}$$

where $P_n(\lambda)$ is a polynomial in λ of order n, possessing no zeros in the right half plane, and where $|P_n(j\Omega)| \geq |(1 + \Omega^2)^{n/2}|$. In evolving equation 13, we have restricted consideration to the specific case of 1 ohm normalizations. This approach was adopted for reasons of simplicity and is intended merely to provide heuristic justification for the statement of the generic forms. Equation 13 and subsequent equations 18-20 are general in nature.

Having this general expression for the cascade, we must now determine the manner in which the incorporation of stubs effects the resultant $s_{12}(\lambda)$ scattering coefficient. Consider, as an example, the shunt short-circuited stub, of characteristic impedance Z_o, depicted in Figure 5.

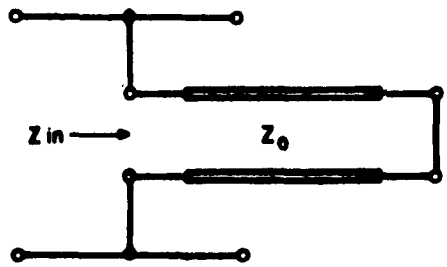

Figure 5 - Shunt Short-Circuited Stub

For this element,

$$Z_{in} = Z_o \tanh \frac{\ell}{v} p = Z_o \lambda \tag{14}$$

Thus, the short-circuited stub, under the Richards transformation, becomes a λ inductor of inductance Z_o. (Likewise, an open-circuited stub transforms into a λ capacitor of capacitance $Y_o = \frac{1}{Z_o}$.) Regarding the above shunt, short-circuited stub as a two-port, we may write its normalized impedance matrix as:

$$[Z] = Z_o \lambda \begin{bmatrix} 1 & 1 \\ 1 & 1 \end{bmatrix} \tag{15}$$

where Z_o is assumed normalized.

Its corresponding scattering matrix normalized to the number for the port at which it is located is, if Z_o is presumed so normalized:

$$[S] = \frac{1}{2 Z_o \lambda + 1} \begin{bmatrix} -1 & 2 Z_o \lambda \\ 2 Z_o \lambda & -1 \end{bmatrix} \tag{16}$$

Thus, if equation 12 is now applied to the configuration of Figure 6, the resulting $s_{12}(\lambda)$ scattering coefficient will have the general form:

$$s_{12}(\lambda) = \frac{\lambda (1 - \lambda^2)^{\frac{n}{2}}}{P_{n+1}(\lambda)} \tag{17}$$

where $P_{n+1}(\lambda)$ is a polynomial of order $(n+1)$ in λ, having no zeros in the right half λ-plane, and where $|P_{n+1}(j\Omega)| \geq |j\Omega(1 + \Omega^2)^{n/2}|$

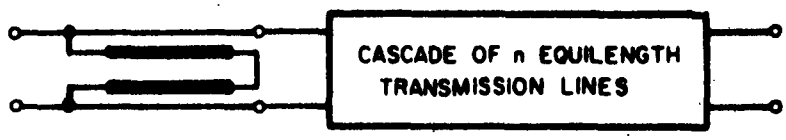

Figure 6 - Cascade of Transmission Lines Augmented by a Shunt Short-Circuited Stub

Hence, $s_{12}(\lambda)$ in equation 17 has a zero (called a zero of transmission) at d.c. (i.e., $\lambda = 0$), the frequency at which the shunt, short-circuited stub behaves as a true short circuit. A similar expression as equation 17 would have been obtained had the cascade been augmented by a series open-circuited stub, rather than the shunt shorted stub; such an element would also introduce a single order d.c. zero of transmission.

By arranging shunt short-circuited stubs and series open-circuited stubs in a highpass ladder configuration, one may achieve multiple-order d.c. zeros of transmission. For a structure containing n cascaded transmission lines and possessing an r^{th} order d.c. zero of transmission:

$$s_{12}(\lambda) = \frac{\lambda^r (1 - \lambda^2)^{\frac{n}{2}}}{P_{n+r}(\lambda)} \tag{18}$$

In a similar fashion, one may incorporate series short-circuited stubs and shunt open-circuited stubs to produce a multiple order zero of transmission at the quarter-wave frequency. For an equalizer containing n cascaded transmission lines

and a q^{th} order quarter-wave zero of transmission:

$$s_{12}(\lambda) = \frac{(1 - \lambda^2)^{\frac{n}{2}}}{P_{n+q}(\lambda)} \tag{19}$$

Finally, for the most general case of n cascaded lines, an r^{th} order d.c. zero of transmission and a q^{th} quarter-wave zero of transmission:

$$s_{12}(\lambda) = \frac{\lambda^r (1 - \lambda^2)^{\frac{n}{2}}}{P_{n+r+q}(\lambda)} \tag{20}$$

These are the generic forms for whose magnitude squared, along the $j\Omega$ axis, equiripple specification is desired.

II. DEVELOPMENT OF THE EQUIRIPPLE FUNCTION

A. D.C. Zero of Transmission

The initial case to be considered is that of an equalizer containing n cascaded transmission lines and an r^{th} order d.c. zero of transmission. For convenience, however, the particular case of r = 1 will first be treated; the generalization to an arbitrary positive integral r will then subsequently be made. Thus, from equation 18 with r = 1, the general form to be considered is:

$$s_{12}(\lambda) = \frac{\lambda(1 - \lambda^2)^{\frac{n}{2}}}{P_{n+1}(\lambda)} \tag{21}$$

Therefore:

$$s_{12}(\lambda)\, s_{12}(-\lambda) = \frac{\lambda^2(1 - \lambda^2)^n}{P_{n+1}(\lambda^2)} \tag{22}$$

where $P_{n+1}(\lambda^2)$ now denotes a polynomial of order n+1 in λ^2.

Along the $j\Omega$ axis, then:

$$|s_{12}(j\Omega)|^2 = \frac{\Omega^2(1 + \Omega^2)^n}{P_{n+1}(\Omega^2)} \quad ; \quad 0 \leq |s_{12}(j\Omega)|^2 \leq 1 \tag{23}$$

From equation 9b:

$$\Omega = \tan \beta \ell \tag{24a}$$

For convenience, let:

$$\theta = \beta \ell \tag{24b}$$

Then, substituting into equation 23:

$$|s_{12}|^2 = \frac{\tan^2\theta \sec^{2n}\theta}{P_{n+1}(\tan^2\theta)} = \frac{\sin^2\theta}{P_{n+1}(\cos^2\theta)} \tag{25}$$

Let, now:

$$x = a \cos \theta \tag{26a}$$

for which:

$$\sin^2\theta = 1 - \cos^2\theta = \frac{a^2 - x^2}{a^2} \tag{26b}$$

where a is an arbitrary positive constant greater than unity.

Substituting equation 26 in 25:

$$|s_{12}|^2 = \frac{\frac{a^2 - x^2}{a^2}}{P_{n+1}\left(\frac{x^2}{a^2}\right)} = \frac{a^2 - x^2}{G_{n+1}(x^2)} =$$

$$= \frac{a^2 - x^2}{a^2 - x^2 + H_{n+1}(x^2)} = \frac{1}{1 + \frac{H_{n+1}(x^2)}{a^2 - x^2}} \qquad (27)$$

The motivation for the preceding manipulations becomes more evident if one considers again the basic end to be achieved. A Tchebycheff-type shape is desired for $|s_{12}|^2$, as this parameter can be equated to a power transfer ratio. That is, we seek an analytic expression describing a shape having the basic form of Figure 7.

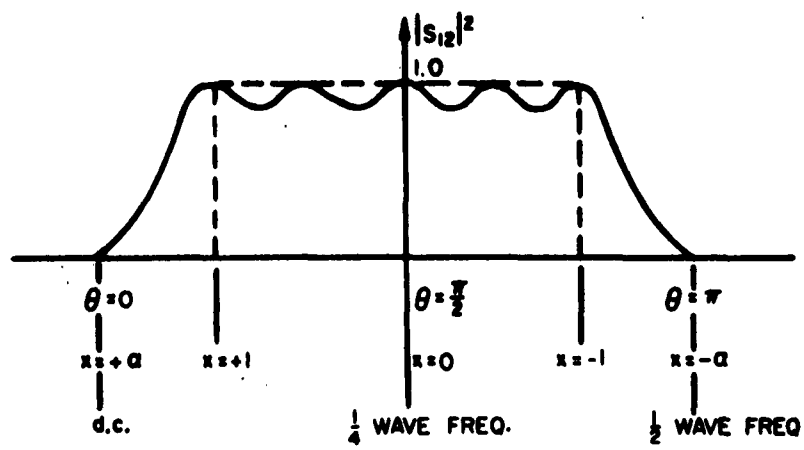

Figure 7 - Desired Tchebycheff-type Shape

The problem thus becomes, noting equation 27, that of specifying $H_{n+1}(x^2)/(a^2 - x^2)$ in such a fashion that it oscillates between finite bounds over a given interval and then increases monotonically outside of this interval. The single order d.c. zero of transmission necessitates that this function have poles at $x = \pm a$. These points correspond to d.c. and the half-wave frequency.

If a function exhibiting this behavior can be found, then the multiplication of it by a constant, call it ε^2 (where $\varepsilon^2 << 1$), when inserted into 27 will generate the basic shape of Figure 7. That is, $\varepsilon^2 H_{n+1}(x^2)/a^2 - x^2$ will slightly perturb $|s_{12}|^2$ in the interval wherein the function oscillates between fixed bounds; in the region where $\varepsilon^2 H_{n+1}(x^2)/a^2 - x^2$ monotonically increases, eventually becoming infinite at $x = \pm a$, $|s_{12}|^2$ will monotonically decrease, becoming zero at $x = \pm a$.

The boundedness constraint, $0 \leq |s_{12}|^2 \leq 1$, when imposed upon equation 27 requires that $H_{n+1}(x^2)/a^2 - x^2$ remain non-negative in the entire real frequency domain corresponding to $-a \leq x \leq a$ which in turn demands that the function oscillate between finite positive bounds. This latter constraint, however, is not stringent; the form of equation 27 may be remanipulated in such a fashion as to accommodate any finite bounds of oscillation and still satisfy the condition, $0 \leq |s_{12}|^2 \leq 1$. In the region of monotonic variation, however, $H_{n+1}(x^2)/a^2 - x^2$ must be a positive increasing function.

A further restriction upon $H_{n+1}(x^2)$, which as yet has not been explicitly stated, is the fact that it must be a rational function of x^2 with real coefficients. This demand becomes obvious if one recalls that in the generic form of $|s_{12}(j\Omega)|^2$, $P_{n+1}(\Omega^2)$ was constrained to be a polynomial of order $n + 1$ in Ω^2.

Thus, if for simplicity of notation, we define $F(x^2) = H_{n+1}(x^2)/a^2 - x^2$, we may summarize the requisite properties of $F(x^2)$ as:

a) $F(x^2)$ must possess poles at $x = \pm a$.
b) $F(x^2)$ must oscillate between finite bounds over a given portion of the total interval $-a \leq x \leq +a$.
c) $F(x^2)$ must be a positive, monotonically increasing function outside of the interval of oscillation.
d) $F(x^2)$ must be a rational function of x^2, whose numerator is a polynomial of order $n + 1$ in x^2 and whose denominator is the $(a^2 - x^2)$ factor.

We are seeking, basically, a modified Tchebycheff function. The substitution, $x = a \cos \theta$, with a stipulated as a positive constant > 1, was made in view of this fact and with a foreknowledge of the behavior of ordinary Tchebycheff polynomials. These polynomials, defined by:

$$T_n(x) = \cos(n \cos^{-1} x) \tag{28}$$

oscillate in amplitude between ± 1 for $-1 \leq x \leq +1$ and behave monotonically outside this interval. We must incorporate this type of behavior into the modified Tchebycheff function. Thus the parameter a was prescribed to establish the width of the passband

relative to the total band of interest. The total band, as shown in Figure 7, extends from $\theta = 0$ to $\theta = \pi$, i.e., from $x = +a$ to $x = -a$. The edges of the passband are at $\theta_o = \cos^{-1} \pm \frac{1}{a}$, i.e., at $x = \pm 1$. Hence, by increasing or decreasing a, subject to the aforementioned constraint, one may respectively decrease or increase the relative width of the passband.

Consider as a possible specification of $F(x^2)$, the function:

$$F(x^2) = \cos(2n\phi + \delta)$$

where

$$\phi = \cos^{-1} x = \cos^{-1} (a \cos \theta) \tag{29}$$

$$\delta = \cos^{-1} \frac{f(x^2)}{a^2 - x^2}$$

From the trigonometric identities:

$$\cos(a + b) = \cos a \cos b - \sin a \sin b \tag{30}$$

$$\sin a = \sqrt{1 - \cos^2 a}$$

it becomes evident that $F(x^2)$ will have the general form:

$$F(x^2) = \cos 2n\phi \cdot \frac{f(x^2)}{a^2 - x^2} - \sin 2n\phi \cdot \frac{\sqrt{(a^2 - x^2)^2 - f^2(x^2)}}{a^2 - x^2} \tag{31}$$

Thus, the function will possess the $(a^2 - x^2)$ denominator factor, i.e., poles at $x = \pm a$.

The function we desire must be a function of the variable x^2, noting equation 27. The polynomials defined by equation 28 do not, for odd n, satisfy this demand. However,

$$T_{2n}(x) = \cos(2n \cos^{-1} x) = \cos(2n\phi) = \cos(n\,[2\phi]) = T_n(2x^2 - 1) \tag{32}$$

does satisfy this requirement of evenness. Thus, $2n\phi$, rather than ϕ, was incorporated into the argument of equation 29.

The development of this general Tchebycheff-type function, as well as the proper analytic form for δ, was accomplished by Sharpe[5] and Helman.[6] The specification they formulated is:

$$\delta = \cos^{-1}\left\{\frac{(1 - 2a^2)x^2 + a^2}{x^2 - a^2}\right\} \tag{33a}$$

or

$$\cos\delta = \frac{(1 - 2a^2)x^2 + a^2}{x^2 - a^2} = \frac{(2a^2 - 1)x^2 - a^2}{a^2 - x^2} \tag{33b}$$

Consider Figure 8, wherein cos δ (for a = 2.00) and cos 2φ are both plotted versus x in the interval $-1 \leq x \leq 1$, i.e., the passband. Since both functions are bounded in magnitude by unity in this interval, the arguments δ and 2φ remain real. Furthermore, the similar behavior of the functions implies that the angles 2φ and δ must vary in like fashion across this interval.

It is a well-established property of Tchebycheff polynomials, though, that the argument φ traverses through π radians as x varies from +1 to -1. Thus, 2φ will cover 2π radians; δ, then, should likewise go through 2π radians. The manner in which these two angles vary relative to each other, however, has not, as yet, been established. That is, although they both cover 2π radians in the passband, no indication has been given as to whether their representative phasors would rotate in a similar or opposite directions.

To establish this point, consider the definition:

$$\sin\phi = \sin(\cos^{-1} x) = \sqrt{1 - x^2} \tag{34}$$

By convention, the positive sign is associated with the square root. This fixes the interval $0 \leq x \leq 1$ as corresponding to $\frac{\pi}{2} \geq \phi \geq 0$ or $\pi \geq 2\phi \geq 0$. Likewise, the interval $-1 \leq x \leq 0$ corresponds $\pi \geq \phi \geq \frac{\pi}{2}$ or $2\pi \geq 2\phi \geq \pi$. Hence,

$$\frac{d\phi}{dx} < 0 \quad \text{for} \quad -1 < x < 1 \tag{35}$$

since

$$\frac{d\phi}{dx} = -\frac{1}{\sin\phi}$$

If, then, we wish δ to vary in a similar manner as 2φ, we must select sin δ in such a manner that the first and second quadrants of δ correspond to $0 < x < 1$ and the third and fourth to $-1 < x < 0$. To accomplish this, we take:

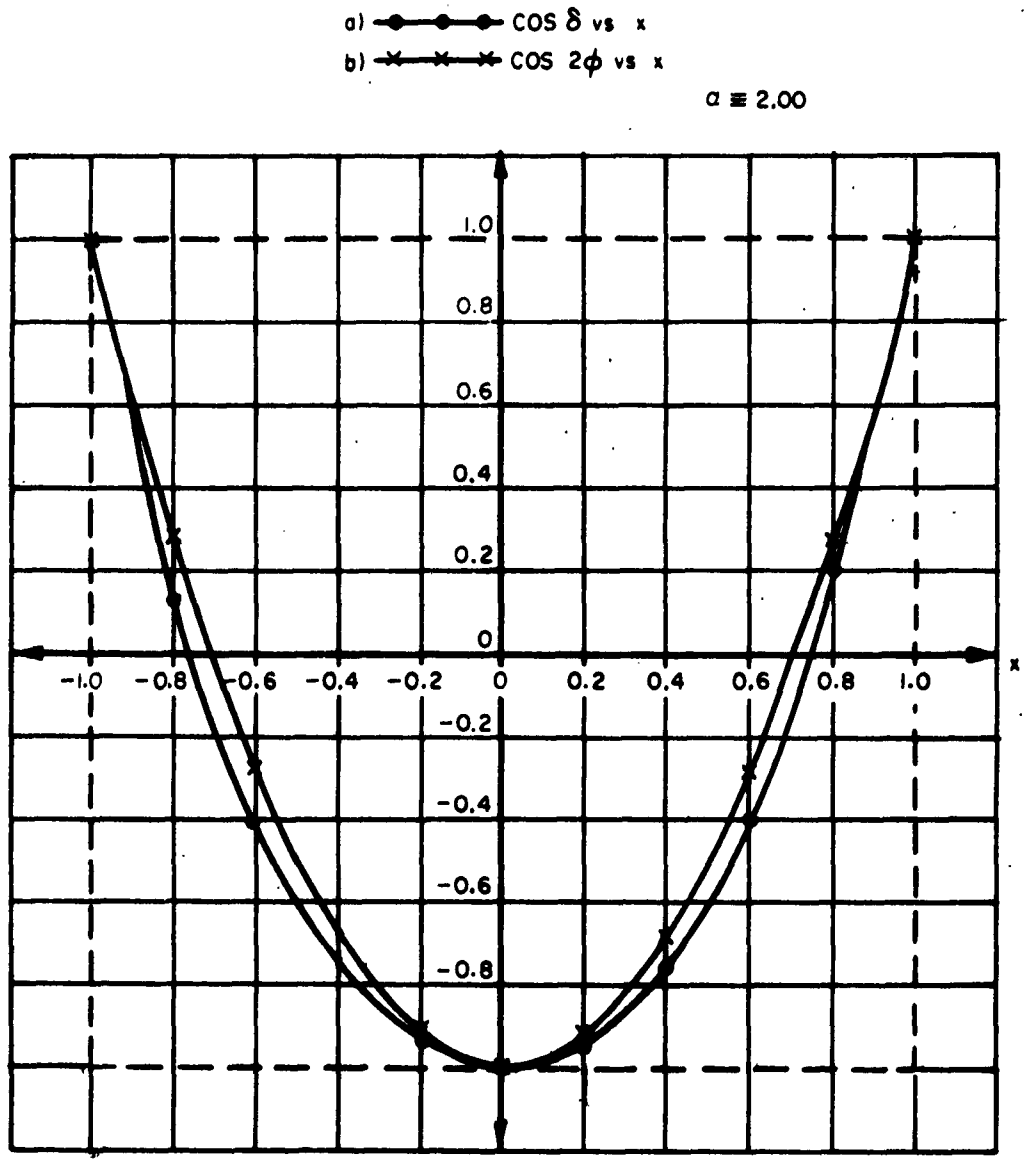

Fig. 8 a) cos δ vs. χ
b) cos 2φ vs. χ

$$\sin\delta = \sqrt{1 - \cos^2\delta} = \frac{2a x\sqrt{(1 - x^2)(a^2 - 1)}}{a^2 - x^2} \tag{36}$$

where the square root of this last expression is taken as positive. Since $a^2 - x^2 > 0$, $a > 1$, and $x^2 < 1$ in the passband, $\sin\delta$ takes on the same sign as x; this, from the above considerations, is the condition desired. Thus,

$$\frac{d\delta}{dx} = \frac{-4a^2 x (a^2 - 1)}{(a^2 - x^2)^2 \sin\delta} < 0 \quad \text{for} \quad -1 < x < +1 \tag{37}$$

Figure 9 depicts the variation of δ and 2ϕ with x for $a = 2.00$.

Hence, the argument $(2n\phi + \delta)$ ranges over $(n+1)$ cycles of 2π in the passband. $\cos(2n\phi + \delta)$, therefore, repeats $(n+1)$ times with $2(n+1)$ zeros and $[2(n+1) + 1]$ points of maximum deviation, i.e., points where $|\cos(2n\phi + \delta)| = 1$.

The effect of the angle δ in the passband is merely to add another ripple. It is important for our purposes that this angle add and not detract from the total argument; the stopband attenuation of $|s_{12}|^2$ proves much steeper in the former instance.

The important feature of this development is the fact that the basic Tchebycheff property of oscillation between fixed bounds (i.e., ± 1) over a subinterval of the total band of interest is preserved. Thus, requirement (b) is established. The passband behavior of a representative function is shown in Figure 10.

Up to this point, we have dealt solely with a single order d.c. zero of transmission. This enabled is to consider the angle δ as such, rather than multiples of this angle. Had an m^{th} order d.c. zero of transmission been initially specified, however, the counterpart to equation 27 would have been:

$$|s_{12}|^2 = \frac{1}{1 + \dfrac{H_{n+m}(x^2)}{(a^2 - x^2)^m}} \tag{38}$$

For this form:

$$F(x^2) = \frac{H_{n+m}(x^2)}{(a^2 - x^2)^m} = \cos(2n\phi + m\delta) \tag{39}$$

would be the requisite equiripple function.

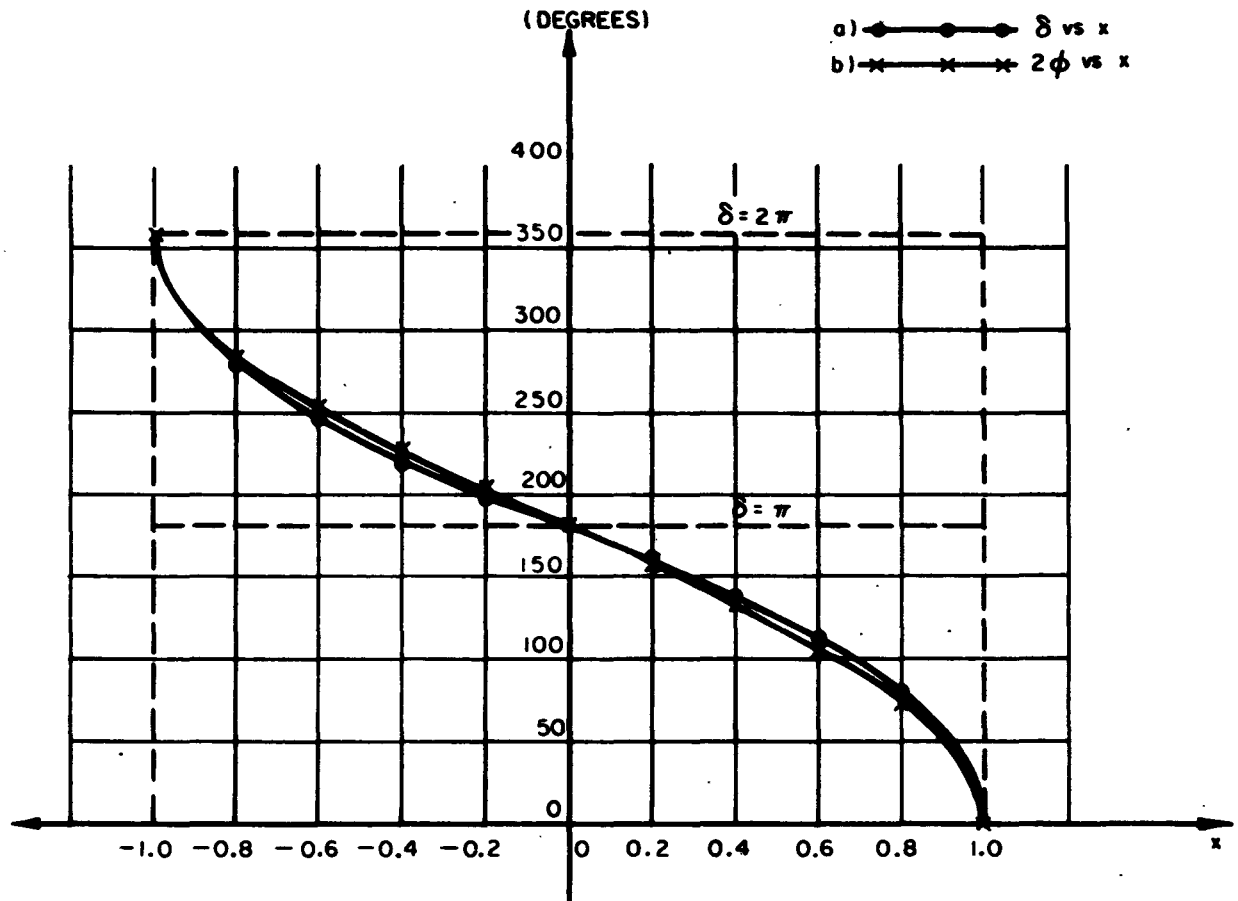

Fig. 9 a) δ vs χ
b) 2φ vs χ

MRI—18854

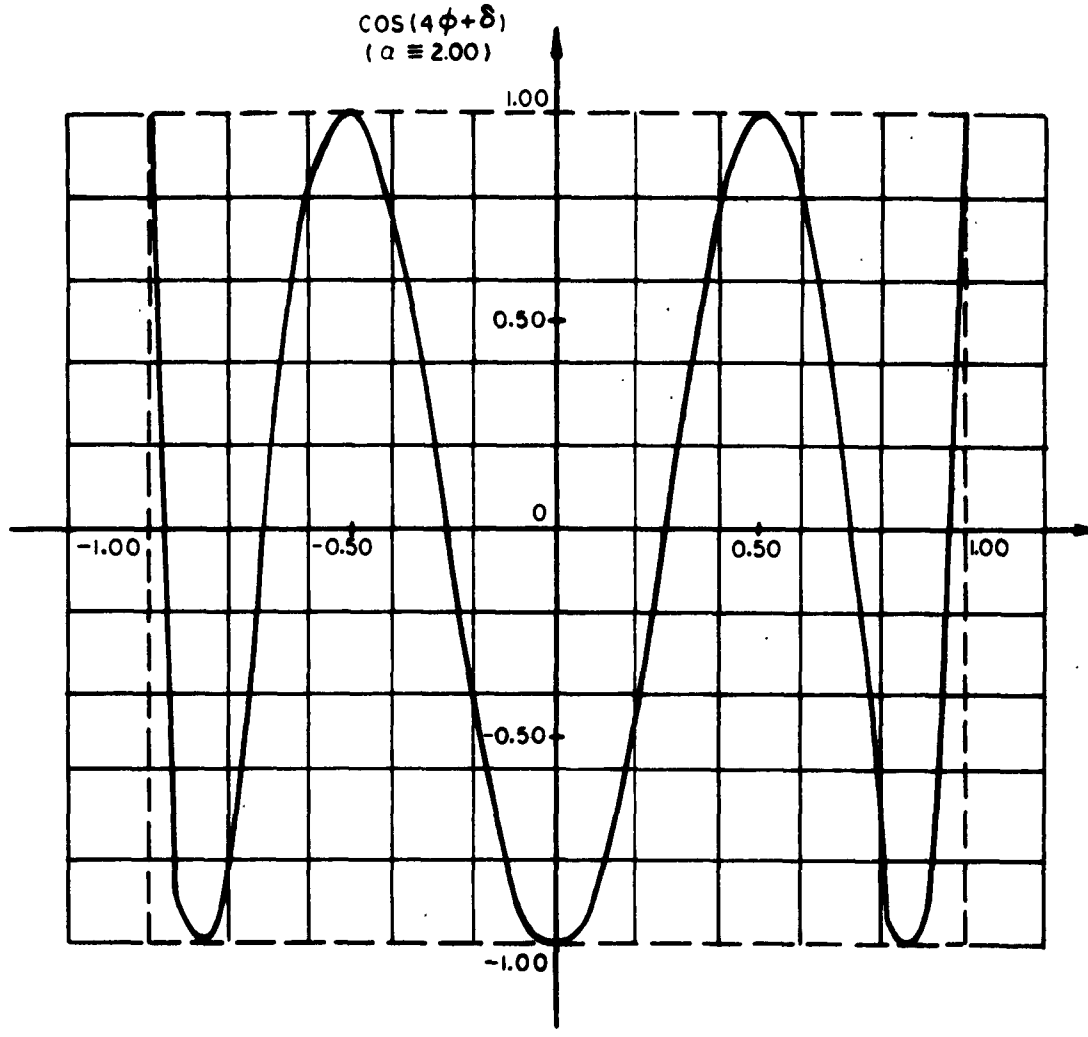

FOR $\alpha = 2.00$:

$$\cos(4\phi+\delta) = \frac{1}{4-x^2}\left[(56+32\sqrt{3})x^6+(-88-48\sqrt{3})x^4+(39+16\sqrt{3})x^2-4\right]$$

Fig 10 cos (4φ + δ) vs. χ

Consider the following expansion of (39):

$$\cos(2n\phi + m\delta) = \frac{1}{2}\left[e^{j(2n\phi + m\delta)} + e^{-j(2n\phi + m\delta)}\right] =$$

$$= \frac{1}{2}\left[(\cos\phi + j\sin\phi)^{2n}(\cos\delta + j\sin\delta)^{m} + (\cos\phi - j\sin\phi)^{2n}(\cos\delta - j\sin\delta)^{m}\right] =$$

$$= \frac{(x+\sqrt{x^2-1})^{2n}\left([2a^2-1]x^2 - a^2 + 2ax\sqrt{(x^2-1)(a^2-1)}\right)^{m} + (x-\sqrt{x^2-1})^{2n}\left([2a^2-1]x^2 - a^2 - 2ax\sqrt{(x^2-1)(a^2-1)}\right)^{m}}{2(a^2-x^2)^{m}} \qquad (40)$$

In this form, the fact that (39) does possess the requisite $(a^2 - x^2)^m$ denominator becomes explicit.

Likewise, the passband behavior of $\cos(2n\phi + m\delta)$ would be qualitatively similar to that of $\cos(2n\phi + \delta)$. The argument $(2n\phi + m\delta)$ would range over $(n+m)$ cycles of 2π, the function repeating $(n+m)$ times with $2(n+m)$ zeros and $[2(n+m)+1]$ points of maximum deviation.

The remaining properties which must be established are the positive, monotonic stopband variation and the constraint of rationality. These properties will be verified for the general case.

Consider again the function:

$$\cos(2n\phi + m\delta)$$

where

$$2\phi = \cos^{-1}(2x^2 - 1)$$

$$\delta = \cos^{-1}\left\{\frac{(2a^2-1)x^2 - a^2}{a^2 - x^2}\right\} = \cos^{-1} g(x^2) \qquad (41a)$$

For $1 < |x| < a$,

$$(2x^2 - 1) > 1 \qquad (41b)$$

$$g(x^2) > 1$$

Therefore, in this interval,

$$2\phi = \cos^{-1}(2x^2 - 1) = j\cosh^{-1}(2x^2 - 1) \tag{41c}$$

$$\delta = \cos^{-1} g(x^2) = j\cosh^{-1} g(x^2)$$

and

$$\cos(2n\phi + m\delta) = \cos\left\{j\left[n\cosh^{-1}(2x^2 - 1) + m\cosh^{-1}(g(x^2)\right]\right\} =$$

$$= \cosh\left\{n\cosh^{-1}(2x^2 - 1) + m\cosh^{-1}(g(x^2))\right\} \tag{41d}$$

As one proceeds from the passband edges (i.e., $|x| = 1$) to the edges of the useful band ($|x| = a$), the parameters of (41b) increase monotonically, $g(x^2)$ approaching infinity as $|x|$ approaches a. Hence the function (41d) is also a positive, monotonically increasing function in this interval; it varies from 1 to ∞ as $|x|$ varies from 1 to a. Thus the desired behavior is achieved. Note that, from (41d), one may readily deduce the primed nature of the polynomial numerator with respect to the factor, $(a^2 - x^2)^m$.

The necessary general rationality of $\cos(2n\phi + m\delta)$ may be explicitly shown if one considers the following expansion:

$$\cos(2n\phi + m\delta) = \cos 2n\phi \cos m\delta - \sin 2n\phi \sin m\delta \tag{42a}$$

Again, for simplicity of notation, let:

$$\cos\delta = \frac{(2a^2 - 1)x^2 - a^2}{a^2 - x^2} = g(x^2) \tag{42b}$$

Then, noting (42a)

$$\cos(2n\phi + m\delta) = T_{2n}(x)\, T_m(g(x^2)) - U_{2n}(x)\, U_m(g(x^2)) \tag{42c}$$

where

$$T_k(\xi) = \cos(k\cos^{-1}\xi)$$

$$U_k(\xi) = \sin(k\cos^{-1}\xi) \tag{42d}$$

Using, now, several established functional relations[7]

$$U_m(g(x^2)) = \sqrt{1 - (g(x^2))^2}\; Q_{m-1}(g(x^2)) \tag{42e}$$

where

$$Q_{m-1}(g) = \left[\binom{m}{1} g^{m-1} - \binom{m}{3} g^{m-3}(1-g^2) + \binom{m}{5} g^{m-5}(1-g^2)^2 - \ldots \right]$$

and

$$\binom{m}{q} = \frac{m!}{(m-q)!\, q!} \tag{42f}$$

Thus, noting (42b) and (36) in conjunction with (42e)

$$U_m(g(x^2)) = \sin\delta\, Q_{m-1}(g(x^2)) = \frac{2ax\sqrt{(a^2-1)(1-x^2)}}{a^2-x^2}\, Q_{m-1}(g(x^2)) \tag{42g}$$

However,

$$-\sqrt{1-x^2}\, U_{2n}(x) = T_{2n+1}(x) - x\, T_{2n}(x) \tag{42h}$$

Thus,

$$\cos(2n\phi + m\delta) = T_{2n}(x)\, T_m(g(x^2)) - U_{2n}(x)\, U_m(g(x^2)) =$$

$$= T_{2n}(x)\, T_m(g(x^2)) + \frac{2ax\sqrt{a^2-1}}{a^2-x^2} \left(T_{2n+1}(x) - x\, T_{2n}(x)\right) Q_{m-1}(g(x^2)) \tag{42i}$$

Since

$$x\, T_{2n+1}(x) = \tfrac{1}{2}\, T_{2n+2}(x) + \tfrac{1}{2}\, T_{2n}(x)$$

$$= \tfrac{1}{2}\, T_{n+1}(2x^2-1) + \tfrac{1}{2}\, T_n(2x^2-1)\,, \tag{42j}$$

$$\cos(2n\phi + m\delta) = T_n(2x^2-1)\, T_m(g(x^2)) + \frac{2a\sqrt{a^2-1}}{a^2-x^2} \left[\tfrac{1}{2}\, T_{n+1}(2x^2-1)\right.$$

$$\left. + \tfrac{1}{2}\, T_n(2x^2-1) - x^2\, T_n(2x^2-1)\right] Q_{m-1}(g(x^2)) \tag{42k}$$

From equation 42b, one notes that $g(x^2)$ is a rational function of x^2. Since equation 42k involves rational functions of x^2 and $g(x^2)$, it is itself a rational function of x^2.

Having established the previously-outlined requisite properties, we may now incorporate this general Tchebycheff function into the equiripple specification of $|s_{12}|^2$. From Figure 10, it is evident that the function oscillates between ± 1 in the passband. Therefore, the form of equation 38 must be slightly adjusted to insure $0 \leq |s_{12}|^2 \leq 1$. A proper form, for n cascaded lines and an m^{th} order

d.c. zero of transmission, is, then:

$$|s_{12}|^2 = \frac{1 - \epsilon^2}{1 + \epsilon^2 \cos(2n\phi + m\delta)} \tag{43}$$

An alternate form may be obtained by defining:

$$\beta = \frac{\delta}{2} \tag{44a}$$

for which:

$$\cos\beta = \sqrt{\frac{1 + \cos\delta}{2}} = x\sqrt{\frac{a^2 - 1}{a^2 - x^2}} \tag{44b}$$

and

$$\sin\beta = a\sqrt{\frac{1 - x^2}{a^2 - x^2}} \tag{44c}$$

Employing this function, we may specify $|s_{12}|^2$ as:

$$|s_{12}|^2 = \frac{1}{1 + \epsilon^2 \cos^2(n\phi + m\beta)} \tag{45}$$

Note that since:

$$\cos^2(n\phi + m\beta) = \frac{1}{2} + \frac{1}{2}\cos(2n\phi + 2m\beta) = \frac{1}{2} + \frac{1}{2}\cos(2n\phi + m\delta), \tag{46}$$

all prior discussions concerning the necessary properties of the equiripple function are equally satisfied.

B. Quarter-Wave Frequency Zeros of Transmission

The general Tchebycheff function will now be applied to the case of quarter-wave frequency (i.e., $\beta\ell = \frac{\pi}{2}$) zeros of transmission. For a network comprised of n cascaded lines and possessing, in addition, a q^{th} order quarter-wave zero of transmission i.e., short circuited stubs in series, open circuited stubs in shunt, (from eq. 19):

$$s_{12}(\lambda) = \frac{(1 - \lambda^2)^{\frac{n}{2}}}{P_{n+q}(\lambda)} \tag{47}$$

Therefore:

$$s_{12}(\lambda)\, s_{12}(-\lambda) = \frac{(1 - \lambda^2)^n}{P_{n+q}(\lambda^2)}$$

with $P_{n+q}(\lambda^2)$ a polynomial of order $n+q$ in λ^2.

Thus, along the $j\Omega$ axis:

$$|s_{12}(j\Omega)|^2 = \frac{(1+\Omega^2)^n}{P_{n+q}(\Omega^2)}; \quad 0 \leq |s_{12}(j\Omega)|^2 \leq 1 \tag{49}$$

Noting that: $\Omega = \tan \beta \ell = \tan \theta$,

$$|s_{12}|^2 = \frac{\sec^{2n}\theta}{P_{n+q}(\tan^2\theta)} = \tag{50a}$$

$$= \frac{\dfrac{1}{\cos^{2n}\theta}}{a_{n+q}\dfrac{\sin^{2n+2q}\theta}{\cos^{2n+2q}\theta} + a_{n+q-1}\dfrac{\sin^{2n+2q-2}\theta}{\cos^{2n+2q-2}\theta} + \cdots + a_1\dfrac{\sin^2\theta}{\cos^2\theta} + a_o} \tag{50b}$$

$$= \frac{1}{a_{n+q}\dfrac{\sin^{2n+2q}\theta}{\cos^{2q}\theta} + a_{n+q-1}\dfrac{\sin^{2n+2q-2}\theta}{\cos^{2q-2}\theta} + \cdots + a_1\sin^2\theta\cos^{2n-2}\theta + a_o\cos^{2n}\theta} \tag{50c}$$

Note that equation (50c) involves only even powers of the trigonometric quantities. Since $\sin^2\theta = 1 - \cos^2\theta$, one may further manipulate equation (50c) into the form:

$$|s_{12}|^2 = \frac{1}{1 + \dfrac{1}{\cos^{2q}\theta} \cdot G_{n+q}(\sin^2\theta)} \tag{51}$$

with no loss of generality. $G_{n+q}(\sin^2\theta)$ is a polynomial of order $n+q$ in $\sin^2\theta$.

Thus, if the transformation:

$$x = a \sin\theta \tag{52a}$$

is made, for which,

$$\cos^2\theta = 1 - \sin^2\theta = \frac{a^2 - x^2}{a^2}, \tag{52b}$$

equation 51 will assume the form:

$$|s_{12}|^2 = \frac{1}{1 + \dfrac{H_{n+q}(x^2)}{(a^2 - x^2)^q}} \tag{53}$$

This form is identical to that of equation (38). Therefore, if $|s_{12}|^2$ is specified as:

$$|s_{12}|^2 = \frac{1 - \varepsilon^2}{1 + \varepsilon^2 \cos(2n\phi + q\delta)} \quad , \tag{54}$$

where $x = a \sin\theta$, an equiripple shape is attained. Note that this is a low pass characteristic; the d.c. point corresponds to $x = o$, the passband edge to $x = +1$, and the quarter-wave frequency to $x = +a$. Figure 11 shows a generic shape of this type.

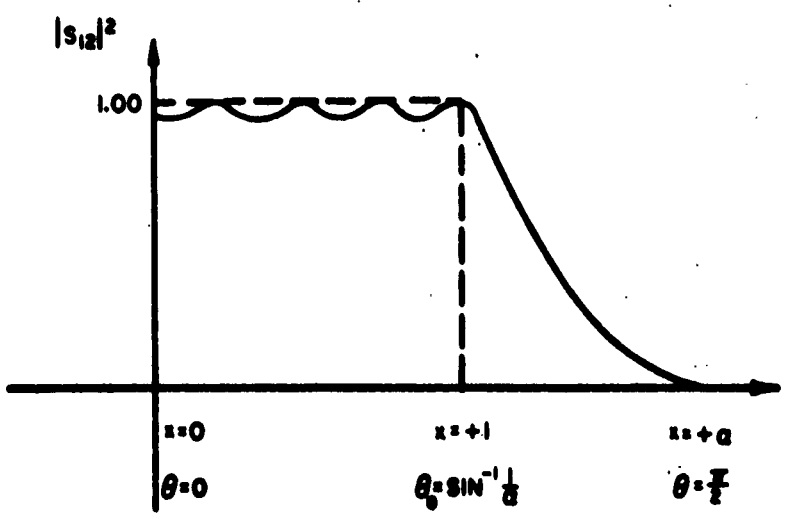

Figure 11 - Equiripple Shape for the Case of a Quarter-Wave Zero of Transmission

C. Zeros of Transmission at D.C. and the Quarter-Wave Frequency

The network structure to be herein considered is one which possesses zeros of transmission at both d.c. and the quarter-wave frequency (i.e., at $\Omega = 0$ and $\Omega = \infty$, respectively). No equiripple specification technique has been devised to handle the most general case of this class; however, we may accommodate the case wherein the pertinent network is comprised of an even number of cascaded lines and equal order zeros of transmission at d.c. and the quarter-wave frequency. Imposing these restrictions upon equation (20), we have, for $n = 2m$ cascaded lines and an r^{th} order zero at d.c. and the quarter-wave:

$$s_{12}(\lambda) = \frac{\lambda^r (1 - \lambda^2)^m}{P_{2m + 2r}(\lambda)} \tag{55}$$

Along the $j\Omega$ axis, then:

$$|s_{12}(j\Omega)|^2 = \frac{\Omega^{2r}(1+\Omega^2)^{2m}}{P_{2m+2r}(\Omega^2)}, \quad 0 \leq |s_{12}(j\Omega)|^2 \leq 1 \tag{56}$$

Since $\Omega = \tan \beta \ell = \tan \theta$:

$$|s_{12}|^2 = \frac{\tan^{2r}\theta \sec^{4m}\theta}{P_{2m+2r}(\tan^2\theta)} \tag{57a}$$

$$= \frac{\dfrac{\sin^{2r}\theta}{\cos^{4m+2r}\theta}}{a_{2m+2r}\dfrac{\sin^{4m+4r}\theta}{\cos^{4m+4r}\theta} + a_{2m+2r-1}\dfrac{\sin^{4m+4r-2}\theta}{\cos^{4m+4r-2}\theta} + \cdots + a_1\dfrac{\sin^2\theta}{\cos^2\theta} + a_o} \tag{57b}$$

$$= \frac{1}{a_{2m+2r}\dfrac{\sin^{4m+2r}\theta}{\cos^{2r}\theta} + a_{2m+2r-1}\dfrac{\sin^{4m+2r-2}\theta}{\cos^{2r-2}\theta} + \cdots + a_1\dfrac{\cos^{4m+2r-2}\theta}{\sin^{2r-2}\theta} + a_o\dfrac{\cos^{4m+2r}\theta}{\sin^{2r}\theta}} \tag{57c}$$

Noting that equation (57c) involves only even powers of the trigonometric functions, we may rewrite it as:

$$|s_{12}|^2 = \frac{1}{1 + \dfrac{G_{2m+2r}(\sin^2\theta)}{(\cos^2\theta \sin^2\theta)^r}} \tag{58}$$

with no loss of generality; $G_{2m+2r}(\sin^2\theta)$ is a polynomial of order $2m+2r$ in $\sin^2\theta$.

Let us now make the transformation:

$$x = a \cos 2\theta \tag{59a}$$

for which,

$$\frac{x}{a} = \cos 2\theta = 2\cos^2\theta - 1 = 1 - 2\sin^2\theta . \tag{59b}$$

Thus,

$$\cos^2\theta = \frac{1}{2a}(a + x)$$

$$\sin^2\theta = \frac{1}{2a}(a - x) \tag{60}$$

Equation (60), when introduced into (58), will yield a form:

$$|s_{12}|^2 = \frac{1}{1 + \dfrac{H_{2m+2r}(x)}{(a^2 - x^2)^r}} \tag{61}$$

However, we require symmetric behavior about x = o; $|s_{12}|^2$ must be ≥ 0 for $1 \leq |x| \leq a$. Hence, let us restrict $H_{2m+2r}(x)$ to be an even function of x; that is, we set the coefficients of all odd powers equal to zero. Then,

$$|s_{12}|^2 = \frac{1}{1 + \dfrac{H_{m+r}(x^2)}{(a^2 - x^2)^r}} \tag{62}$$

This form is identical to that of equations (38) and (53). Thus, by specifying

$$|s_{12}|^2 = \frac{1 - \varepsilon^2}{1 + \varepsilon^2 \cos(2m\phi + r\delta)} \quad , \tag{63}$$

we realize the desired equiripple shape.

Figure 12 depicts a generic shape of this class.

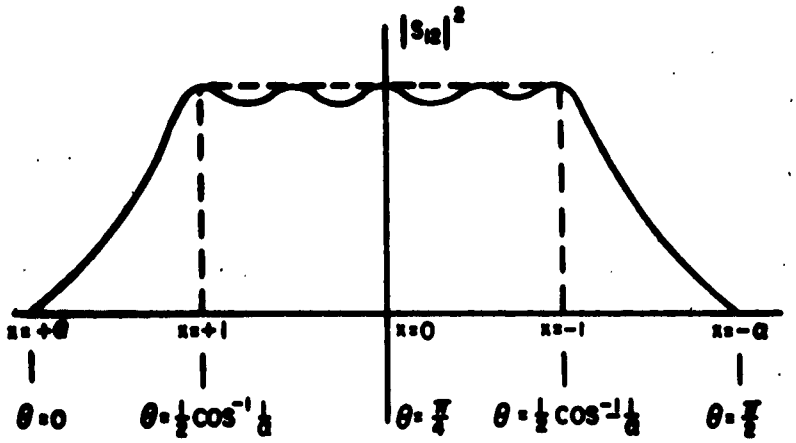

Figure 12 - Equiripple Shape for the Case of D.C. and Quarter-Wave Frequency Zeros of Transmission

Examples, wherein networks realizing these Tchebycheff shapes are synthesized, will be given in subsequent sections of the text. The shunt, short-circuited stub band pass filter, treated in the following segment, will utilize the transformation of Section II A; that of Section II B will be employed in the tunnel

diode amplifier design. Appendix A contains an elementary example of a synthesis, realizing a network of the Section II C type.

An integral part of these synthesis procedures is the factorization of $s_{11}(\lambda)\, s_{11}(-\lambda) = 1 - s_{12}(\lambda)\, s_{12}(-\lambda)$, as outlined in reference 1. Thus, it would be highly desirable to have an explicit factorization of $s_{11}(\lambda)\, s_{11}(-\lambda)$. This factorization, for the general case, has not been achieved. However, for the specific case of Section II A or Section II B wherein the number of lines and the order of the zero of transmission are equal (i.e., where $\cos(2n\phi + n\delta)$ is encountered), the roots may be found in a manner similar to that employed with regular Tchebycheff polynomials. This factorization is outlined in Appendix B.

III. THE SINGLE-STUB BANDPASS FILTER

A. Determination of Load Resistance and Stub Characteristic Admittance

The network to be considered in this section is, as shown in Figure 13, a cascade of transmission lines shunted by a short-circuited stub. The problem to be treated is the apriori determination of the load resistance and stub characteristic admittance, so that the structure can be designed to operate between prescribed terminations.

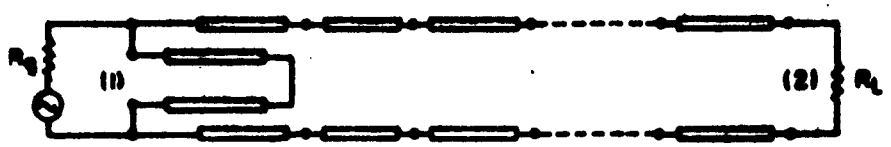

Figure 13 - Shunt, Short-Circuited Stub, Bandpass Filter

For a network comprised solely of a cascade of equilength transmission lines operating between a resistive generator and a resistive load, the determination of the load resistance is straightforward. The transparency of the lines at d.c. ($\Omega = 0$) enables one to calculate the load termination R_L from the relation[1]

$$s_{11}(0) = \frac{R_L - R_g}{R_L + R_g} \quad . \tag{64}$$

That is, since $s_{11}(0)$ is real and since $|s_{11}|^2 = 1 - |s_{12}|^2$, the load resistance may be easily determined from a knowledge of the insertion gain (i.e., $|s_{12}|^2$) shape.

The insertion of the shunt, shorted stub into the equalizer, as is shown in Figure 13, necessitates that $s_{11}(0) = -1$ regardless of the termination. One loses the d.c. point access to the load.

The problem thus becomes, given the insertion gain shape (i.e., equation (43) or (45)) and a foreknowledge of the desired physical position of the stub relative to the generator and load, the determination in an a priori fashion of the values of load resistance and stub characteristic admittance which the synthesis will yield.

We shall obtain these parameters by considering the representation of Figure 14,

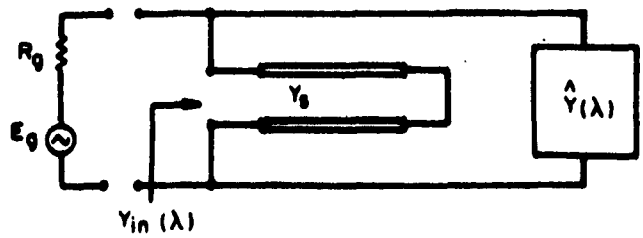

Figure 14 - Bandpass Filter Schematic

where $\hat{Y}(\lambda)$ represents the unnormalized input admittance of a cascade of n equi-length lossless transmission lines terminated in conductance Y_L.

Y_s = stub characteristic admittance.

$Y_{in}(\lambda)$ = unnormalized input admittance of the stub-shunted cascade. That is,

$$Y_{in}(\lambda) = \frac{Y_s}{\lambda} + \hat{Y}(\lambda) \tag{65}$$

Normalizing this admittance to $Y_g = R_g^{-1}$:

$$\frac{Y_{in}}{Y_g} = \frac{R_g Y_s}{\lambda} + R_g \hat{Y}(\lambda) , \tag{66}$$

for which:

$$s_{in}(\lambda) = \frac{1 - R_g Y_{in}}{1 + R_g Y_{in}} = s_{11}(\lambda) \tag{67}$$

if we constrain port 2 of the equalizer to be normalized to the load.

The first relation that will be derived is the familiar Fano-Bode integral restriction.[8, 11] Substituting equation (65) into (67):

$$s_{11}(\lambda) = \frac{1 - \frac{R_g Y_s}{\lambda} - R_g \hat{Y}(\lambda)}{1 + \frac{R_g Y_s}{\lambda} + R_g \hat{Y}(\lambda)} = -\left\{ \frac{1 - \frac{\lambda}{R_g Y_s}(1 - R_g \hat{Y}(\lambda))}{1 + \frac{\lambda}{R_g Y_s}(1 + R_g \hat{Y}(\lambda)} \right\} \tag{68}$$

Note from the above definition that $\hat{Y}(\lambda)$ is a regular function in the neighborhood of the origin; that is, its series expansion about this point would be of the form:

$$\hat{Y}(\lambda) = Y_L + a_1\lambda + a_2\lambda^2 + \cdots \tag{69}$$

Hence, in the neighborhood of the origin $s_{11}(\lambda)$ is a ratio of two quantities differing slightly from unity. Let us expand $\frac{1}{s_{11}(\lambda)}$ about the origin:

$$\frac{1}{s_{11}(\lambda)} = - \left\{1 + \frac{\lambda}{R_g Y_s}(1 + R_g \hat{Y}(\lambda))\right\} \left\{1 + \frac{\lambda}{R_g Y_s}(1 - R_g \hat{Y}(\lambda)) + \cdots\right\} \quad (70)$$

since $\frac{1}{1-\varepsilon} = 1 + \varepsilon + \varepsilon^2 + \cdots$.

Thus:

$$\frac{1}{s_{11}(\lambda)} = (-1)(1 + \frac{2}{R_g Y_s}\lambda + \sum_{n=2}^{\infty} b_n \lambda^n) \quad (71)$$

and

$$\ln(\frac{1}{s_{11}(\lambda)}) = j\pi + \frac{2}{R_g Y_s}\lambda + \sum_{n=2}^{\infty} c_n \lambda^n . \quad (72)$$

or

$$\frac{1}{\lambda^2}\ln(\frac{1}{s_{11}(\lambda)}) = \frac{j\pi}{\lambda^2} + \frac{2}{R_g Y_s}\frac{1}{\lambda} + \frac{1}{\lambda^2}\sum_{n=2}^{\infty} c_n \lambda^n . \quad (73)$$

Consider the integration of equation (73) about the contour shown in Figure 15.

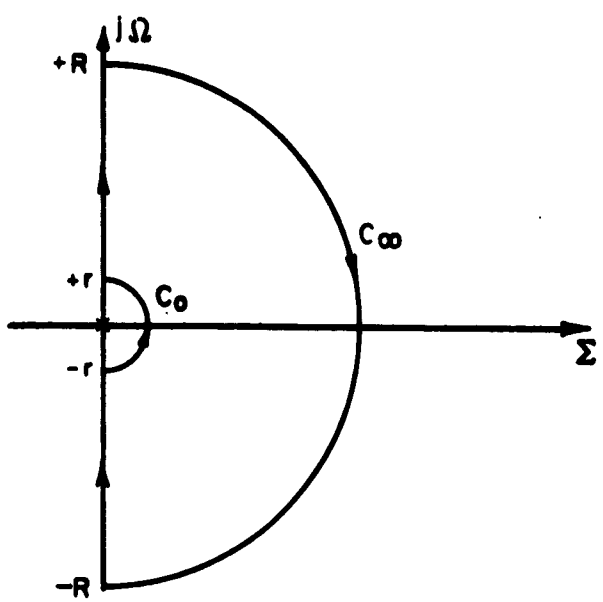

Figure 15 - Path of Contour Integration

Let us now constrain $\frac{1}{\lambda^2} \ln \left(\frac{1}{s_{11}(\lambda)}\right)$ to be analytic within and on the closed contour of Figure 15. Then, by the Cauchy-Goursat theorem:

$$\oint_c \frac{1}{\lambda^2} \ln \left(\frac{1}{s_{11}(\lambda)}\right) d\lambda = 0 \tag{74}$$

The integrand vanishes on c_∞, i.e.,

$$\lim_{R \to \infty} \left\{ \oint_{c_\infty} \frac{1}{\lambda^2} \ln \left(\frac{1}{s_{11}(\lambda)}\right) d\lambda \right\} = 0$$

Furthermore:

$$\oint_{c_o} \frac{1}{\lambda^2} \ln \left(\frac{1}{s_{11}(\lambda)}\right) d\lambda = +j\pi \left(\frac{2}{R_g Y_s}\right) \tag{75}$$

since the integration about the pole at the origin is taken in the "positive-phase", i.e., counterclockwise, direction. Thus,

$$\oint_c \frac{1}{\lambda^2} \ln \left(\frac{1}{s_{11}(\lambda)}\right) d\lambda = j \int_{-\infty}^{o-r} -\frac{1}{\Omega^2} \ln \left(\frac{1}{s_{11}(j\Omega)}\right) d\Omega + j \int_{o+r}^{\infty} -\frac{1}{\Omega^2} \ln \left(\frac{1}{s_{11}(j\Omega)}\right) d\Omega +$$

$$+ j\pi \left(\frac{2}{R_g Y_s}\right) = 0 \tag{76a}$$

or, in the limit as $r \to 0$,

$$\int_{-\infty}^{o-} \frac{1}{\Omega^2} \ln \left(\frac{1}{s_{11}(j\Omega)}\right) d\Omega + \int_{o+}^{\infty} \frac{1}{\Omega^2} \ln \left(\frac{1}{s_{11}(j\Omega)}\right) d\Omega = \frac{2\pi}{R_g Y_s} \tag{76b}$$

Let $\frac{1}{s_{11}(j\Omega)}$ be represented as:

$$\frac{1}{s_{11}(j\Omega)} = \left| \frac{1}{s_{11}(j\Omega)} \right| e^{j\phi(\Omega)} \tag{77}$$

Then:

$$\int_{-\infty}^{o^-} \frac{1}{\Omega^2} \ln \left| \frac{1}{s_{11}(j\Omega)} \right| d\Omega + \int_{o+}^{\infty} \frac{1}{\Omega^2} \ln \left| \frac{1}{s_{11}(j\Omega)} \right| d\Omega = \frac{2\pi}{R_g Y_s} \tag{78}$$

since the integral of the phase component is zero; every point on the $j\Omega$ axis has its corresponding conjugate and from (10), $s_{11}(\lambda^*) = s_{11}^*(\lambda)$.

Thus,

$$\int_o^\infty \frac{1}{\Omega^2} \ln \left| \frac{1}{s_{11}(j\Omega)} \right|^2 d\Omega = \frac{2\pi}{R_g Y_s} \tag{79}$$

This gives us one of the required relations. To obtain the second, let us consider again Figure 14. From equation (67):

$$|s_{11}(j\Omega)|^2 = 1 - |s_{12}(j\Omega)|^2 = \frac{1 - R_g Y_{in}(j\Omega)}{1 + R_g Y_{in}(j\Omega)} \cdot \frac{1 - R_g Y_{in}(-j\Omega)}{1 + R_g Y_{in}(-j\Omega)} \tag{80a}$$

or:

$$1 - |s_{12}(j\Omega)|^2 = \frac{1 + |R_g Y_{in}(j\Omega)|^2 - 2\,\mathrm{Re}\left\{R_g Y_{in}(j\Omega)\right\}}{1 + |R_g Y_{in}(j\Omega)|^2 + 2\,\mathrm{Re}\left\{R_g Y_{in}(j\Omega)\right\}} \tag{80b}$$

Rearranging equation (80b):

$$|R_g Y_{in}(j\Omega)|^2 = \frac{4\,\mathrm{Re}\left\{R_g Y_{in}(j\Omega)\right\}}{|s_{12}(j\Omega)|^2} - (1 + 2\,\mathrm{Re}\left\{R_g Y_{in}(j\Omega)\right\}) \tag{80c}$$

From equation (66);

$$R_g Y_{in}(j\Omega) = \frac{R_g Y_s}{j\Omega} + R_g \hat{Y}(j\Omega) \tag{81}$$

Hence:

$$\mathrm{Re}\left\{R_g Y_{in}(j\Omega)\right\} = \mathrm{Re}\left\{R_g \hat{Y}(j\Omega)\right\} \tag{82}$$

since R_g and Y_s are real quantities (stub is lossless).

Also:

$$|R_g Y_{in}(j\Omega)|^2 = R_g^2 \left(\frac{Y_s^2}{\Omega^2} + \frac{Y_s}{j\Omega} \cdot \hat{Y}(-j\Omega) - \frac{Y_s}{j\Omega} \cdot \hat{Y}(j\Omega) + |\hat{Y}(j\Omega)|^2 \right) \tag{83}$$

Thus, noting equation (69) in conjunction with (82) and (83):

$$\left[\Omega^2 |R_g Y_{in}(j\Omega)|^2\right]_{\Omega=o} = R_g^2 Y_s^2 = \left[\frac{\Omega^2\, 4\,\mathrm{Re}\left\{R_g \hat{Y}(j\Omega)\right\}}{|s_{12}(j\Omega)|^2} \right]_{\Omega=o} \tag{84a}$$

since:

$$\left[\Omega^2\left(1 + 2\,\mathrm{Re}\left\{R_g Y_{in}(j\Omega)\right\}\right)\right]_{\Omega=o} = \left[\Omega^2\left(1 + 2\,\mathrm{Re}\left\{R_g \hat{Y}(j\Omega)\right\}\right)\right]_{\Omega=o} = 0 \quad (84b)$$

Let us transform equation (84a) to the x-domain. From Section II-A, $x = a\cos\theta$. Thus:

$$\Omega^2 = \tan^2\theta = \frac{a^2 - x^2}{x^2}$$

We shall adopt, as our equiripple form, that of equation (45). Let:

$$|s_{12}|^2 = \frac{1 - \kappa^2}{1 + \varepsilon^2 \cos^2(n\phi + \beta)} = \frac{1 - \kappa^2}{1 + \dfrac{\varepsilon^2 G_{n+1}(x^2)}{a^2 - x^2}} \quad (86)$$

where $0 < \kappa^2 << 1$.

From equation (69):

$$\left[\mathrm{Re}\ (R_g \hat{Y}(j\Omega))\right]_{\Omega=o} = R_g Y_L \quad (87)$$

Thus, from equation (84a):

$$R_g^2 Y_s^2 = \left[\frac{\Omega^2\ 4\,\mathrm{Re}\ (R_g \hat{Y}(j\Omega))}{|s_{12}(j\Omega)|^2}\right]_{\Omega=o} = 4 R_g Y_L \left\{\frac{\varepsilon^2 G_{n+1}(a^2)}{a^2(1 - \kappa^2)}\right\} \quad (88)$$

Therefore, using equation (79) in conjunction with (88):

$$Y_s = \frac{2\pi}{R_g\left\{\int_o^\infty \frac{1}{\Omega^2} \ln \frac{1}{|s_{11}(j\Omega)|^2}\, d\Omega\right\}}$$

and

$$R_L = \frac{R_g}{\pi^2}\left(\frac{\varepsilon^2 G_{n+1}(a^2)}{a^2(1 - \kappa^2)}\right)\left[\int_o^\infty \frac{1}{\Omega^2} \ln \frac{1}{|s_{11}(j\Omega)|^2}\, d\Omega\right]^2 \quad (89)$$

These relations pertain to the case wherein the stub shunts the generator. Instances may arise in which the desired orientation has the stub shunting the load, as is shown in Figure 16b. For this case, in view of reciprocity, we may first treat the case of Figure 16a. Proceeding in an analogous fashion from port 2, we may predetermine the pertinent parameters by the relations:

$$Y_s = \frac{2\pi}{R_L \left[\int_o^\infty \frac{1}{\Omega^2} \ln \frac{1}{|s_{22}(j\Omega)^2|} \, d\Omega \right]} \tag{90}$$

and

$$R_g = \frac{R_L}{\pi^2} \left(\frac{\varepsilon^2 G_{n+1}(a^2)}{a^2 (1 - \kappa^2)} \right) \left[\int_o^\infty \frac{1}{\Omega^2} \ln \frac{1}{|s_{22}(j\Omega)|^2} \, d\Omega \right]^2$$

Because of reciprocity, $|s_{12}(j\Omega)|^2 = |s_{21}(j\Omega)|^2$. Thus, if we now move the ideal generator E_g to port 1 to form the configuration of Figure 16b, the power transfer ratio will not change; the network of 16a, with the power measured across R_g, has a transducer power gain identical to that of 16b, wherein power is measured across R_L.

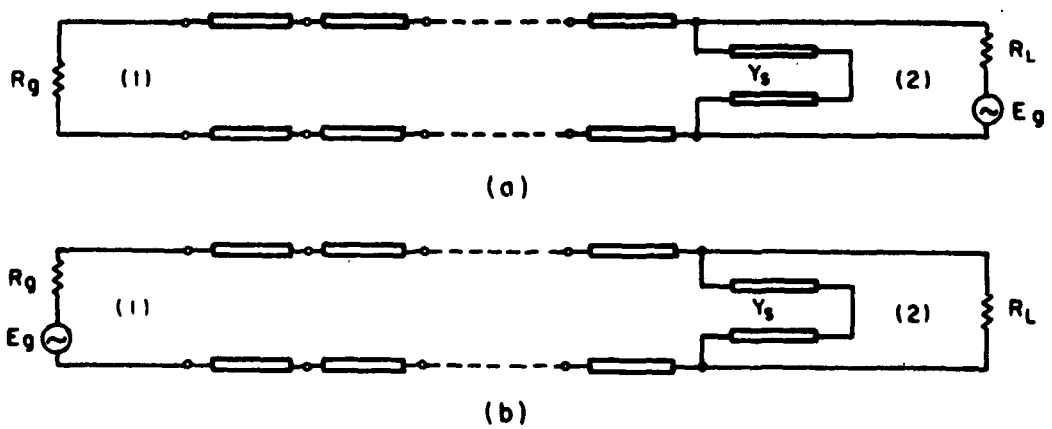

Figure 16 - Bandpass Filter with Stub Shunting Load

A necessary condition for the validity of equation (74) was the analyticity of the Fano integrand within the closed contour of Figure 15. This constraint, which permitted the derivation of equation (79), thus restricts the validity of equations (89) and (90). These relations will predict the desired parameters for the case of Figure 13 or Figure 16 only if, in the ensuing synthesis factorization, $s_{11}(\lambda)$ or $s_{22}(\lambda)$, respectively, is chosen such that it possesses no zeros in the right half plane.

The constant κ^2 was introduced in equation (86) to serve a dual purpose. For a given α, ε^2 and n, it may be used to vary the stub and load immittances. Secondly, in lowering the passband ripple peaks of $|s_{12}|^2$ to below unity, the parameter κ^2 prevents $j\Omega$-axis zeros of $s_{11}(\lambda)$ or $s_{22}(\lambda)$ and thus serves to prevent $j\Omega$-axis singularities of the Fano integrand; equation (74) demands that the integrand be analytic on the contour.

The lack of an explicit analytic evaluation of the Fano integral for the gain functions used here restricts this determination of parameters to a semi-graphical procedure. Its primary advantage lies in the fact that design curves may be tabulated for cases of interest.

To demonstrate how these design curves (e.g., Y_s v.s. κ^2 and R_L v.s. κ^2) would be computed, a relatively simple example will now be offered. Let the pertinent design parameters be specified as:

a) $n = 1$

b) $\alpha = 1.50$

c) $\varepsilon^2 = 0.01$

d) the shorted stub is to shunt the generator

As a reasonable designation for κ^2, let $\kappa^2 = 0.04$. Then:

$$|s_{12}|^2 = \frac{1 - 0.04}{1 + 0.01\cos^2(\phi + \beta)} = \frac{0.96}{1 + 0.01\,\frac{(1 + \cos(2\phi + \delta))}{2}} \qquad (91)$$

which, for $\alpha^2 = 2.25$, becomes:

$$|s_{12}|^2 = \frac{0.96}{1 + 0.005\left[1 + \frac{13.7082x^4 - 14.7082x^2 + 2.25}{2.25 - x^2}\right]} \qquad (92)$$

From equation (86):

$$\varepsilon^2 \cdot G_{n+1}(\alpha^2) = 0.01\,G_2(2.25) = 0.005\Big[2.25 - x^2 + 13.7082x^4 - 14.7082x^2 + 2.25\Big]_{x^2 = 2.25} = 0.19277 \qquad (93)$$

To evaluate the Fano integral, we initially formulate $\frac{1}{|s_{11}|^2} = \frac{1}{1 - |s_{12}|^2}$. The

integration is then separated into two phases. Noting that,

$$\Omega^2 = \tan^2\theta = \frac{a^2 - x^2}{x^2} = \frac{2.25 - x^2}{x^2}, \tag{94a}$$

we determine the lower passband edge as:

$$\Omega_o = \left[\frac{2.25 - x^2}{x^2}\right]^{\frac{1}{2}}_{x=1} = 1.118 \tag{94b}$$

Figure 17 depicts the stopband variation of the Fano integrand. By numerical integration, the integral was evaluated to be:

$$\int_o^{1.118} \frac{1}{\Omega^2} \ln \frac{1}{|s_{11}(j\Omega)|^2}\, d\Omega = 6.82 \tag{95}$$

The integration was divided into two parts because, in the passband, $1/|s_{11}|^2$ ripples about a mean value, call it $1/|s_o|^2$. Since the logarithm of a function varies less than the function itself:

$$\int_{1.118}^{\infty} \frac{1}{\Omega^2} \ln \frac{1}{|s_{11}(j\Omega)|^2}\, d\Omega \cong \int_{1.118}^{\infty} \frac{1}{\Omega^2} \ln \frac{1}{|s_o|^2}\, d\Omega = \int_{1.118}^{\infty} \frac{1}{\Omega^2} \ln\left(\frac{1.005}{0.045}\right) d\Omega = 2.78 \tag{96}$$

Thus, from equation (89) (for R_g = 1 ohm):

$$Y_s = \frac{6.2832}{9.60} = 0.654 \text{ mho}$$

$$R_L = \frac{(0.19277)(9.60)^2}{(9.8697)(2.25)(0.96)} = 0.833 \text{ ohm} \tag{97}$$

The actual synthesis, performed to verify these results, yielded the following:

From equations (92) and (94a):

$$|s_{11}(j\Omega)|^2 = \frac{0.11250\Omega^4 - 0.0417173\Omega^2 + 0.1927716}{2.27250\Omega^4 + 2.1182827\Omega^2 + 0.1927716} \tag{98}$$

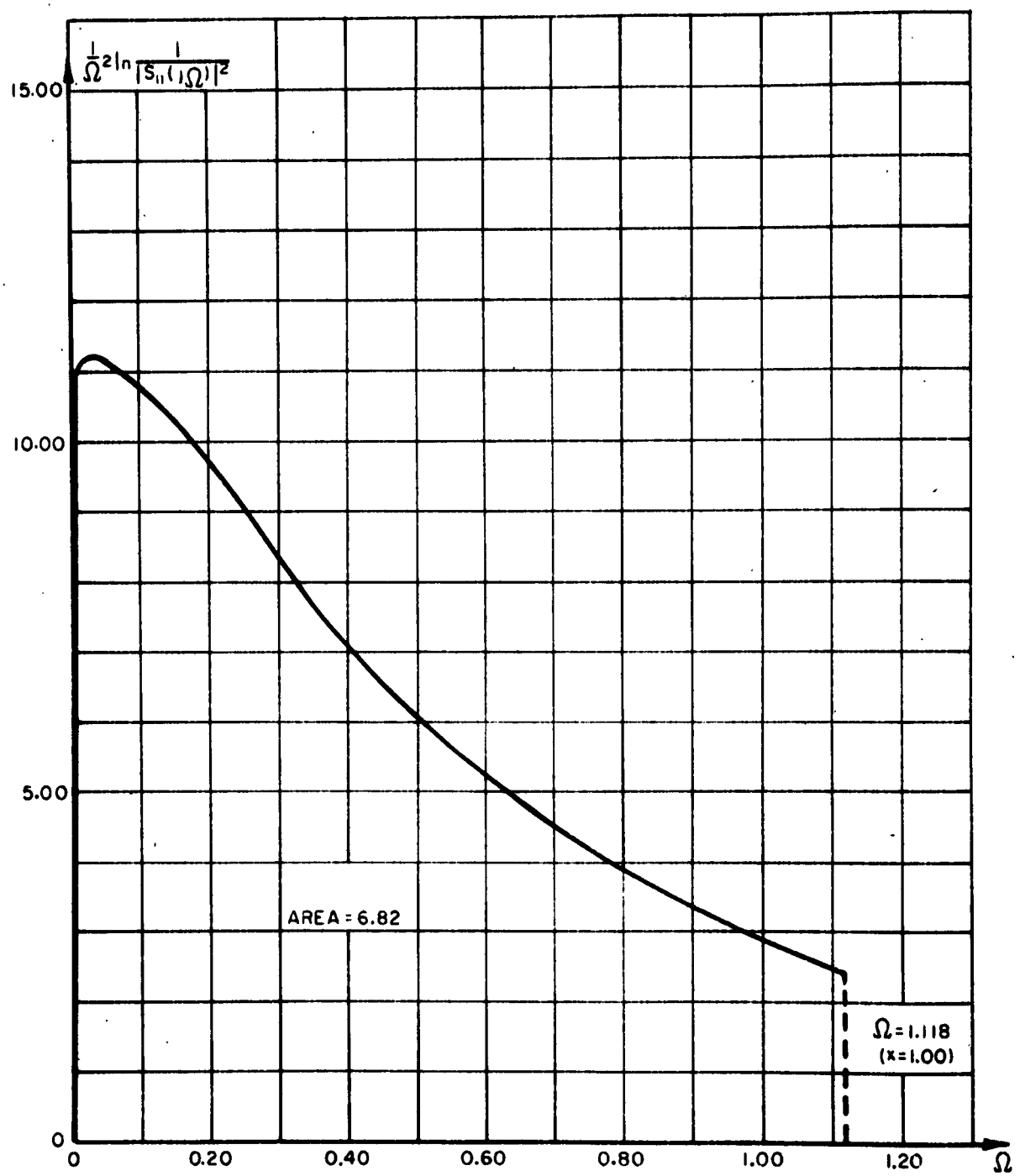

Fig. 17 Stopband Variation of Fano Integrand

Selecting left-hand plane zeros and noting that $s_{11}(0) = -1$:

$$s_{11}(\lambda) = \frac{-0.222498\lambda^2 - 0.333571\lambda - 0.291252}{\lambda^2 + 1.230708\lambda + 0.291252}, \tag{99}$$

for which the corresponding input admittance is:

$$Y_{in}(\lambda) = \frac{1.222498\lambda^2 + 1.564279\lambda + 0.582504}{0.777502\lambda^2 + 0.897137\lambda} \tag{100}$$

The resulting network is shown in Figure 18:

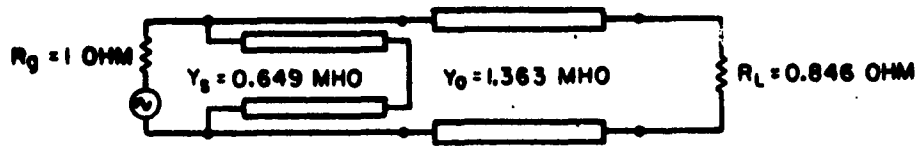

Figure 18 - Synthesized One-line Bandpass Filter

Note that in cases where a single design for a specific R_L is required, one must use a cut and try procedure in adjusting the shape parameters, until the integration yields the desired value.

A word of explanation is in order concerning the forms of equations (89) and (90). The Fano integral is specified in the Ω-domain whereas the other parameters are evaluated in the x-domain. In lieu of the fact that $|s_{12}|^2$ is initially specified as a function of x, one might question the merit of an x-to-Ω transformation for the integrand.

The motivation for this transformation lies in the fact that the integrand is composed of the product of two terms which respectively increase and decrease as one proceeds to the edge of the useful band. Thus, a stopband maximum occurs. If, as in the example, the stopband attenuation of $|s_{12}|^2$ is not relatively steep, this peak will occur in the immediate vicinity of the band edge (i.e., $\Omega = 0$). In this region:

$$\left|\frac{dx}{d\Omega}\right| = \frac{a\ \Omega}{(1 + \Omega^2)^{3/2}} \tag{101}$$

is correspondingly small. Hence, the stopband peak in the x-domain becomes accordingly greater and numerical integration is, thus, more difficult.

For equalizers comprised of greater numbers of lines, the stopband attenuation of $|s_{12}|^2$ becomes greater and the stopband peak shifts inward from the band edge. In these cases, choice of domain is relatively academic.

B. Partial Residue Technique for the Adjustment of the Load Immittance

In the preceding section, the use of the Fano integral necessitated a definite physical positioning of the shunt short-circuited stub relative to the generator or load; the stub had to be positioned distinct from the cascade if any useful information was to be extracted. This orientation, however, is not the most general.

The shunt s.c. stub introduces a d.c. zero of transmission. Since this zero occurs at the frequency at which the lines become transparent, it becomes evident that equation (17) is the form for any positioning of the shunt s.c. stub. The d.c. input immittance will be that of a short circuit, irrespective of the stub location. Moreover, since the parallel combination of an arbitrary number of these stubs (λ inductors) will still produce a single order d.c. zero of transmission (i.e., act as a single equivalent shunt inductance), equation (17) does not constrain the resulting equalizer to be of canonic form (i.e., minimum number of elements).

In the synthesis of these networks, this lack of uniqueness carries over to the input immittance expression. Thus, for a given input immittance function, the sequence of synthesis is not fixed. One may, for such a function, extract a total residue, a partial residue or a transmission line (i.e., delay the residue extraction to a later stage in the cascade synthesis). In each instance, the load termination which is ultimately realized will be different.

This fact affords one an added degree of freedom in load realization. If this change in load immittance can be predicted, the delayal of stub extraction will provide a stage-by-stage procedure whereby the load may be adjusted. That is, if this variation is monotonic, one may in certain cases converge upon the desired value of load immittance.

Consider Figure 19, wherein the alternatives at one's disposal are shown. In this development, capital letters will be used to designate unnormalized admittances; lower case letters will indicate normalized ones.

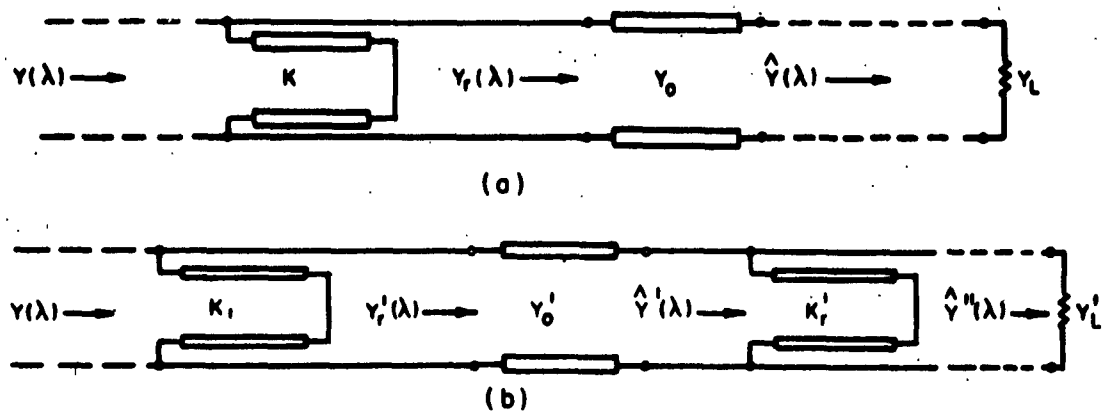

Figure 19 - Alternative Synthesis Procedures

In Figure 19:

$Y(\lambda)$ = input admittance physically realizable as a cascade of n-1 lossless equi-length transmission lines shunted by a lossless s.c. stub of commensurate length and terminated by a pure conductance.

K, K_1, K_r' = stub characteristic admittances.

Y_o, Y_o' = line characteristic admittances.

$Y_r(\lambda)$, $\hat{Y}(\lambda)$, $Y_r'(\lambda)$, $\hat{Y}'(\lambda)$, $\hat{Y}''(\lambda)$ = input admittances whose relations to $Y(\lambda)$ and the other parameters is indicated in the diagrams.

Y_L, Y_L' = terminating conductances

The object of the following derivation will be to obtain an expression for Y_L' in terms of Y_L and other quantities which can be readily determined at the $Y(\lambda)$ input stage.

To begin this development, we shall use the transmission line relation:

$$y_r(\lambda) = \frac{Y_r(\lambda)}{Y_o} = \frac{\hat{Y}(\lambda) + \lambda Y_o}{Y_o + \lambda \hat{Y}(\lambda)} \qquad (102a)$$

or rearranging,

$$\hat{y}(\lambda) = \frac{\hat{Y}(\lambda)}{Y_o} = \frac{\lambda Y_o - Y_r(\lambda)}{\lambda Y_r(\lambda) - Y_o}$$

For n-1 lines and the shunt s.c. stub:

$$Y(\lambda) = \frac{\sum_{k=o}^{n} a_n \lambda^n}{\sum_{p=1}^{n} b_p \lambda^p} = \frac{K}{\lambda} + \frac{\sum_{k=1}^{n} c_k \lambda^{k-1}}{\sum_{p=1}^{n} b_p \lambda^{p-1}} = \frac{K}{\lambda} + Y_r(\lambda)$$

where

$$K = \frac{a_o}{b_1} \tag{103}$$

Let us now designate

$$K = K_1 + K_r \quad \text{where} \quad 0 \leq K_r \leq K \tag{104}$$

Then:

$$Y(\lambda) = \frac{K_1}{\lambda} + \left\{ \frac{K_r}{\lambda} + \frac{\sum_{k=1}^{n} c_k \lambda^{k-1}}{\sum_{p=1}^{n} b_p \lambda^{p-1}} \right\} = \frac{K_1}{\lambda} + \frac{\sum_{k=o}^{n} d_k \lambda^k}{\sum_{p=1}^{n} b_p \lambda^p} = \frac{K_1}{\lambda} + Y_r'(\lambda) \tag{105a}$$

where:

$$\sum_{p=1}^{n} K_r b_p \lambda^{p-1} + \sum_{k=1}^{n} c_k \lambda^k = \sum_{k=o}^{n} d_k \lambda^k \tag{105b}$$

From equation (105a):

$$Y_o' = Y_r'(1) = \frac{\sum_{k=o}^{n} d_k}{\sum_{p=1}^{n} b_p} = \frac{D}{B} \tag{106a}$$

where:

$$D = \sum_{k=o}^{n} d_k \quad \text{and} \quad B = \sum_{p=1}^{n} b_p \tag{106b}$$

That is, from equation (104) and the definition of $Y(\lambda)$, $Y_r'(\lambda)$ is similarly realizable as a cascade of n-1 lines, shunted by a s.c. stub and terminated by a conductance. Thus, from (102b):

$$\hat{y}'(\lambda) = \frac{\hat{Y}'(\lambda)}{Y'_o} = \frac{\lambda \frac{D}{B} - \frac{\Sigma\, d_k \lambda^k}{\Sigma\, b_p \lambda^p}}{\frac{\lambda \Sigma\, d_k \lambda^k}{\Sigma\, b_p \lambda^p} - \frac{D}{B}} = \frac{D\lambda \Sigma\, b_p \lambda^p - B \Sigma\, d_k \lambda^k}{B\lambda \Sigma\, d_k \lambda^k - D \Sigma\, b_p \lambda^p} =$$

$$= \frac{D b_n \lambda^{n+1} + (D b_{n-1} - B d_n)\lambda^n + \cdots + (D b_1 - B d_2)\lambda^2 + (-B d_1)\lambda + (-B d_o)}{B d_n \lambda^{n+1} + (B d_{n-1} - D b_n)\lambda^n + \cdots + (B d_1 - D b_2)\lambda^2 + (B d_o - D b_1)\lambda} \tag{107}$$

A necessary consequence of the realizability of $Y'_r(\lambda)$ is the fact that:

$$Y'_r(1) + Y'_r(-1) = 0 \tag{108}$$

Noting equation (102b), this, in turn, demands that both numerator and denominator of equation (107) be reducible by the factor $(1 - \lambda^2)$. Let the reduced form of $\hat{y}'(\lambda)$ be represented as:

$$\hat{y}'(\lambda) = \frac{e_{n-1}\lambda^{n-1} + \cdots + e_2\lambda^2 + e_1\lambda + e_o}{f_{n-1}\lambda^{n-1} + \cdots + f_2\lambda^2 + f_1\lambda} \tag{109}$$

Let now both numerator and denominator of equation (109) be multiplied by the factor $(1-\lambda^2)$ and the resulting coefficients be associated with those of (107). The ensuing pertinent relations are:

$$\begin{aligned} e_o &= -B d_o & f_1 &= B d_o - D b_1 \\ e_1 &= -B d_1 & f_2 &= B d_1 - D b_2 \\ e_2 - e_o &= (D b_1 - B d_2) \end{aligned} \tag{110}$$

or

$$e_2 = D b_1 - B d_2 - B d_o$$

Thus:

$$\hat{y}'(\lambda) = \frac{e_{n-1}\lambda^{n-1} + \cdots + e_2\lambda^2 + e_1\lambda + e_o}{f_{n-1}\lambda^{n-1} + \cdots + f_2\lambda^2 + f_1\lambda} = \frac{k'_r}{\lambda} + \frac{g_{n-2}\lambda^{n-2} + \cdots + g_1\lambda + g_o}{f_{n-1}\lambda^{n-2} + \cdots + f_2\lambda + f_1}$$

$$= \frac{k'_r}{\lambda} + \hat{y}''(\lambda) \tag{111}$$

From (110) and (111):

$$k_r' = \left[\lambda \hat{y}'(\lambda)\right]_{\lambda=0} = \frac{e_o}{f_1} = \frac{-B d_o}{B d_o - D b_1} \tag{112a}$$

Also:

$$g_o = e_1 - f_2 k_r' = -B d_1 - (B d_1 - D b_2)\left(\frac{-B d_o}{B d_o - D b_1}\right) \tag{112b}$$

and

$$y_L' = \hat{y}''(0) = \frac{g_o}{f_1} = \frac{B D(b_1 d_1 - d_o b_2)}{(B d_o - D b_1)^2} \tag{112c}$$

Unnormalizing:

$$K_r' = Y_o' k_r' = \frac{D}{B} k_r' = \frac{-D d_o}{B d_o - D b_1} \tag{113}$$

and

$$Y_L' = Y_o' y_L' = \frac{D^2(b_1 d_1 - d_o b_2)}{(B d_o - D b_1)^2}$$

From equation (105b), at $\lambda = 1$:

$$\Sigma K_r b_p + \Sigma c_k = \Sigma d_k$$

or

$$K_r B + C = D \tag{114a}$$

Also:

$$d_o = K_r b_1 \tag{114b}$$

$$d_1 = c_1 + K_r b_2$$

Substituting equations (114) into (113):

$$K_r' = K_r\left(1 + K_r \frac{B}{C}\right)$$

and

$$Y_L' = \frac{c_1}{b_1}\left(1 + K_r \frac{B}{C}\right)^2 \tag{115}$$

From equation (103):

$$Y_o = Y_r(1) = \frac{\Sigma c_k}{\Sigma b_p} = \frac{C}{B}$$

and

$$Y_L = Y_r(0) = \frac{c_1}{b_1} \tag{116}$$

Thus:

$$K_r' = K_r(1 + K_r Z_o)$$

and

$$Y_L' = Y_L(1 + K_r Z_o)^2. \tag{117}$$

Also:

$$Y_o' = Y_o(1 + K_r Z_o)$$

Since K_r and Z_o, representing immittances, are inherently positive, equation (117) indicates that by delaying stub extraction to the next stage one necessarily increases the value of load conductance ultimately realized. Note that all pertinent parameters can be determined at the $Y(\lambda)$ input stage. At a given stage, any load conductance between the bounds Y_L and $Y_L(1 + K Z_o)^2$ may be realized by the proper specification of K_r.

These relations may then be used in a stage-by-stage load adjustment procedure. For any given synthesis, the minimum value of load admittance is realized by immediate total residue extraction; the maximum value is obtained by delaying stub extraction until last. The inability to predict the characteristic impedance of the succeeding line, however, prevents the predictions of the overall bounds on the load.

In the preceding derivation, use was made of the coefficients e_1, e_o, f_2, and f_1 of equation (111). For the case where $n \geq 3$, these coefficients appear in the form shown, and the prior general derivation applies. For the special case of $n = 2$ (i.e., one line and the shunt s.c. stub), f_2 does not appear, and additional algebraic manipulation is required to obtain the desired forms.

For $n = 2$:

$$Y_r'(\lambda) = \frac{d_2\lambda^2 + d_1\lambda + d_o}{b_2\lambda^2 + b_1\lambda} \tag{118}$$

for which:

$$\hat{y}'(\lambda) = \frac{Db_2\lambda^3 + (Db_1 - Bd_2)\lambda^2 + (-Bd_1)\lambda + (-Bd_o)}{Bd_2\lambda^3 + (Bd_1 - Db_2)\lambda^2 + (Bd_o - Db_1)\lambda} \tag{119}$$

In reduced form:

$$\hat{y}'(\lambda) = \frac{e_1\lambda + e_o}{f_1\lambda} \tag{120}$$

Multiplying numerator and denominator of (120) by $(1 - \lambda^2)$ and associating coefficients:

$$e_o = -B d_o = -(D b_1 - B d_2) \qquad f_1 = (B d_o - D b_1) = -B d_2$$
$$e_1 = -B d_1 = -D b_2 \qquad B d_1 - D b_2 = 0 \tag{121}$$

Thus:

$$k_r' = \frac{-B d_o}{B d_o - D b_1} \quad \text{as before.}$$

However:

$$y_L' = \frac{e_1}{f_1} = \frac{e_1 f_1}{f_1^2} = \frac{-B d_1 (B d_o - D b_1)}{(B d_o - D b_1)^2}$$

or

$$Y_L' = \frac{D}{B} y_L' = \frac{-D(B d_1 d_o - D b_1 d_1)}{(B d_o - D b_1)^2} \tag{122}$$

From equations (121), $B d_1 = D b_2$. Therefore:

$$Y_L' = \frac{D^2 (b_1 d_1 - d_o b_2)}{(B d_o - D b_1)^2}$$

which is the desired form, that of equation (113).

An elementary example will now be presented to demonstrate the technique. Let the network of Figure 20 be given.

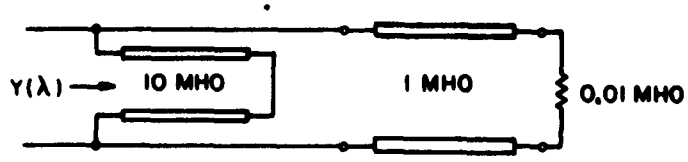

Figure 20 - Given Network

From Figure 20:

$$Y(\lambda) = \frac{10}{\lambda} + \frac{0.01 + \lambda}{1 + 0.01\lambda} \tag{123}$$

We desire now to obtain a network which will have the same input admittance but a 1-mho termination. Consider:

$$Y'_L = Y_L(1 + K_r Z_o)^2 \tag{117}$$

For the given example:

$$Y_L = 0.01 \text{ mho}$$

$$Z_o = 1 \text{ ohm}$$

$$K = 10 \text{ mho} .$$

Substituting into (117) to determine the required K_r, we find:

$$1 = 0.01\ (1 + K_r \cdot 1)^2$$

or

$$K_r = 9.00 \tag{124}$$

Since $0 \leq 9 \leq 10$, the desired network is physically realizable. From (117), the parameters of the equivalent network may be predicted to be:

$$\begin{aligned} K_1 &= K - K_r = 1 \text{ mho} \\ Y'_o &= 1 \cdot 10 = 10 \text{ mho} \\ K'_r &= 9 \cdot 10 = 90 \text{ mho} \\ Y'_L &= (0.01)(100) = 1 \text{ mho} . \end{aligned} \tag{125}$$

In the actual synthesis:

$$Y'_r(\lambda) = \frac{9}{\lambda} + \frac{0.01 + \lambda}{1 + 0.01\lambda} = \frac{\lambda^2 + 0.10\lambda + 9}{0.01\lambda^2 + \lambda} \tag{126}$$

for which:

$$Y'_o = Y'_r(1) = \frac{10.10}{1.01} = 10 \text{ mho}$$

Thus:

$$\hat{y}'(\lambda) = \frac{\lambda Y'_o - Y'_r(\lambda)}{\lambda Y'_r(\lambda) - Y'_o} = \frac{0.10\lambda^3 + 9\lambda^2 - 0.10\lambda - 9}{\lambda^3 - \lambda} =$$

$$= \frac{0.10\lambda + 9}{\lambda} = \frac{9}{\lambda} + 0.10 = \frac{k'_r}{\lambda} + y'_L \tag{127}$$

Unnormalizing:

$$K_r' = Y_o' k_r' = (10)(9) = 90 \text{ mho}$$

$$Y_L' = Y_o' y_L' = (10)(0.10) = 1 \text{ mho}$$

The resulting equivalent network is:

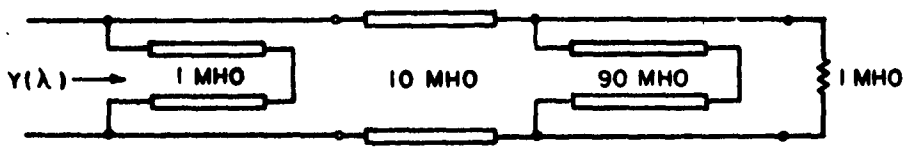

Figure 21 - Equivalent Network

This partial residue technique has been offered in conjunction with the material of Section III-A since, if one is willing to tolerate the disadvantages of the manipulation (i.e., non-canonic equalizers with unpredictable stub positioning), it appears possible to greatly expedite certain filter designs by avoiding the necessity of numerical integration.

Let us suppose that, in the broadband matching of a specified resistance to a given generator, one desires substantial stopband attenuation. This requirement will necessitate an equalizer comprised of an appreciable number of cascaded lines. Hence, the equiripple specification of $|s_{12}|^2$ will involve high-order functions; numerical integration of the Fano integrand will become correspondingly tedious.

Note, however, that the constraint of rapid stopband attenuation will cause a considerable portion of the area of the plotted Fano integrand to fall within the passband. Thus, if we use the passband approximation of (96) and then approximate the total integral by this value, we can obtain a reasonable lower bound on the value of the total integral.

A lower bound on the integral yields, from (89), a lower bound on the load. Therefore, let us determine a κ^2 such that the lower bound on the load equals the specified load resistance. We can then be assured that, in the ensuing synthesis, the load resistance obtained by immediate stub extraction will prove $\geq$ the desired load.

Noting (117), however, the load resistance may then be decreased by partial residue manipulation. The appreciable number of lines, necessitated by the desired rapid stopband attenuation, provides a considerable number of stages for this manipulation.

There are two obvious shortcomings to this proposed procedure. From (89), the load is seen to vary as the square of the integral. Thus, the above-mentioned bound on the load will be relatively low. Secondly, the inability to predict the overall bounds of the partial residue adjustment prevents an absolute assurance of desired load realization. Thus, this procedure affords one no positive guarantee of success. Rather, it has been offered as a technique which, when properly used, has a good probability of success and, in view of the work it curtails, might therefore be of value.

IV. TUNNEL DIODE AMPLIFIER DESIGN

The small-signal network equivalent circuit of the tunnel diode is shown in Figure 22. This model, which is valid up to microwave frequencies, is composed of lumped parameter elements. Thus any attempt to design a distributed parameter amplifier encounters an initial difficulty; the network description of such a transmission line-lumped reactance mixture would involve transcendental relations.

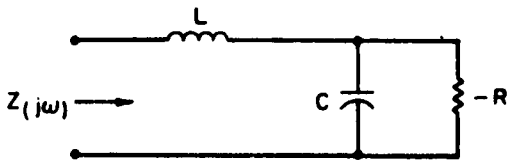

Figure 22 - Equivalent Circuit of a Tunnel Diode (neglecting junction spreading resistance)

To avoid this difficulty, we shall adopt the distributed parameter approximation of the diode, developed by L.I. Smilen.[9] This model is shown in Figure 23.

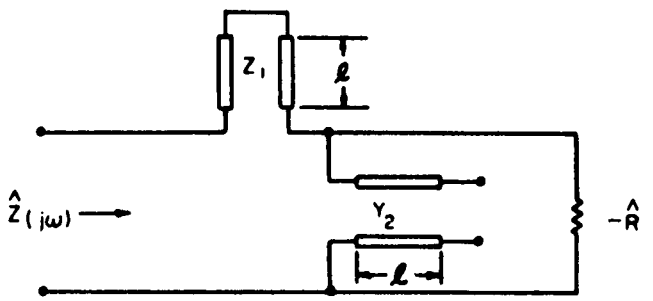

Figure 23 - Approximate Model for the Tunnel Diode (neglecting junction spreading resistance)

Thus, the p-plane reactances of Figure 22 are approximated by λ-plane reactances in Figure 23. This model is to approximate the diode behavior over a frequency band. From Figures 22 and 23:*

$$Z(j\omega) = \frac{-R}{1 + \omega^2 R^2 C^2} + j\omega\left(L - \frac{R^2 C}{1 + \omega^2 R^2 C^2}\right) \tag{128a}$$

$$\hat{Z}(j\omega) = \frac{-\hat{R}}{1 + \hat{R}^2 Y_2^2 \tan^2 \frac{\pi f}{2 f_o}} + j \tan \frac{\pi f}{2 f_o}\left(Z_1 - \frac{\hat{R}^2 Y_2}{1 + \hat{R}^2 Y_2^2 \tan^2 \frac{\pi f}{2 f_o}}\right) \tag{128b}$$

*Equations (128) and (129) are taken directly from Smilen.[9]

where f_o represents the quarter-wave frequency.

The imposition of the following constraints:

$$\text{a)} \quad \text{Real } Z(0) = \text{Real } \hat{Z}(0)$$

At a given frequency $f_c (0 < f_c < f_o)$:

$$\text{b)} \quad \text{Real } Z(j f_c) = \text{Real } \hat{Z}(j f_c) \tag{129a}$$

$$\text{c)} \quad \text{Imag } Z(j f_c) = \text{Imag } \hat{Z}(j f_c)$$

necessitates that:

$$\text{a)} \quad \hat{R} = R$$

$$\text{b)} \quad Y_2 = \omega_c C \cot \frac{\pi f_c}{2 f_o} \tag{129b}$$

$$\text{c)} \quad Z_1 = \omega_c L \cot \frac{\pi f_c}{2 f_o}$$

Using this approximation, we wish to design a tunnel diode reflection amplifier. This type of configuration is shown in Figure 24:

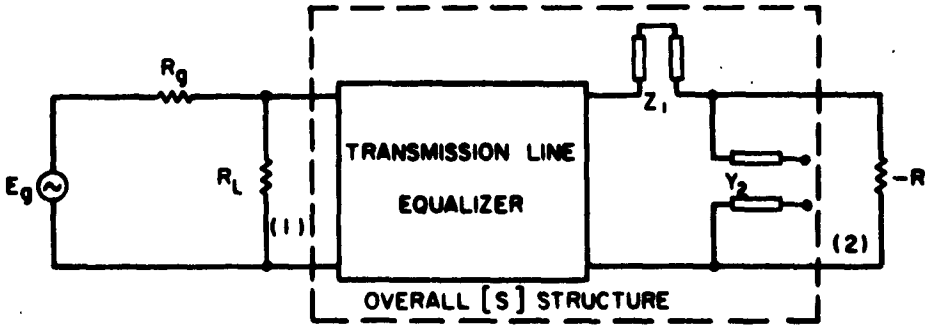

Figure 24 - Tunnel Diode Reflection Amplifier, with Diode Approximated by Transmission Line Model

As is shown in the diagram, the stubs may be incorporated with the equalizer to form a composite structure with resistive termination. This procedure is that developed by Smilen and Youla.[10] In accord with their derivation, the overall scattering matrix [S] will be normalized at port 1 to the parallel combination of R_g and R_L and at port 2 to +R. Then, for port 2 terminated in -R as shown, the transducer power gain becomes:

$$G(\omega^2) = \frac{P_L}{P_m} = \frac{1}{4} \sin^2 2\psi \left| 1 + \frac{1}{s_{11}(j\omega)} \right|^2 \tag{130}$$

where P_L = power to the load

P_m = maximum available power from the generator

$$\sin^2\psi = \frac{R_L}{R_L + R_g}$$

(The derivation of (130), which appears in reference 10, is presented in Appendix C.)

The composite [S] structure of Figure 24 is of the class treated in Section II-B, that is, a cascade of lossless equilength transmission lines augmented by a stub configuration producing a second order zero of transmission at the quarter-wave frequency. (We constrain the stubs to be lossless and of length commensurate with the lines). Thus, we may specify $|s_{12}|^2$, corresponding to the structure of Figure 24, in equiripple fashion; to achieve appreciable stopband fall-off, let the equalizer be prescribed as composed of four cascaded lines. Then:

$$|s_{12}|^2 = \frac{1 - b^2}{1 + \varepsilon^2 \cos^2(4\phi + 2\beta)} = \frac{1 - b^2}{1 + \frac{\varepsilon^2}{2} + \frac{\varepsilon^2}{2}\cos(8\phi + 2\delta)} \qquad (131)$$

where $x = \cos\phi = \alpha \sin\theta$.

The $|s_{12}|^2$ so defined pertains to the network wherein the diode approximate model is used; we anticipate no substantial change in behavior over the frequency band of interest when we revert back to lumped reactances. Thus, by so specifying $|s_{12}|^2$, we approximate the transducer power gain as an equiripple shape. This can be seen by noting that for the lossless reciprocal structure:

$$|s_{11}|^2 = 1 - |s_{12}|^2 = |s_{22}|^2 \qquad (132a)$$

and in the passband (i.e., region of high gain), $\left|\frac{1}{s_{11}}\right| >> 1$ so that:

$$G(\omega^2) \cong \frac{\sin^2 2\psi}{4}\left|\frac{1}{s_{11}}\right|^2 \qquad (132b)$$

Having the form of $|s_{12}|^2$, we must now prescribe the constants α, b^2, and ε^2. The first of these, α, is fixed by the desired bandwidth and certain practical considerations. If, as an illustration, we seek amplification over a frequency band extending from d.c. to 1 kmc, then at $f = f_1 = 10^9$ cps, $x = 1$. Moreover, suppose further, we do not wish the transmission lines which will constitute the equalizer, to be of length less than one inch. These constraints essentially fix the upper

bound of α at 2.00. For $\alpha = 2.00$:

$$1 = 2 \sin \theta_1 \quad \text{and} \quad 2 = 2 \sin \theta_o$$

or

$$\theta_1 = \frac{\pi}{6} \quad \text{and} \quad \theta_o = \frac{\pi}{2}$$

(where the subscript 1 denotes passband edge parameters and the subscript o denotes $\frac{1}{4}$-wave frequency parameters).

Consequently:

$$\theta_1 = \beta_1 \ell = \frac{2\pi f_1 \ell}{v} = \frac{\pi}{6}$$

$$\theta_o = \beta_o \ell = \frac{2\pi f_o \ell}{v} = \frac{\pi}{2} .$$

or $f_o = 3 f_1 = 3$ kmc, and since $v = 3 \times 10^{10}$ cm/sec., $\ell = 2.50$ cm.

Another factor influencing the choice of α arises from the approximate model being used for the diode. This model is to approximate the diode behavior over a frequency band. As is indicated in reference 9, this approximation is enhanced by decreasing the ratio f_c/f_o, which for our design will become f_1/f_o (i.e., we set $f_c = f_1 = 10^9$ cps); hence, the approximation is bettered by increasing α.

A compromise must therefore be made to accommodate these considerations. A reasonable value, and that which will be adopted, is $\alpha = 2.00$.

The parameters b^2 and ϵ^2 must be selected in such a manner as to make the diode approximate model applicable. We are designing a network which will initially be realized in the form of Figure 24; then, using equations (129b) in inverted form, we will substitute the diode lumped reactances for the stubs. If this procedure is to be successful, the value of the stub immittances which result in the synthesis, must transform into lumped reactances having values consistent with those encountered in tunnel diodes. Essentially, then, we must be able to prescribe proper values for the stub characteristic immittances. These values must be transformable to tunnel diode-type lumped reactances; the resultant amplifier must in turn realise a reasonable transducer power gain.

The second order zero of transmission at the quarter-wave frequency, created by the stub configuration, provides the means by which the stub characteristic immittances may be predicted. Two integral restrictions[11] pertain. We shall constrain $s_{22}(\lambda)$ to have no zeros in $\mathrm{Re}(\lambda) \geq 0$ such that these restrictions become

equalities. Then, from Figure 23 with $E_g = 0$ and -R disconnected:

$$\int_0^\infty \ln \frac{1}{|s_{22}(j\Omega)|^2}\, d\Omega = \frac{2\pi}{RY_2}$$

and (133)

$$\int_0^\infty \Omega^2 \ln \frac{1}{|s_{22}(j\Omega)|^2}\, d\Omega = \frac{2\pi}{3}\left[\frac{3R^2Y_2 - Z_1}{Z_1 Y_2^3 R^3}\right]$$

One notes from equations (131) and (132a) that the parameters b^2 and ε^2 influence the integrands of equations (133) and therefore influence the values of the stub immittances. ($b^2 > 0$ is prescribed to prevent both gain oscillations and $j\Omega$-axis logarithmic singularities of the integrands.)

Using the relations of (133), suitable stub immittances may be determined through a trial and error procedure. A reasonable gain and tolerance is initially chosen (essentially by guesswork guided by experience). Then, using equations (131) and (132a) in conjunction with (132b), the constants b^2 and ε^2 are evaluated. Equation (131) is thereby completely specified. (Note that, in view of the approximated gain and the approximate diode model, the specified tolerance should be less than the desired.)

The integral relations may then be numerically evaluated and the corresponding stub immittances determined. If the associated lumped elements prove of the magnitude encountered in tunnel diodes, one may proceed with the synthesis; if not, one must select another gain-tolerance combination and repeat the procedure.

The angle ψ in equation (132b) may be arbitrarily prescribed beforehand; any subsequent alteration required to accommodate a particular load or generator impedance will alter only the gain level and not the integral relations.

For the design in question, with $\psi = 45^\circ$, a suitable specification proved to be a gain of 19.0 db $\pm$ 1.0 db, over the desired 1 kmc band. From equation (132b):

$$G_{max} = 100.00 = \frac{1}{4b^2}$$

and

$$G_{min} = 63.0957 = \frac{1}{4}\left(\frac{1+\varepsilon^2}{b^2+\varepsilon^2}\right)$$

or (134)

$$b^2 = 0.002500$$

$$\varepsilon^2 = 0.001468$$

Substituting these values into equation (131) and applying (132a), we obtain:

$$|s_{22}|^2 = \frac{0.003234 + 0.000734\cos(8\phi + 2\delta)}{1.000734 + 0.000734\cos(8\phi + 2\delta)} \qquad (135a)$$

where, for $a = 2.00$:

$$\cos(8\phi + 2\delta) = \frac{1}{(x^2 - 4)^2}\left[(128x^8 - 256x^6 + 160x^4 - 32x^2 + 1)(97x^4 - 104x^2 + 16) + \right. \qquad (135b)$$

$$\left. + 13.85641(7x^2 - 4)(128x^{10} - 320x^8 + 272x^6 - 88x^4 + 8x^2)\right]$$

The integral relations were then evaluated in the x-domain. Since $x = a \sin\theta$, $\Omega^2 = \tan^2\theta = \frac{x^2}{a^2 - x^2}$. Equations (133) thus become:

$$a^2 \int_0^a (a^2 - x^2)^{-\frac{3}{2}} \ln \frac{1}{|s_{22}|^2}\, dx = \frac{2\pi}{RY_2}$$

and (136)

$$a^2 \int_0^a x^2(a^2 - x^2)^{-\frac{5}{2}} \ln \frac{1}{|s_{22}|^2}\, dx = \frac{2\pi}{3}\left[\frac{3R^2Y_2 - Z_1}{Z_1 Y_2^3 R^3}\right]$$

Figures25 and 26 show the plots of the respective integrands. The dashed curve in Figure 25 indicates the behavior of the integrand wherein the passband behavior of $|s_{22}|^2$ is approximated by its mean value (i.e., $\frac{0.003234}{1.000734}$). As the graph indicates, this approximation is quite good; in using it, one can avoid a considerable amount of calculation.

For R = 30 ohm, the stub immittances were subsequently evaluated as:

$$Y_2 = 0.05477$$

$$Z_1 = 69.8011 \qquad (137a)$$

Using equations (129b) (for $f_c = 10^9$ cps), the corresponding lumped elements were determined to be:

$$C = 5.035 \text{ pf}$$

$$L = 6.417 \text{ nh} \qquad (137b)$$

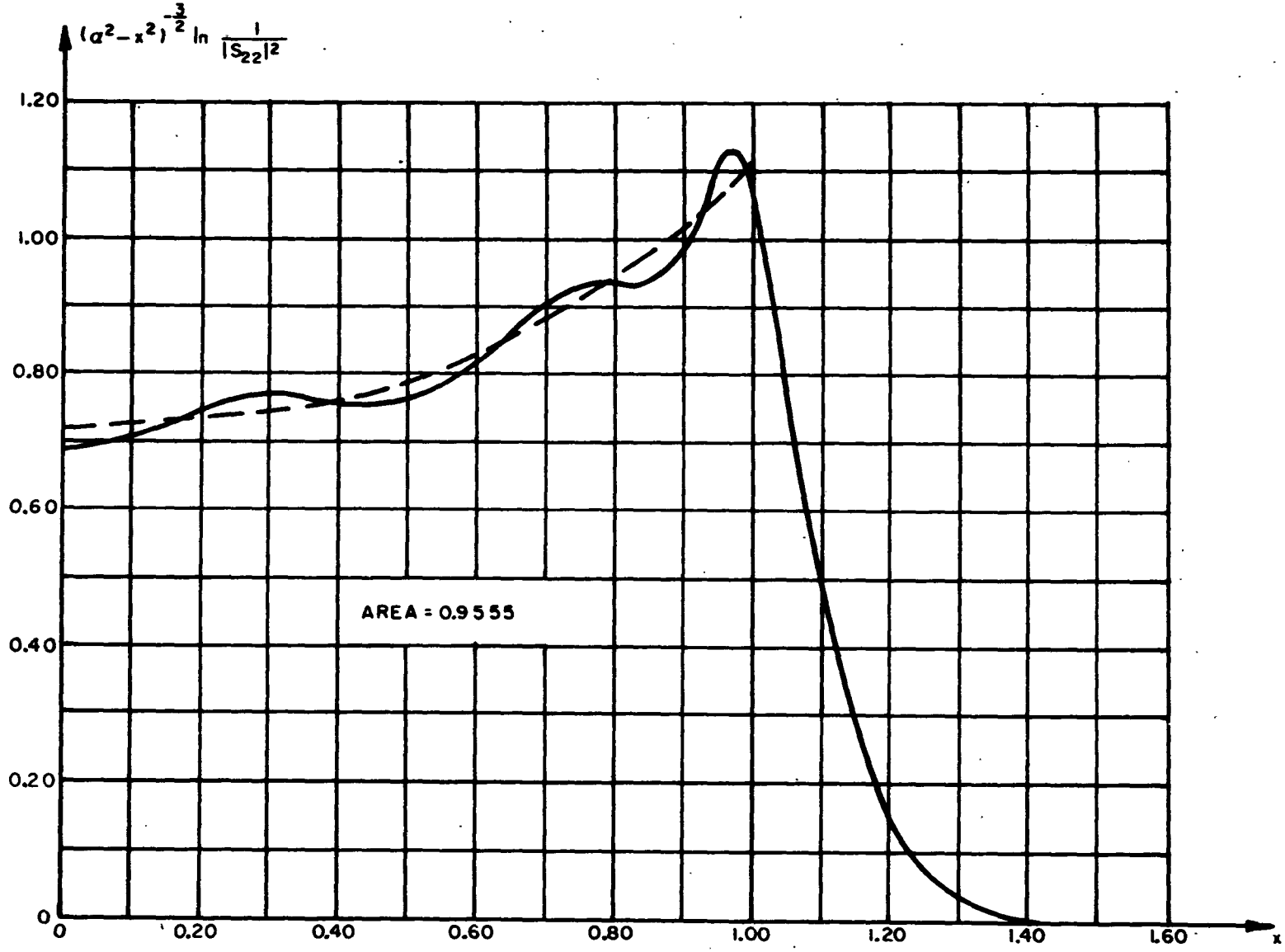

Fig. 25 $(a^2 - x^2)^{-3/2} \ln \frac{1}{|S_{22}|^2}$ vs. x

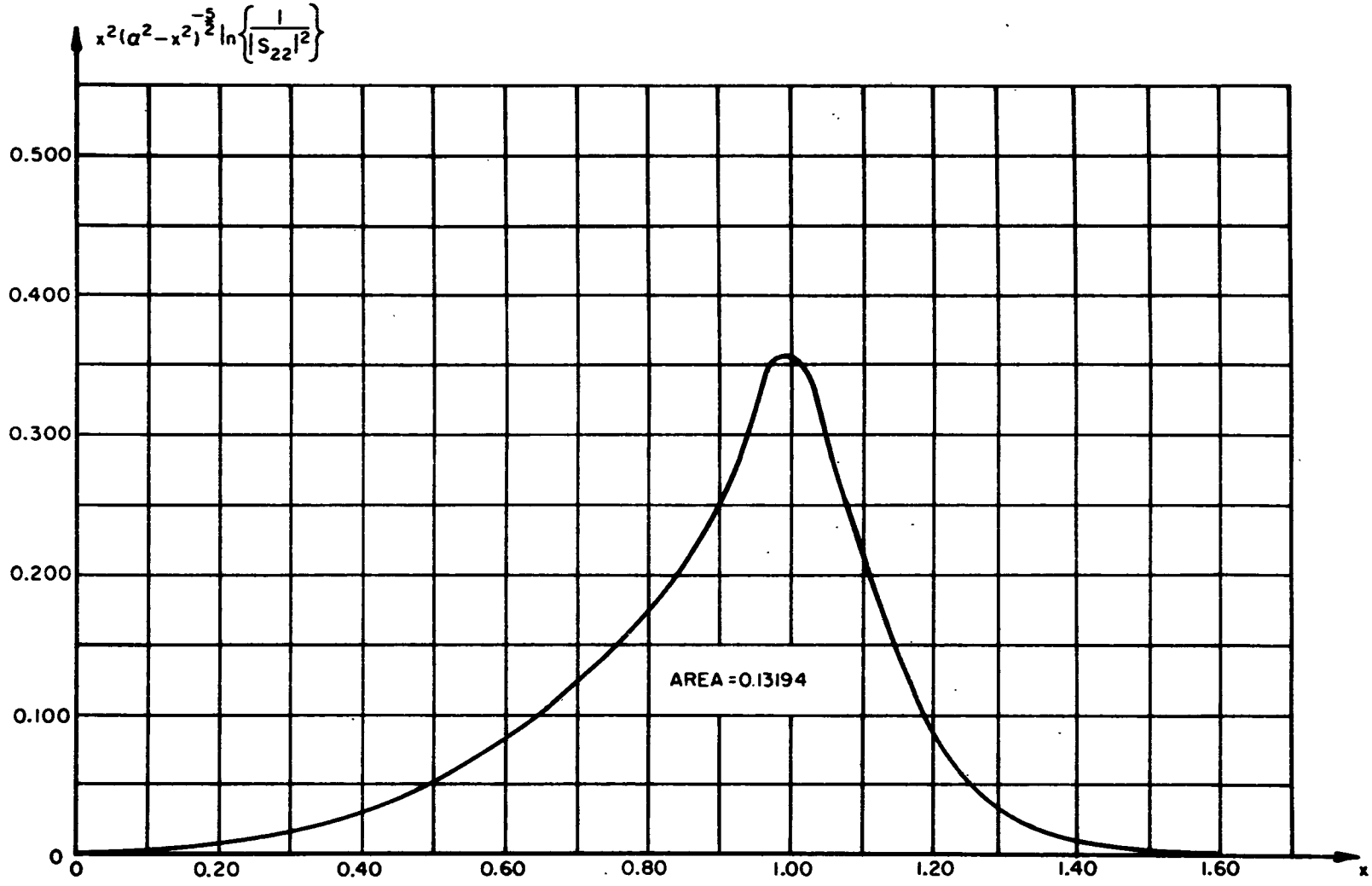

Fig. 26 $x^2 (a^2 - x^2)^{-5/2} \ln \frac{1}{|S_{22}|^2}$ vs. x

MRI-18862

The resistance and capacitance thus determined have magnitudes typical of tunnel diodes; the inductance, however, is somewhat high. Thus, it will prove necessary to add series inductance. This is not too stringent a condition, since in ordinary tunnel diodes the inductance depends on the lengths of the leads.

Since the reactances prove acceptable, we may proceed with the synthesis. From equation (135):

$$|s_{22}|^2 = \frac{18.226206\,x^{12} - 55.987201\,x^{10} + 64.820134\,x^8 - 34.829271\,x^6 + 8.545831\,x^4 - 0.8029056\,x^2 + 0.063488}{18.226206\,x^{12} - 55.987201\,x^{10} + 64.820134\,x^8 - 34.829271\,x^6 + 9.543331\,x^4 - 8.7829056\,x^2 + 16.023488} \tag{138a}$$

For $\alpha = 2.00$, $x^2 = \frac{4\Omega^2}{\Omega^2 + 1}$. Therefore

$$|s_{22}(j\Omega)|^2 = \frac{31822.1284576\Omega^{12} - 30298.949248\Omega^{10} + 10695.970144\Omega^8 - 1712.986624\Omega^6 + 121.627504\Omega^4 - 2.8306944\Omega^2 + 0.063488}{31822.1284576\Omega^{12} - 30298.949248\Omega^{10} + 10711.930144\Omega^8 - 1649.146624\Omega^6 + 217.387504\Omega^4 + 61.0093056\Omega^2 + 16.023488} \tag{138b}$$

Equation (138b) was factored by a computer. Selecting left-hand plane zeros of $s_{22}(\lambda)$ and noting the capacitive nature of port 2 at infinity (i.e., $s_{22}(\infty) = -1$), the resultant form became:

$$s_{22}(\lambda) = \frac{-\lambda^6 - 0.407052\lambda^5 - 0.558913\lambda^4 - 0.157585\lambda^3 - 0.076012\lambda^2 - 0.011215\lambda - 0.001412}{\lambda^6 + 1.614896\lambda^5 + 1.780010\lambda^4 + 1.239671\lambda^3 + 0.586027\lambda^2 + 0.167981\lambda + 0.022439} \tag{139}$$

Using equation (139), the network of Figure 27 was synthesized.

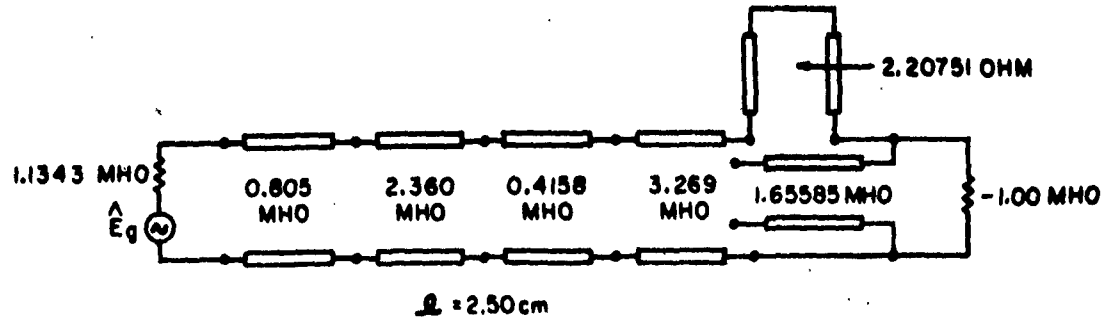

Figure 27 - Synthesized 4-Line Amplifier with Transmission Line Diode Model

If the impedance level of Figure 27 is raised to R = 30 ohm, the stub immittances will become:

$$Y_2 = \frac{1.65585}{30} = 0.055195 \text{ mho}$$

$$Z_1 = (2.20751)(30) = 66.2253 \text{ ohm}$$

From (129b):

$$C = 5.074 \text{ pf.}$$
$$L = 6.088 \text{ nh.}$$

Substituting these lumped elements for the stubs, the resultant amplifier becomes that shown in Figure 28:

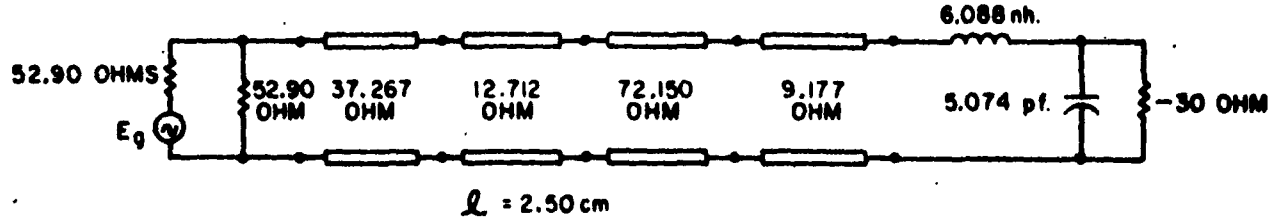

Figure 28 - 4-Line Tunnel Diode Reflection Amplifier

The transducer power gain of the amplifier as a function of frequency is now to be determined. To accomplish this, we must initially consider the network of Figure 28 with port 2 terminated in a +R (i.e., +30 ohm) resistance. This artifice arises from a somewhat subtle but highly important point.

The derivation of the transducer power gain, $G(\omega^2)$, as shown in Appendix C, is done for port normalizations of $\hat{R}_g$ and +R, with the respective terminations being $\hat{R}_g$ and -R. Thus, one might question the above change in the port 2 termination.

Note from equation (130), however, that determining $G(\omega^2)$ necessitates the ascertaining of $s_{11}(j\omega)$. This scattering coefficient is one of four which, for specified port normalizations, characterizes the two-port composed of the transmission line cascade in tandem with the reactive L-section. That is, although the derivation of $G(\omega^2)$ depends upon specific port normalizations and terminations, the scattering coefficient $s_{11}(j\omega)$ itself is independent of terminations.

One observes from Figure 28 that a parameter which can be determined with relative ease is a port 1 input scattering coefficient, normalized to $\hat{R}_g$. Evaluating this term involves essentially Smith Chart techniques. We wish now to relate this input coefficient to $s_{11}(j\omega)$. As reference 2 points out, the port 1 input coefficient equals $s_{11}(j\omega)$ if port 2 is terminated in its match (i.e., +R), upon which a_2 equals zero. If port 2 is terminated in -R, b_2 becomes equal to zero and no simple relation exists between $s_{in_1}(j\omega)$ and $s_{11}(j\omega)$.

Thus we use the +R port 2 termination as a means of readily evaluating $s_{11}(j\omega)$. This parameter, for the same normalization, does not change when we subsequently revert to the -R termination. For this latter configuration, the transducer gain given by equation (130) applies.

Figure 29 shows the variation of $G(\omega^2)$ with frequency for the amplifier of Figure 28. This response was evaluated by an entirely numerical procedure for reasons of accuracy; the Smith Chart was not used.

Throughout the course of this synthesis procedure, two approximations were made; the diode was approximated by the transmission line model and the gain relation was approximated by equation (132b). Thus, as Figure 29 indicates, the exact gain expression, when evaluated for the network of Figure 28, deviated somewhat from the specified 19.0 ± 1.0 db. By sacrificing some gain for better tolerance in the initial specification, it is felt that one may achieve ultimately an even better response.

In the design, R was arbitrarily set equal to 30 ohms, since -R = -30 ohms is a value typical of tunnel diodes. Note that, once $|s_{12}|^2$ and R are numerically specified, the transparency of the system at d.c. fixes $\hat{R}_g \cdot \hat{R}_g$, in turn, involves R_g, R_L and the angle ψ. This angle may be subsequently varied, at the expense of gain, to accommodate, within certain limits, a particular R_L or R_g. If the design in question demands both a particular R_L and R_g, both R and ψ are thereby fixed for a given $|s_{12}|^2$.

Fig. 29 Transducer Power Gain $\left[G(\omega^2)\right]$
vs.
Frequency

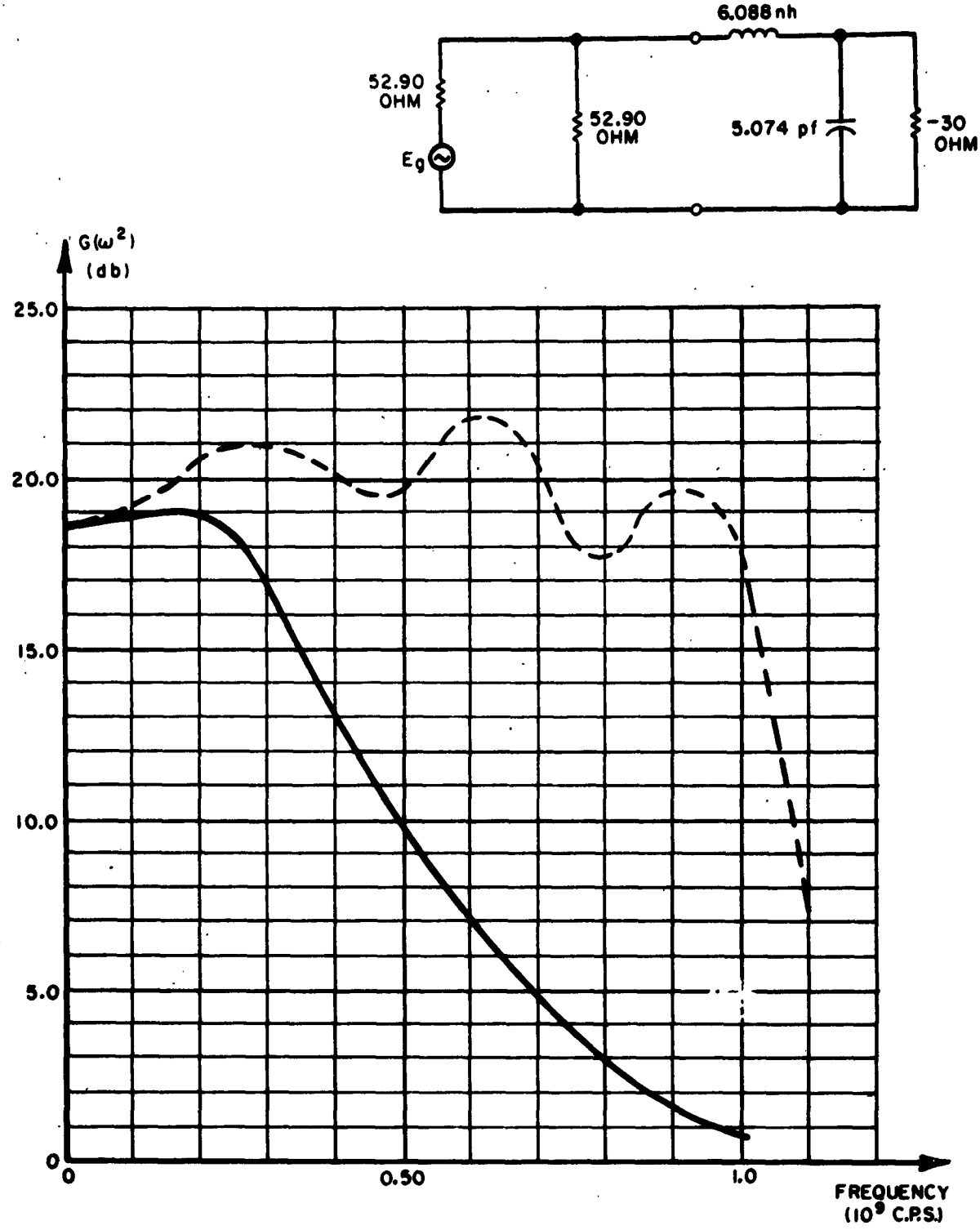

Fig. 30 Transducer Power Gain of Uncompensated Diode vs. Frequency

The major shortcoming of the design procedure is its inability to guarantee a stable amplifier. Smilen and Youla[10] show that any diode for which $L/R^2C < 3$ can be used to design a stable amplifier. Reference 10 further derives the necessary conditions for the stability of a reflection amplifier; $s_{22}(p)$ can have no zeros in $Re(p) \geq 0$ and $s_{11}(p)$ can have no zeros in $Re(p) \leq 0$.

The only condition which we satisfy with certainty is the inequality. From equations (131) and (132a), one notes that $0 < |s_{22}(j\Omega)|^2 \leq 1$. Hence the integrand of equation (133) is non-negative, or $Z_1/R^2Y_2 > 3$. From equations (129b), however, $Z_1/Y_2 = L/C$.

The inability to predict or control the critical frequencies of the scattering coefficients stems basically from the transcendental functions inherent in network descriptions of transmission line-lumped reactance mixtures. The scattering coefficients, over which we have explicit control, are those characterizing the system of Figure 24. The s_{22} coefficient of this system was selected without zeros in $Re(\lambda) \geq 0$. The substitution of the lumped reactances for the stubs essentially creates a new lossless reciprocal two-port, characterized by its own scattering coefficients. Over these latter parameters, we have no explicit control.

APPENDIX I: Synthesis Example of a Type II-C Network (i.e., same order zeros of transmission at d.c. and the quarter-wave frequency)

The most elemental network of this class, a two-line cascade augmented by a stub configuration realizing single order zeros, is to be synthesized. As representative bandwidth and tolerance parameters, we select:

$$a = 2.00$$

$$\varepsilon^2 = 0.01$$

Then, from equation (63) (with $n = 2m = 2$ and $r = 1$):

$$|s_{12}|^2 = \frac{0.99}{1 + 0.01 \cos(2\phi + \delta)} \tag{A-1}$$

Therefore:

$$|s_{11}|^2 = 1 - |s_{12}|^2 = \frac{-0.27856x^4 + 0.29856x^2 - 0.0800}{-0.27856x^4 + 1.28856x^2 - 4.0400} \tag{A-2}$$

$x = a \cos 2\theta$. Thus, $x^2 = \frac{a^2(1 - \Omega^2)^2}{(1 + \Omega^2)^2}$ where $\Omega = \tan\theta$

Substituting into equation (A-2):

$$|s_{11}(j\Omega)|^2 = \frac{-3.34272\Omega^8 + 17.50784\Omega^6 - 29.61024\Omega^4 + 17.50784\Omega^2 - 3.34272}{-3.34272\Omega^8 + 1.66784\Omega^6 - 61.29024\Omega^4 + 1.66784\Omega^2 - 3.34272} \tag{A-3}$$

for which:

$$s_{11}(\lambda) = \frac{\lambda^4 + 2.61875\lambda^2 + 1}{\lambda^4 + 3.5063\lambda^3 + 6.3972\lambda^2 + 3.5063\lambda + 1} \tag{A-4}$$

Note that by selecting $s_{11}(0) = s_{11}(\infty) = +1$, we shall realize the zeros of transmission through series, rather than shunt, stubs.

The corresponding port 1 input impedance is:

$$Z(\lambda) = \frac{2\lambda^4 + 3.5063\lambda^3 + 9.0160\lambda^2 + 3.5063\lambda + 2}{3.5063\lambda^3 + 3.7784\lambda^2 + 3.5063\lambda} \tag{A-5}$$

The network of Figure A-1 resulted.

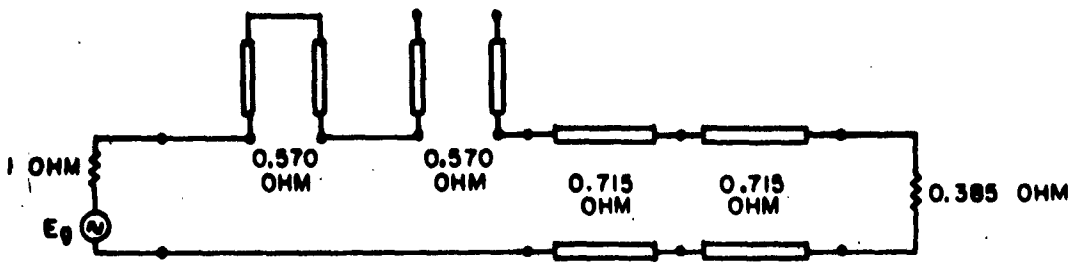

Figure A-1 - Network Realizing Equiripple Response with Zeros of Transmission at D.C. and the Quarter-Wave Frequency

APPENDIX II: Factorization for the Special Case wherein the Order of the Zero of Transmission is Equal to the Number of Cascaded Lines

For this case:

$$|s_{12}|^2 = \frac{1 - (\epsilon^2 + k^2)}{1 + \epsilon^2 \cos(2n\phi + n\delta)}$$

or (B-1)

$$|s_{11}|^2 = 1 - |s_{12}|^2 = \frac{\cos(2n\phi + n\delta) + 1 + k^2/\epsilon^2}{\cos(2n\phi + n\delta) + 1/\epsilon^2}$$

1. Numerator Equation

$$\cos(2n\phi + n\delta) = -(1 + \frac{k^2}{\epsilon^2})$$

Let

$$2n\phi + n\delta = \rho + j\eta \qquad \text{(B-2)}$$

Then:

$$\cos\rho \cosh\eta - j \sin\rho \sinh\eta = -(1 + \frac{k^2}{\epsilon^2})$$

or:

$$\sin\rho \sinh\eta = 0$$

$$\cos\rho \cosh\eta = -(1 + \frac{k^2}{\epsilon^2})$$

Therefore:

$$\rho = \pm (2m + 1)\pi \qquad m = 0, 1, 2, \cdots$$

$$\eta = \pm \cosh^{-1}(1 + \frac{k^2}{\epsilon^2})$$

From equation (B-2), then:

$$2n\phi + n\delta = \pm(2m+1)\pi \pm j \cosh^{-1}\left(1 + \frac{k^2}{\varepsilon^2}\right)$$

or

$$2\phi + \delta = \pm(2m+1)\frac{\pi}{n} \pm j\frac{1}{n}\cosh^{-1}\left(1 + \frac{k^2}{\varepsilon^2}\right)$$

Thus:

$$\cos(2\phi + \delta) = \cos\left\{(2m+1)\frac{\pi}{n} \pm j\frac{1}{n}\cosh^{-1}\left(1 + \frac{k^2}{\varepsilon^2}\right)\right\} \qquad \text{(B-3)}$$

Let these values be represented by ξ_m.

2. Denominator Equation

By an identical procedure:

$$\cos(2\phi + \delta) = \xi_q = \cos\left\{(2q+1)\frac{\pi}{n} \pm j\frac{1}{n}\cosh^{-1}\left(\frac{1}{\varepsilon^2}\right)\right\} \qquad \text{(B-4)}$$

$$q = 0, 1, 2, \cdots$$

3. $\cos(2\phi + \delta) = \cos 2\phi \cos\delta - \sin 2\phi \sin\delta =$

$$= \frac{1}{(a^2 - x^2)}\left\{\left[2x^2 - 1\right]\left[(2a^2 - 1)x^2 - a^2\right] - \left[2x\sqrt{1 - x^2}\right]\left[2a\,x\sqrt{(1 - x^2)(a^2 - 1)}\right]\right\}$$

Therefore, from equations (B-3) and (B-4):

$$x^4(4a^2 + 4a\sqrt{a^2 - 1} - 2) - x^2(4a^2 + 4a\sqrt{a^2 - 1} - 1 - \xi) + a^2(1 - \xi) = 0 \qquad \text{(B-5)}$$

where the proper ξ-set must be used.

4. For zeros of transmission at d.c., $x = a\cos\theta$, or $x^2 = \frac{a^2}{(1 + \Omega^2)}$.
Therefore:

$$\Omega^4(1 - \xi) + \Omega^2(3 - \xi - 4a^2 - 4a\sqrt{a^2 - 1}) + (2 + 4a^4 + 4a^3\sqrt{a^2 - 1} - 4a\sqrt{a^2 - 1} - 6a^2) = 0$$

(B-6)

Therefore:

$$\lambda = \pm j \sqrt{\frac{(4a^2+4a\sqrt{a^2-1}+\xi-3) \pm \sqrt{(3-\xi-4a^2-4a\sqrt{a^2-1})^2 - 4(1-\xi)(2+4a^4+4a^3\sqrt{a^2-1}-4a\sqrt{a^2-1}-6a^2)}}{2(1-\xi)}} \qquad \text{(B-7)}$$

By substituting the ξ_m and ξ_q sets into the above relation, one can obtain the numerator and denominator roots for $s_{11}(\lambda)$. The condition, $s_{11}(0) = \pm 1$, the sign depending upon the type of network desired, determines the required scale factor for the factored $s_{11}(\lambda)$.

5. For zeros of transmission at the quarter-wave frequency, $x = a \sin \theta$, or $x^2 = a^2\Omega^2/\Omega^2 + 1$.

Therefore, substituting into equation (B-5):

$$\Omega^4(2+4a^4+4a^3\sqrt{a^2-1}-4a\sqrt{a^2-1}-6a^2) + \Omega^2(3-\xi-4a^2-4a\sqrt{a^2-1}) + (1-\xi) = 0 \qquad \text{(B-8)}$$

The roots are consequently:

$$\lambda = \pm j \sqrt{\frac{(4a^2+4a\sqrt{a^2-1}+\xi-3) \pm \sqrt{(3-\xi-4a^2-4a\sqrt{a^2-1})^2 - 4(2+4a^4+4a^3\sqrt{a^2-1}-4a\sqrt{a^2-1}-6a^2)(1-\xi)}}{2(2+4a^4+4a^3\sqrt{a^2-1}-4a\sqrt{a^2-1}-6a^2)}} \qquad \text{(B-9)}$$

Since quarter-wave frequency zeros of transmission demand that $s_{11}(\infty) = \pm 1$, the scale factor for this case will involve, at most, a change in sign.

APPENDIX III: Derivation of Reflection Amplifier Transducer Power Gain*

Figure C-1 shows the reflection amplifier, with the input circuit represented by its Thevenin equivalent circuit deduced from Figure 24.

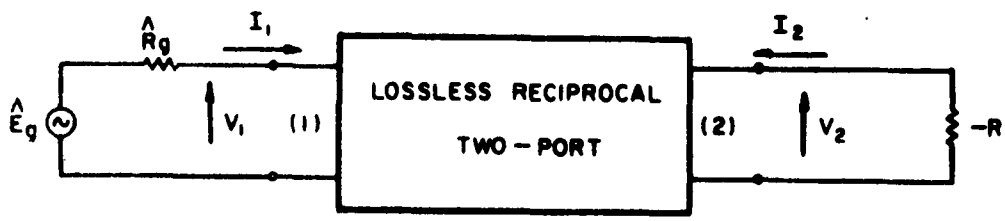

Figure C-1 - Reflection Amplifier Representation, With the Input Circuit Replaced by its Thevenin Equivalent

*This derivation is taken from Smilen and Youla.[10]

$$\hat{R}_g = \frac{R_L R_g}{R_L + R_g} = R_g \sin^2 \psi \tag{C-1}$$

$$\hat{E}_g = E_g \frac{R_L}{R_L + R_g} = E_g \sin^2 \psi \tag{C-2}$$

where $R_L = R_g \tan^2 \psi$. The port normalization numbers are selected as:

$$R_1 = \hat{R}_g \tag{C-3}$$

$$R_2 = R \tag{C-4}$$

In terms of terminal voltages and currents, the incident and reflected "voltages" are given as:

$$a_i = \frac{1}{2}\left[R_i^{-\frac{1}{2}} V_i + R_i^{\frac{1}{2}} I_i\right]$$

$$b_i = \frac{1}{2}\left[R_i^{-\frac{1}{2}} V_i - R_i^{\frac{1}{2}} I_i\right] \qquad (i = 1, 2) \tag{C-5}$$

where the R_i are the normalizing numbers.

From Figure C-1:

$$V_1 = \hat{E}_g - I_1 \hat{R}_g$$

$$V_2 = I_2 R$$

Therefore, for the given normalizations, from equations (C-5):

$$a_1 = \frac{\hat{E}_g}{2\hat{R}_g^{1/2}} \tag{C-6}$$

and

$$b_2 = 0 \tag{C-7}$$

From (C-1) and (C-2):

$$a_1 = \frac{E_g \sin \psi}{2R_g^{1/2}} \tag{C-8}$$

The maximum available power from the generator is:

$$P_m = \frac{|E_g|^2}{4R_g} = |a_1|^2 \csc^2 \psi \tag{C-9}$$

The power to the load is:

$$P_L = \frac{|V_1|^2}{R_L} \tag{C-10}$$

which, from (C-5) in conjunction with (C-1) and (C-2), becomes:

$$P_L = |a_1 + b_1|^2 \cos^2 \psi \tag{C-11}$$

Noting equation (C-7), the equations characterizing the network become:

$$\begin{aligned} b_1 &= s_{11} a_1 + s_{12} a_2 \\ 0 &= s_{12} a_1 + s_{22} a_2 \end{aligned} \tag{C-12}$$

Thus,

$$b_1 = \frac{s_{11} s_{22} - s_{12}^2}{s_{22}} a_1 \tag{C-13}$$

As a consequence of the unitary condition, the following relations apply:

$$s_{11}(-p)\, s_{12}(p) + s_{12}(-p)\, s_{22}(p) = 0 \tag{C-14}$$

$$s_{11}(p)\, s_{11}(-p) + s_{12}(p)\, s_{12}(-p) = 1 \tag{C-15}$$

By multiplying (C-14) by the factor $[s_{11}(p)\, s_{12}(p)]$ and then using (C-15), one can show that:

$$\frac{s_{11}(p)\, s_{22}(p) - s_{12}^2(p)}{s_{22}(p)} = \frac{1}{s_{11}(-p)} \tag{C-16}$$

Therefore:

$$P_L = \left| 1 + \frac{1}{s_{11}(j\omega)} \right|^2 \cos^2 \psi \, |a_1|^2 \qquad \text{(C-17)}$$

and

$$G(\omega^2) = \frac{P_L}{P_m} = \frac{\sin^2 2\psi}{4} \left| 1 + \frac{1}{s_{11}(j\omega)} \right|^2 \qquad \text{(C-18)}$$

REFERENCES

1. Carlin, H.J. - "Cascaded Transmission Line Synthesis", Research Report PIBMRI-889-61, April 1961.

2. Carlin, H.J. - "The Scattering Matrix in Network Theory", I.R.E. Transactions, June 1956, CT-3, pp. 88-97.

3. Youla, D.C. - "Physical Realizability Criteria", I.R.E. International Convention Record, Part 2, 1960.

4. Richards, P.I. - "Resistor-Transmission Lines", Proceedings of the I.R.E., Vol. 37, No. 2, February 1948, pp. 217-219.

5. Sharpe, C.B. - "A General Tchebycheff Rational Function", Proceedings of the I.R.E., Vol. 42, No. 2, February 1954, pp. 454-457.

6. Helman, D. - "Tchebycheff Approximations for Amplitude and Delay with Rational Functions", Reprinted from the Proceedings of the Symposium on Modern Network Synthesis, Polytechnic Institute of Brooklyn, April 1955.

7. Magnus and Oberhettinger - "Formulas and Theorems for the Special Functions of Mathematical Physics", Chelsea Pub. Co., 1949.

8. Bode, H.W. - "Network Analysis and Feedback Amplifier Design", Van Nostrand, 1945.

9. Smilen, L.I. - "A Distributed Parameter Approximation of the Tunnel Diode", PIBMRI-983-61, Memorandum 60, December 1961.

10. Smilen and Youla - "Exact Theory and Synthesis of a Class of Tunnel Diode Amplifiers", Research Report PIBMRI-877-60, October 1960.

11. Fano, R.M. - "Theoretical Limitations on the Broadband Matching of Arbitrary Impedances", Journal of the Franklin Institute, Vol. 249, January 1950 and February 1950.

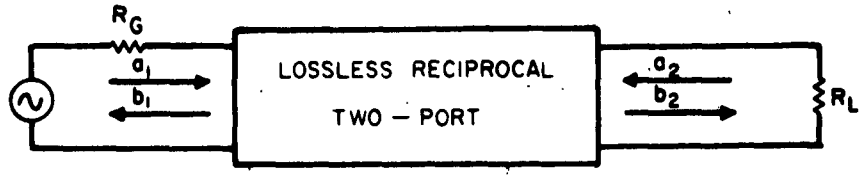

Fig. 1 System Representation

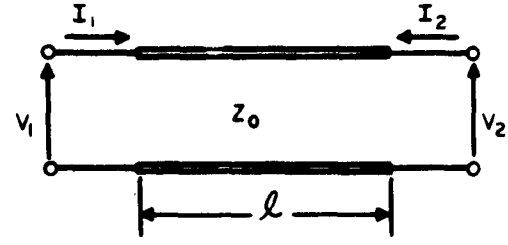

Fig. 2 Transmission Line

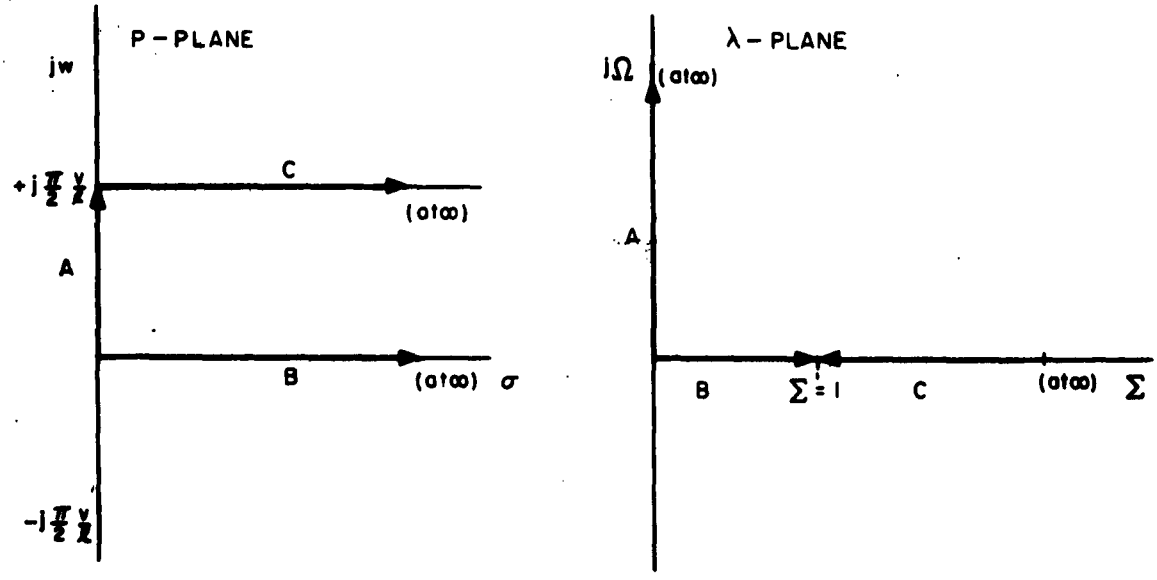

Fig. 3 Richards Frequency Transformation

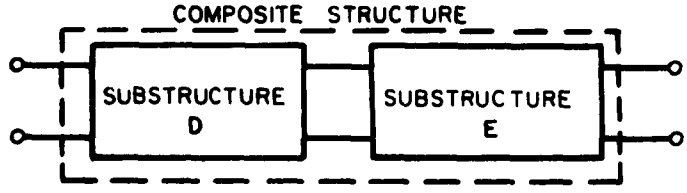

Fig. 4 Cascade Connection of Two Structures

MRI – 18851

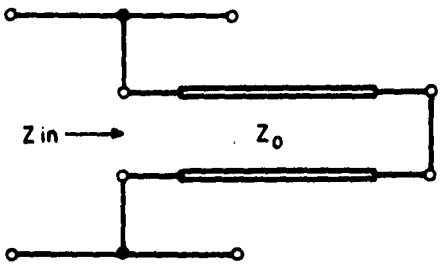

Fig. 5 Shunt Short - Circuited Stub

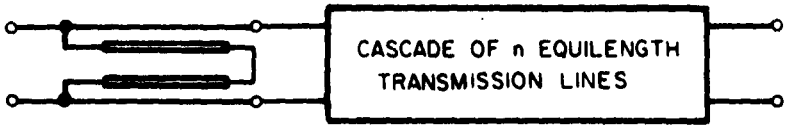

Fig. 6 Cascade of Transmission Lines Augmented by a Shunt Short - Circuited Stub

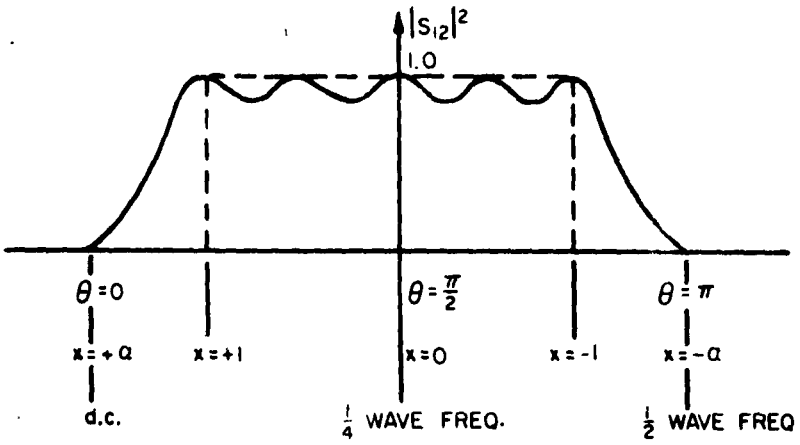

Fig. 7 Desired Tchebycheff - Type Shape

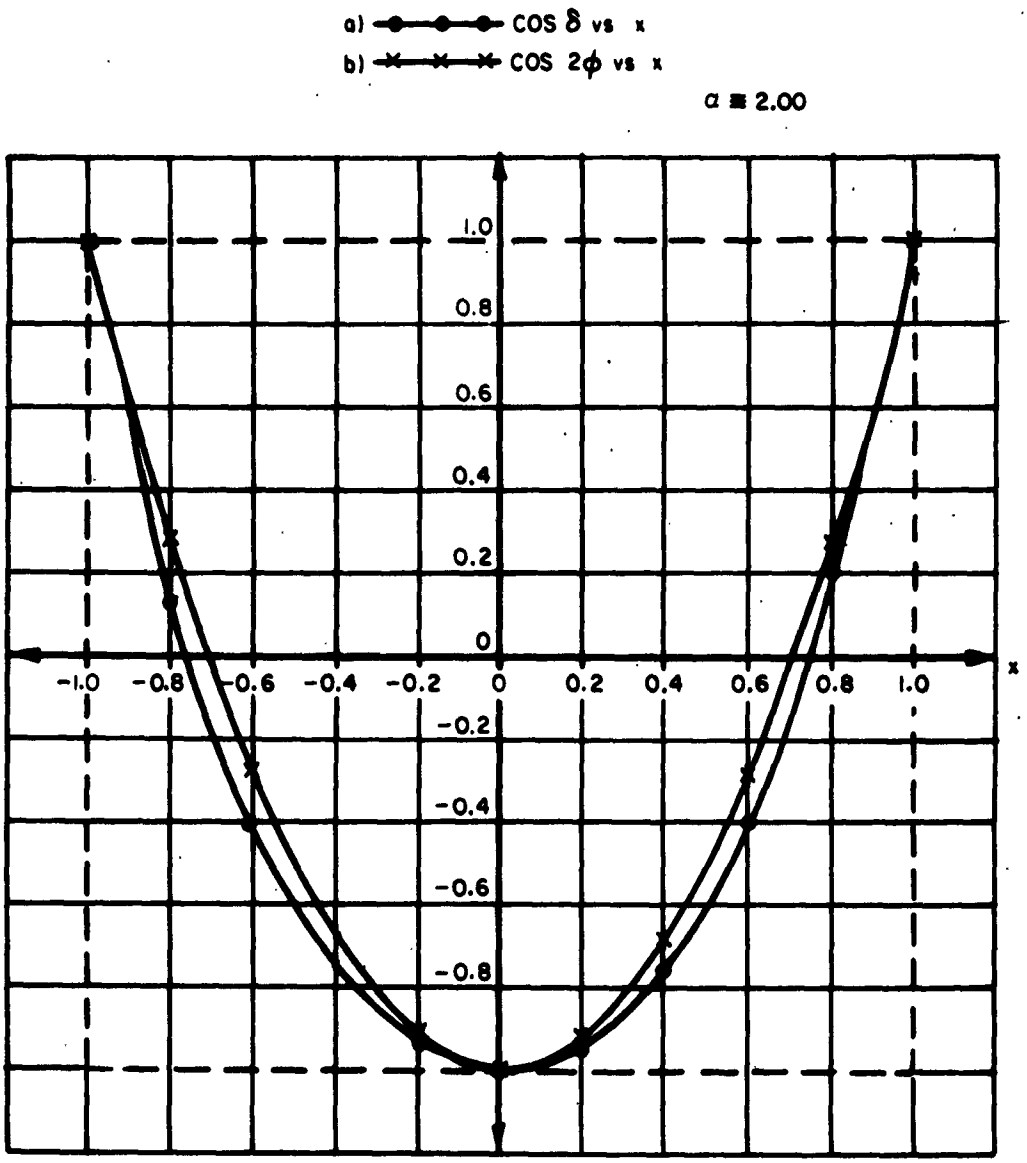

Fig. 8 a) cos δ vs. χ
b) cos 2φ vs. χ

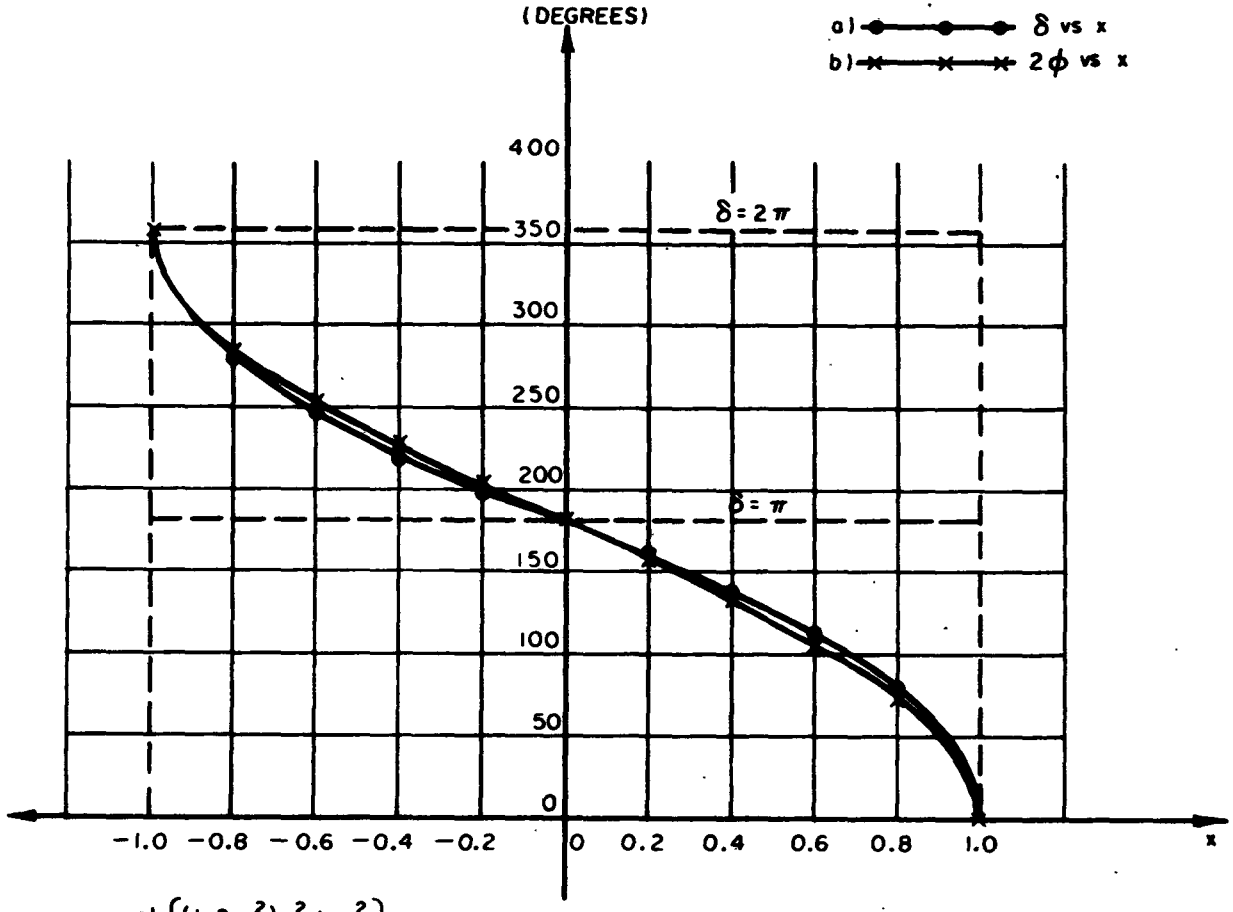

Fig. 9 a) δ vs χ
b) 2ϕ vs χ

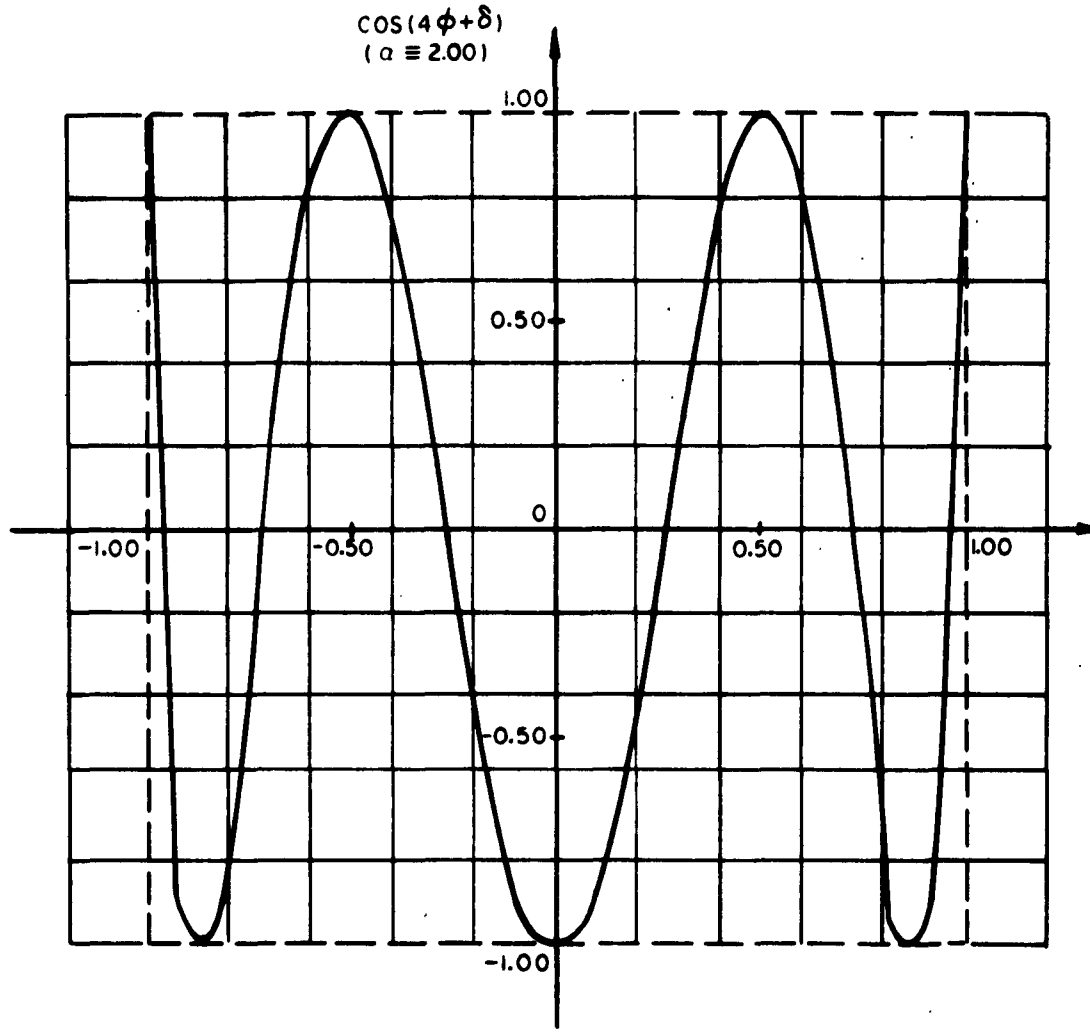

FOR $\alpha = 2.00$:

$$\cos(4\phi+\delta) = \frac{1}{4-x^2}\left[(56+32\sqrt{3})x^6+(-88-48\sqrt{3})x^4+(39+16\sqrt{3})x^2-4\right]$$

Fig 10 cos (4φ + δ) vs. χ

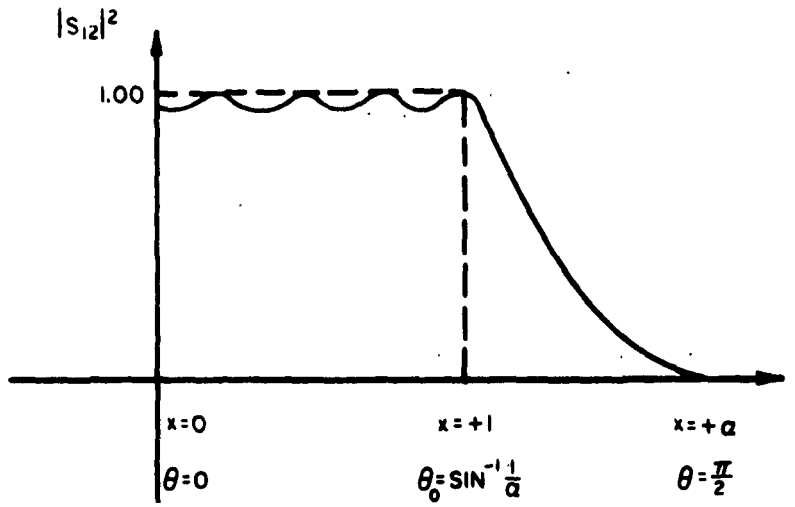

Fig. 11 Equiripple Shape For the Case of a Quarter-Wave Zero of Transmission

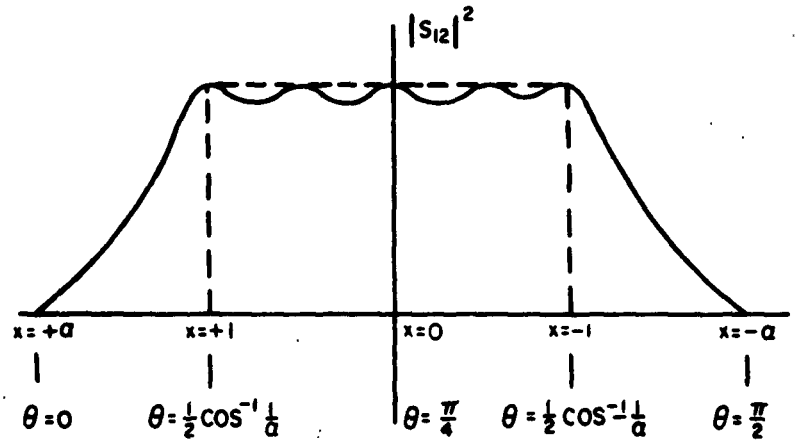

Fig. 12 Equiripple Shape For the Case of D. C. and Quarter-Wave Frequency Zeros of Transmission

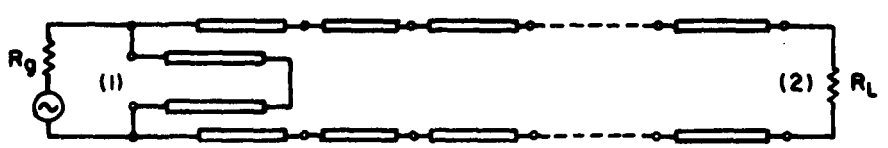

Fig. 13 Shunt, Short - Circuited Stub, Bandpass Filter

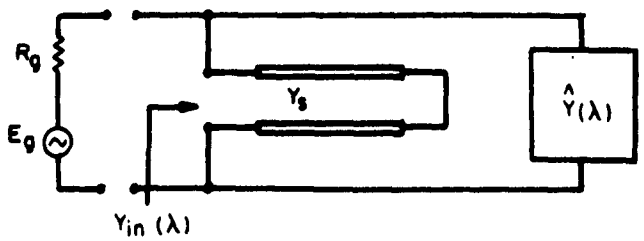

Fig. 14 Bandpass Filter Schematic

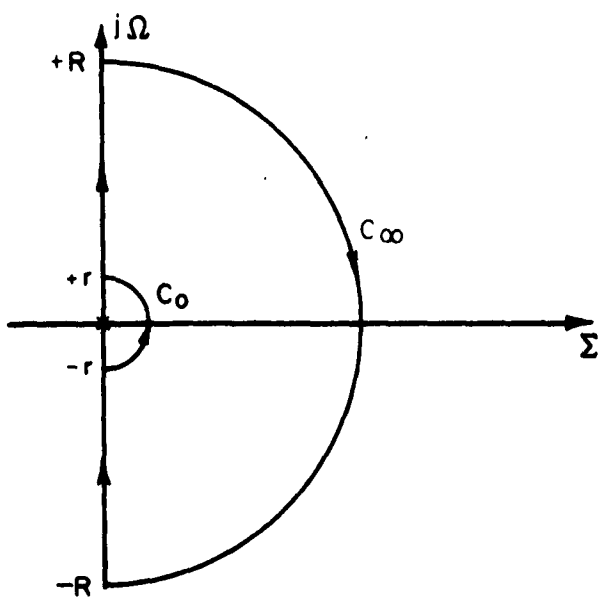

Fig. 15 Path of Contour Integration

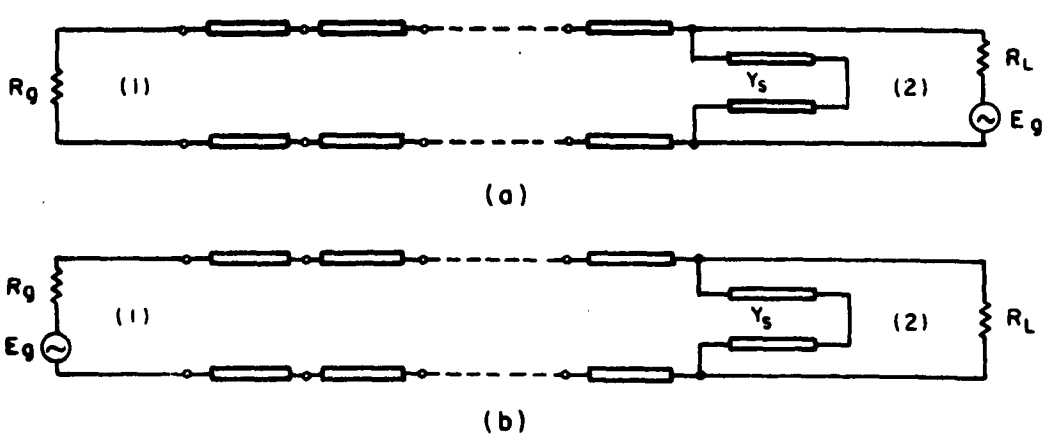

Fig. 16 Bandpass Filter With Stub Shunting Load

MRI-18857

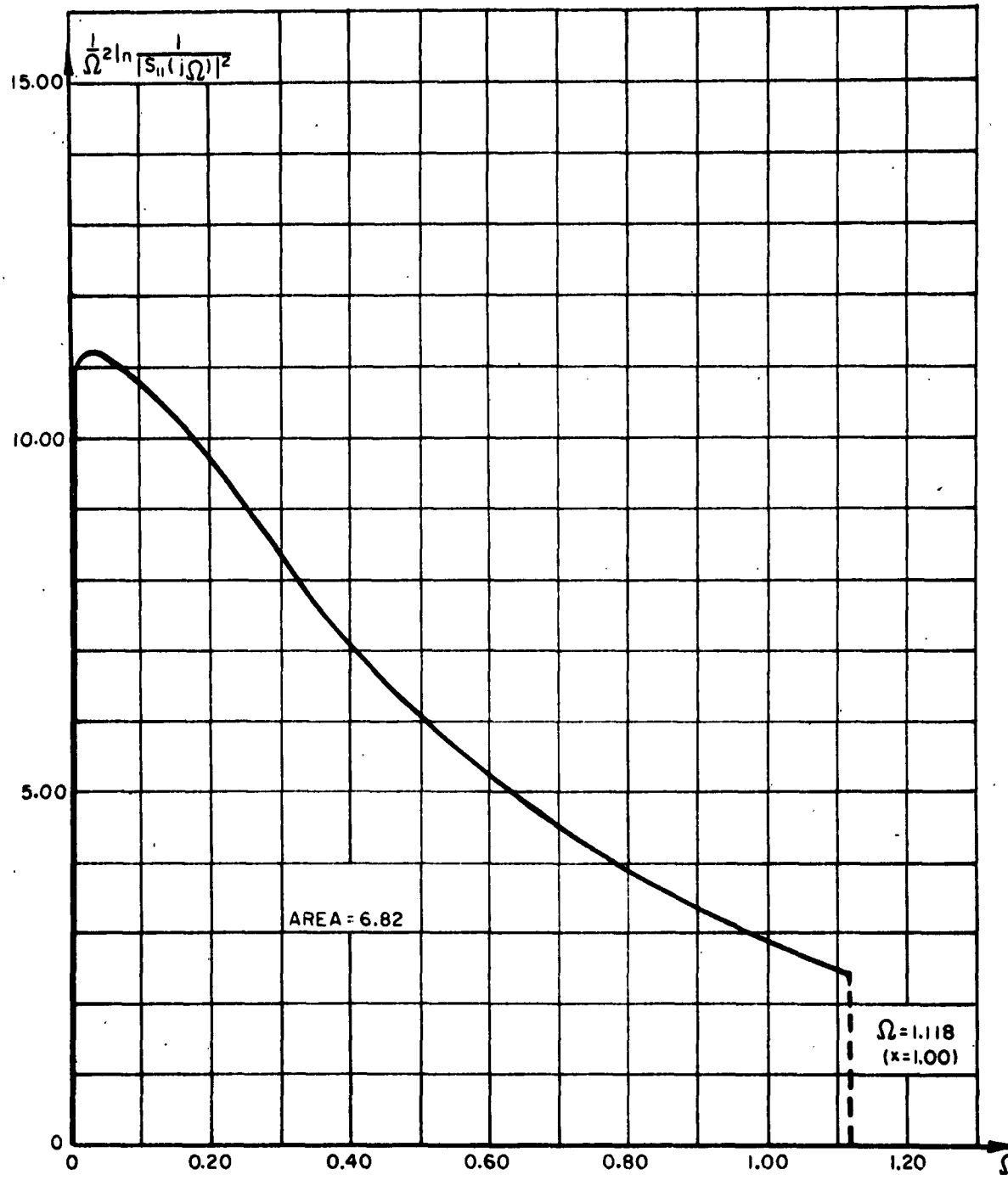

Fig. 17 Stopband Variation of Fano Integrand

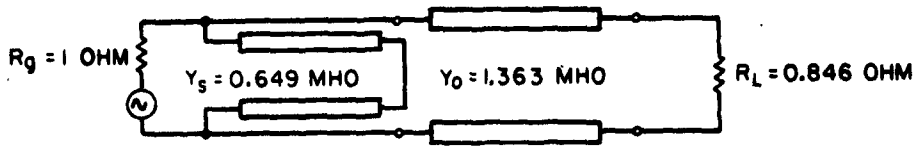

Fig. 18 Synthesized One-Line Bandpass Filter

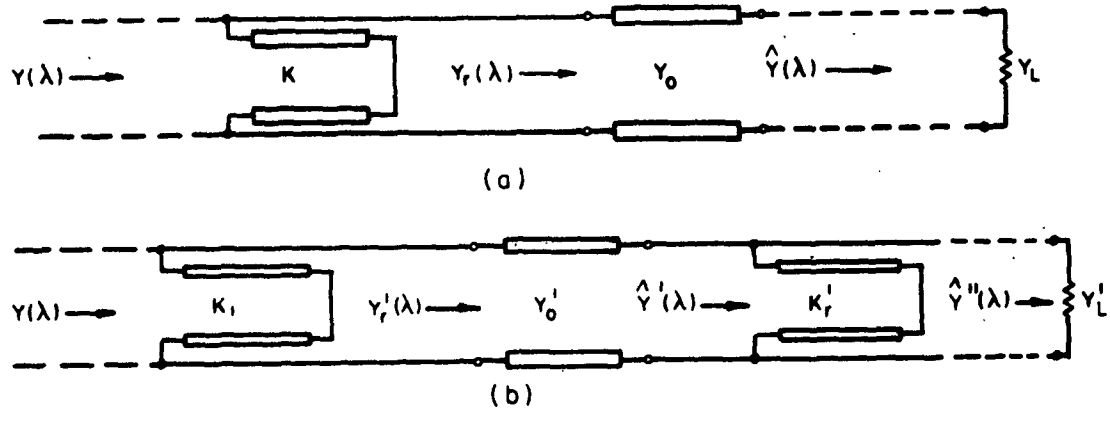

Fig. 19 Alternative Synthesis Procedures

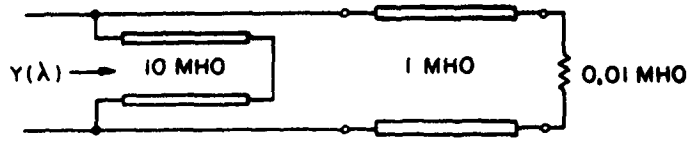

Fig. 20 Given Network

Fig. 21 Equivalent Network

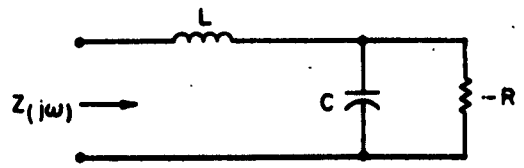

Fig. 22 Equivalent Circuit of a Tunnel Diode (neglecting junction spreading resistance).

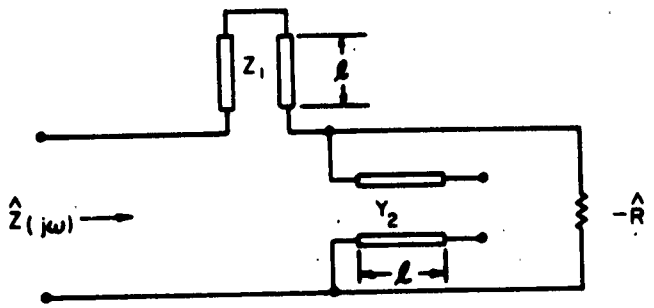

Fig. 23 Approximate Model for the Tunnel Diode (neglecting junction spreading resistance).

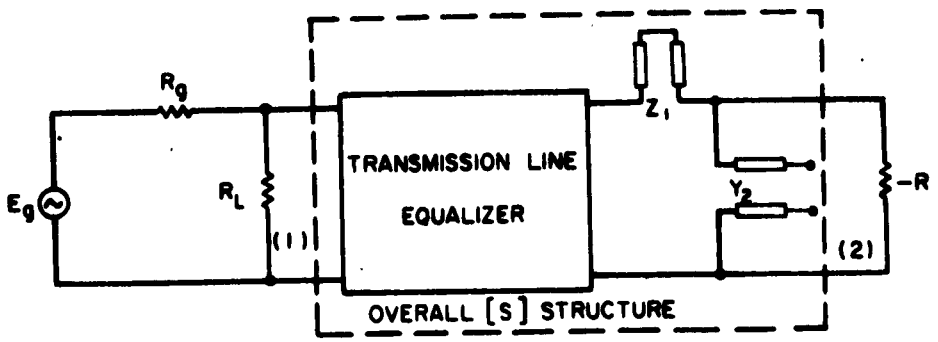

Fig. 24 Tunnel Diode Reflection Amplifier, with Diode Approximated by Transmission Line Model

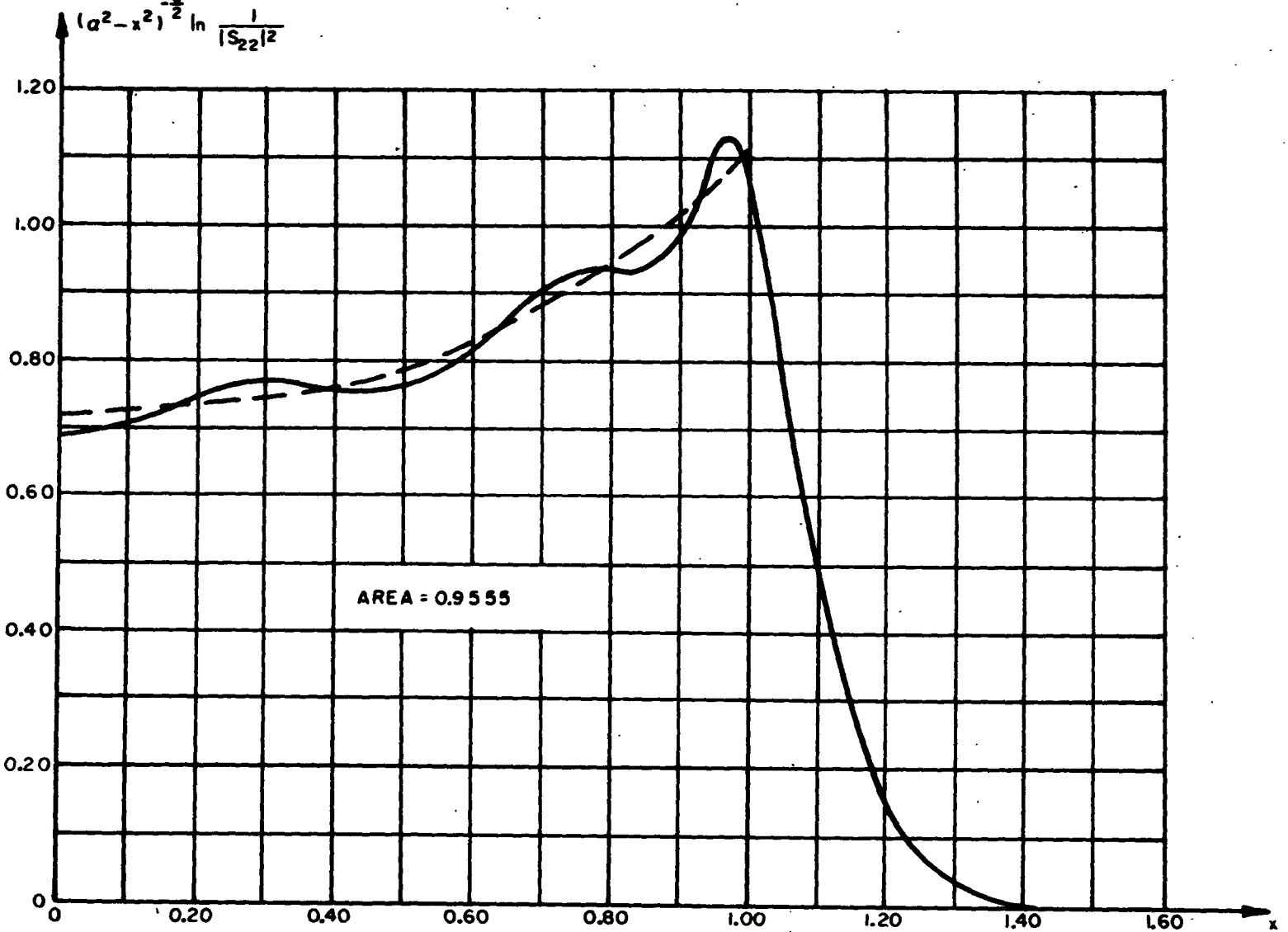

Fig. 25 $(a^2 - x^2)^{-3/2} \ln \frac{1}{|S_{22}|^2}$ vs. x

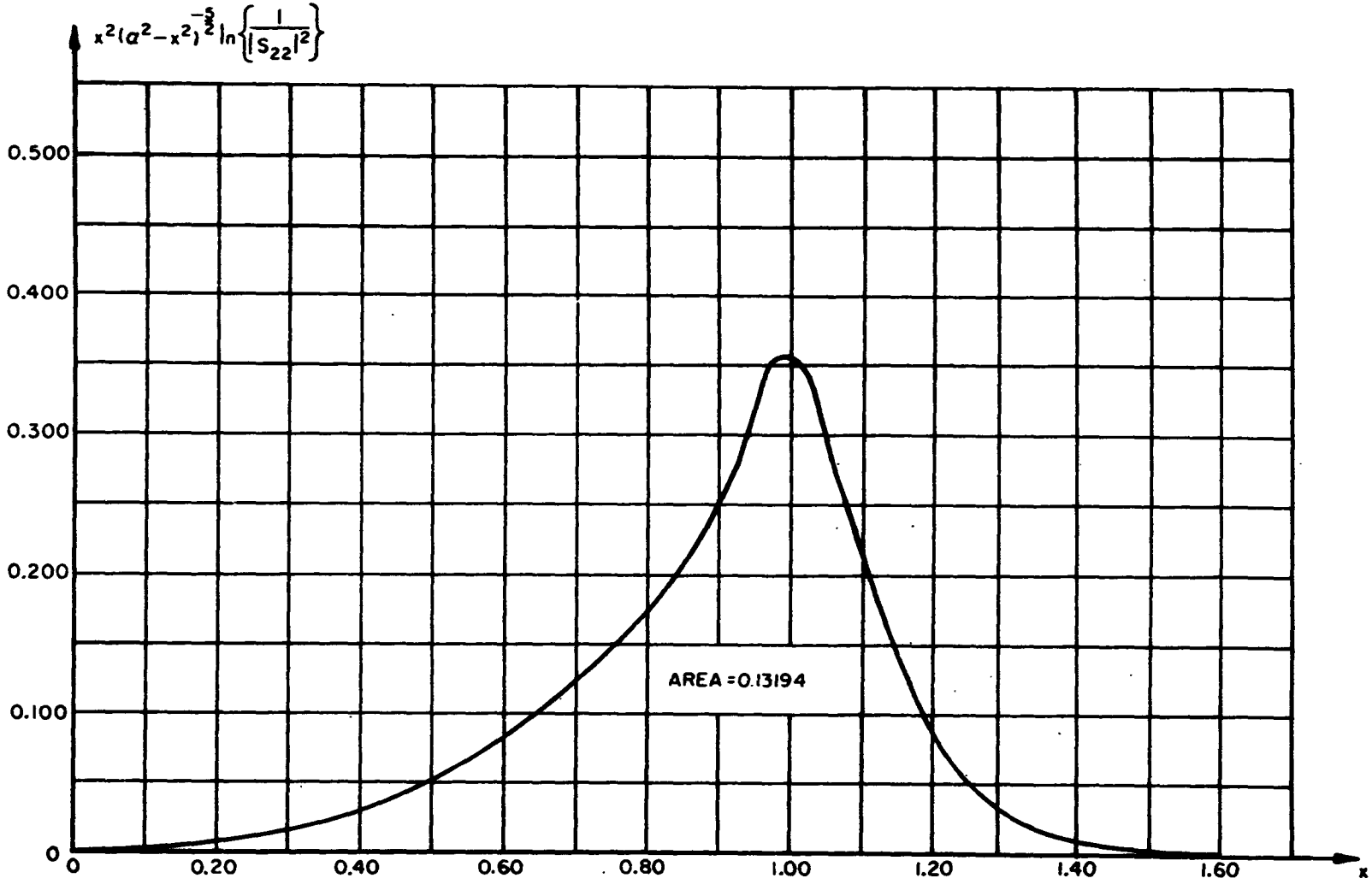

Fig. 26 $x^2 (a^2 - x^2)^{-5/2} \ln \frac{1}{|S_{22}|^2}$ vs. x

MRI-18862

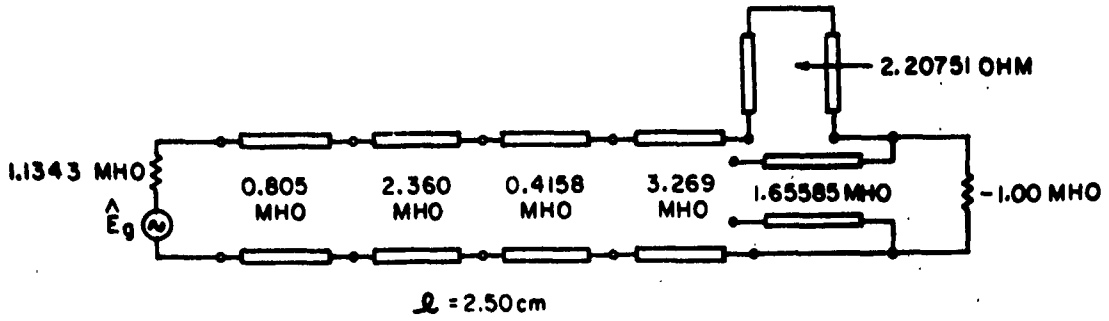

Fig. 27 Synthesized 4 - Line Amplifier With Transmission Line Diode Model

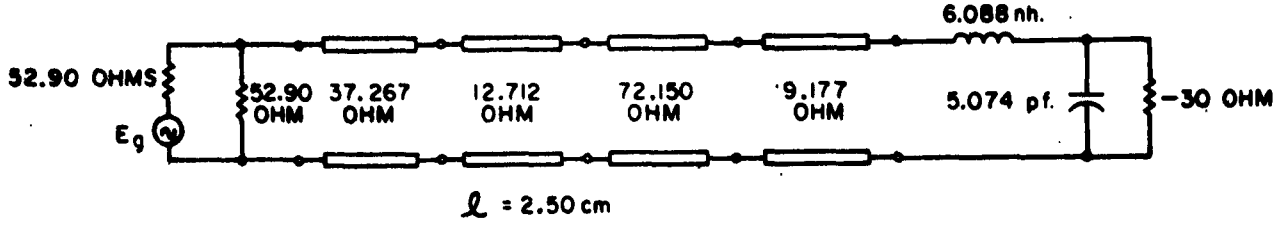

Fig. 28 4 - Line Tunnel Diode Reflection Amplifier

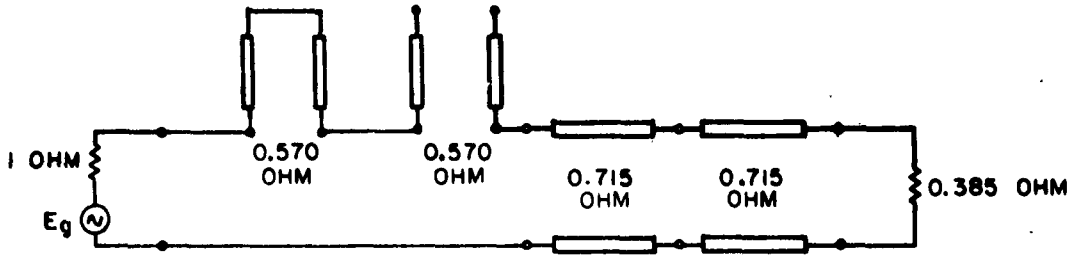

Fig. A-1 Network Realizing Equiripple Response With Zeros of Transmission at D. C. and the Quarter - Wave Frequency

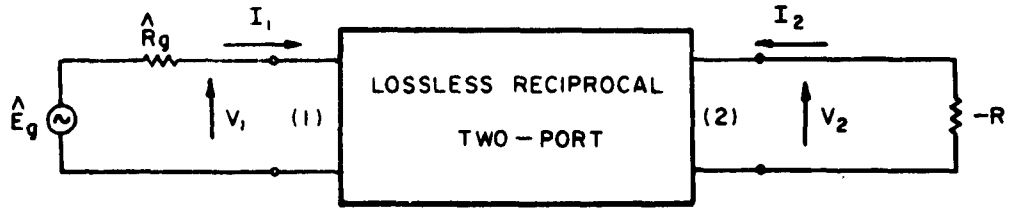

Fig. C-1 Reflection Amplifier Representation With the Input Circuit Replaced by its Thevenin Equivalent

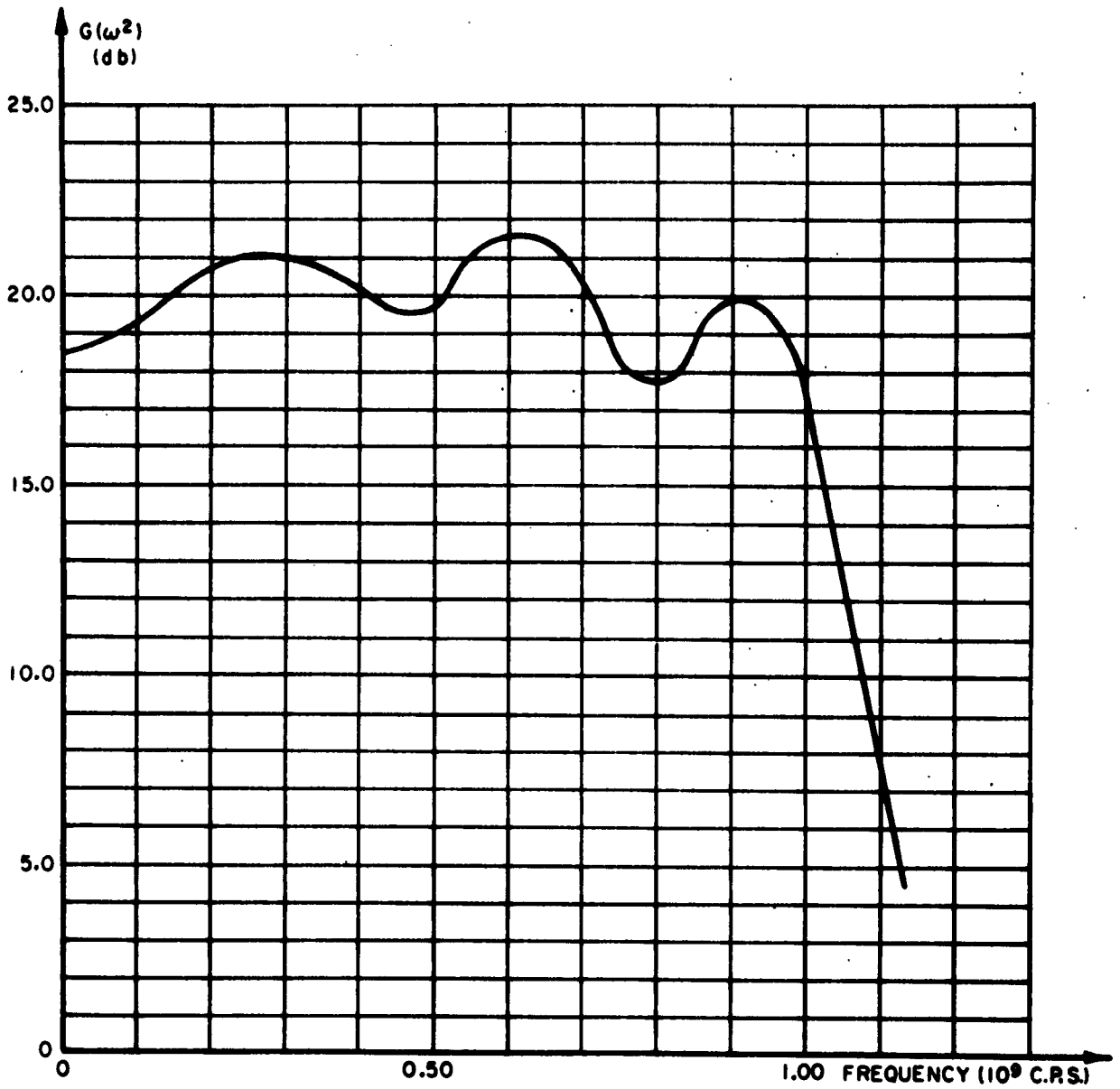

Fig. 29 Transducer Power Gain $\left[G(\omega^2)\right]$
vs.
Frequency

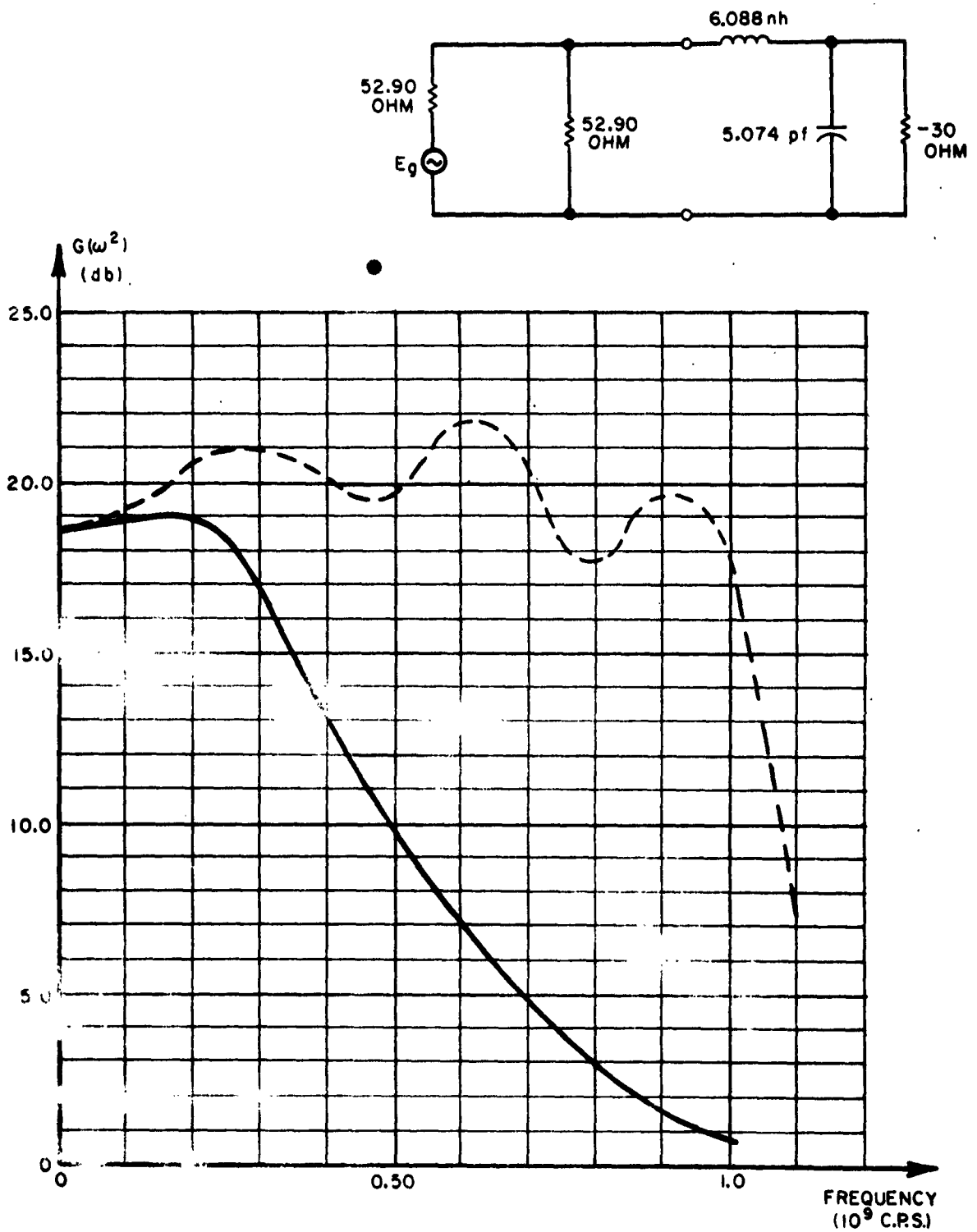

Fig. 30 Transducer Power Gain of Uncompensated Diode vs. Frequency

UNIVERSITIES:

PIBMRI-1038-62

Purdue University
School of Electrical Engineering
Lafayette, Indiana

University of Southern California
Engineering Center
University Park
Los Angeles 7, California
ATTN: Librarian and/or Dr. R. L. Chuan

University of Pennsylvania
Institute for Cooperative Research
Room 306 - Logan Hall, 36th and Spruce
Philadelphia 4, Pennsylvania
ATTN: A. M. Hadley

Syracuse University
Electrical Engineering Dept.
Syracuse 10, New York
ATTN: Dr. David K. Cheng

Department of Electrical Engineering,
University of Toronto
Room 147, Galbraith Building
University of Toronto
Toronto 5, Ontario
ATTN: Professor G. Sinclair

University of Kansas
Electrical Engineering Department
University of Kansas
Lawrence, Kansas
ATTN: Dr. H. Unz

University of Tennessee
Ferris Hall
W. Cumberland Avenue
Knoxville, Tennessee
ATTN: J. D. Tillman

Technical Reports Collection
Gordon McKay Library
Harvard University
Div. of Eng'g. and Applied Physics
Pierce Hall, Oxford St.
Cambridge 38, Massachusetts
ATTN: Mrs. Y. Alland

Brown University
Division of Engineering
Providence 12, Rhode Island
ATTN: B. Hazeltine

Massachusetts Institute of Technology
Research Laboratory of Electronics
77 Massachusetts Avenue
Cambridge 39, Massachusetts
ATTN: Document Room 26-327, John H. Hewitt

Battelle Memorial Institute
505 King Avenue
Columbus 1, Ohio
ATTN: R. T. Compton, Jr.

Cooley Electronics Laboratory
The University of Michigan
Room 262, Cooley Building
Ann Arobr, Michigan

Lowell Technological Institute
Division of Physics and Engineering
Science
Lowell, Massachusetts
ATTN: Dr. C. R. Mingins, Chairman

Case Institute of Technology
University Circle
Cleveland 6, Ohio
ATTN: Prof. R. E. Collin

Dept. of Electrical Engineering
Syracuse University
Syracuse, New York
ATTN: W. R. La Page

Stanford Research Institute
Menlo Park, California
ATTN: External Reports, G-037

Jet Propulsion Laboratory
California Institute of Technology
4800 Oak Grove Drive
Pasadena, California
ATTN: Mr. Huston Denslow, Library Supervisor

Electrical Engineering Research Laboratory
The University of Texas
P. O. Box 7789, University Station
Austin 12, Texas
ATTN: John R. Gerhardt

Geophysical Institute of the
University of Alaska,
College, Alaska
ATTN: Library

Physical Science Laboratory
New Mexico State University
Box 548
University Park, New Mexico
ATTN: Reports Office Librarian

UNIVERSITIES cont'd

Institute of Science and Technology,
University of Michigan
P. O. Box 618, Ann Arbor, Michigan
ATTN: Technical Documents Service

Electronics Research Laboratory
427 Cory Hall
University of California
Berkeley 4, California
ATTN: Librarian

Ohio State University Research Foundation
1314 Kennear Road
Columbus 8, Ohio
ATTN: Robert A. Foutz

University of Oklahoma
Norman, Oklahoma
ATTN: C. D. Farrar

Johns Hopkins University
W. H. Huggins
Dept. of Elec. Engrg.
The Johns Hopkins University
Baltimore 18, Maryland
ATTN: W. H. Huggins

New York University
Department of Electrical Engineering
181st Street and University Avenue
2 cys Bronx 53, N. Y.
ATTN: Benjamin Goldin

The Johns Hopkins University
Carlyle Barton Laboratory
Charles & 34th Streets
Baltimore 18, Maryland
ATTN: Librarian

Illinois Institute of Technology
3300 S. Federal
Chicago 16, Illinois
Dept. of Electrical Engineering
ATTN: Dr. Lester C. Peach

University of Illinois
College of Engineering
ATTN: Dr. P. E. Mayes
Urbana, Illinois

University of Southern California
Electrical Engineering Department
University of Southern California
Los Angeles 7, California
ATTN: Dr. R. M. Gagliardi

University of Wisconsin
Dept. of Electrical Engineering
Engineering Building
Madison 6, Wisconsin
ATTN: Dr. E. H. Scheibe

Space Sciences Laboratory
University of California
Berkeley 4, California
ATTN: S. Silver

University of Hawaii
Electrical Engineering Department
University of Hawaii
Honolulu 14, Hawaii
ATTN: Dr. Paul C. Yuen

University of Illinois Library
Documents Division
Urbana, Illinois

Cornell University
Phillips Hall
Ithaca, New York
ATTN: G. C. Dalman, Prof.

The University of Texas
Dept. of Physics
The University of Texas
Austin 12, Texas
ATTN: Professor Claude W. Horton

Professor Vitold Belevitch
Director,
Comite d'Etude et d'Exploitation
des Calculateurs Electroniques
67 Rue De La Croix de Fer
Brussels, Belgium

Dr. Yosiro Oono
Faculty of Engineering
Kyushu University
Hukuoka, Japan

Dr. B.B.H. Tellegen
Scientific Advisor
Philips Research Laboratory
Eindhoven, Netherlands

Professor Hiroshi Ozaki
Faculty of Engineering
Osaka University
Higashinoda,
Osaka, Japan

UNIVERSITIES Cont'd

W. Olja Saraga
Section Leader
Research Laboratory Siemens Edison Swan, Ltd.
Crootes Place
Blackheate
London S.E. 3, England

Professor T. Pajlasek
Dept of Electrical Engineering
McGill University
Montreal, P.Q.
Canada

Polytechnic Institute of Brooklyn 80 copies
55 Johnson Street
Brooklyn, N.Y.
ATTN: Dr. H. Carlin

Stanford University
Department of Electrical Engineering
Stanford, California

Electronics Research Laboratory
Stanford University
Stanford, California
ATTN: Prof. Buss

Carnegie Institute of Technology
Dept. of Electrical Engineering
Pittsburgh, Pennsylvania
ATTN: Dr. Williams

INDUSTRIAL LABORATORIES

Boulder Laboratories
National Bureau of Standards
Boulder, Colorado
ATTN: Library

Airborne Instruments Laboratory, Inc
Walt Whitman Road
Melville, Long Island, New York
ATTN: Library

The Mitre Corporation
Bedford, Massachusetts
ATTN:Library

Lincoln Laboratory, M I T
P O Box 73
Lexington 73, Mass
ATTN: Library A-082

IBM Research Library
Thomas J Watson Research Center
P O Box 218
Yorktown Heights, New York
ATTN: Reports Section

The Boeing Company
Aero-Space Division
P O Box 3707
Seattle 24, Washington
ATTN: R R Barber, Library Unit Chief

Micro State Electronics Corporation
152 Floral Avenue
Murray Hill, New Jersey
ATTN: Dr Samuel Weisbaum

Space Technology Labs, Inc
STL Technical Library
Space Technology Labs, Inc
One Space Park
Redondo Beach, Calif
ATTN: Acquisitions

RCA Laboratories
David Sarnoff Research Center
Princeton, N J
ATTN: Fern Cloak, Librarian

Hughes Aircraft Company
Florence and Teale Streets
Culver City, California
ATTN: Dr W H Kummer

Sylvania Electronic Systems--West
Electronic Defense Labs
P O Box 205
Mt View, Calif
ATTN: Document Center

Pickard & Burns, Inc
103 Fourth Ave
Waltham 54, Massachusetts

A S Thomas, Incorporated
355 Providence Highway
Westwood, Mass
ATTN: A S Thomas

International Microwave Corporation
105 River Road
COS COB, Conn

TRG, Incorporated
2 Aerial Way
Syosset, N Y
ATTN: Library

The Rand Corporation
1700 Main Street
Santa Monica, California
ATTN: Director, USAF Project RAND
via: AF Liaison Office

Lockheed Missiles & Space Company
Technical Information Center (50-14)
3251 Hanover Street
Palo Alto, California
ATTN: Dr W A Kozumplik, Manager

Chu Associates
Whitcomb Avenue
P O Box 387
Littleton, Massachusetts
ATTN: Ivan M Faigen, General Manager

Mathematical Reviews
190 Hope Street
Providence 6, R. I.

National Research Council
Radio and Electrical Eng Div
Ottawa, Ontario, Canada
ATTN: Dr G A Miller, Head Microwave Section

Texas Instruments Incorporated
Apparatus Division
6000 Lemmon Ave, Dallas 9, Texas

U S Air Force

Ballistic Research Laboratories
Aberdeen Proving Ground
Maryland
ATTN: Dr Keats Pullen

Aeronautical Systems Division
ATTN: ASRNEA-2 (Mr G R Branner)
Wright-Patterson AFB, Ohio

Air Force Academy
Attn: Library
Colorado Springs, Colo.

ASD (ASNRD, Mr A D CLark)
Directorate of System Eng
Dyna Soar Engineering Off
Wright-Patterson AFB, Ohio

AFCRL AFRD (CRRELT)
L G Hanscom Fld, Mass

ESD (ESRDW)
ATTN: Capt John J Hobson
L G Hanscom Fld, Mass

RADC (RAT)
ATTN: Dr John S Burgess
Griffiss AFB, N Y

AF Missile Dev Cen (MDGRT)
ATTN: Technical Library
Holloman AFB, New Mexico

AFOSR (SRY, Technical D
14th St and Constitution Ave
Wash D C

AFCRL AFRD (CRRL)
ATTN: Contract Files
L G Hanscom Fld, Mass

AFSC (SCSE)
Andrews AFB
Wash 25 D C

APGC (PGAPI)
Eglin AFB Fla

AFSWC (SWOI)
Kirtland AFB New Mex

AFMTC (Tech Library MU-135)
(MTBAT)
Patrick AFB Fla

RADC (RAAPT)
Griffiss AFB N Y

RADC (RAALD)
Griffiss AFB N Y

GEEIA (ROZMCAT)
Griffiss AFB N Y

RADC (RAIS, ATTN: Mr Malloy)
Griffiss AFB N Y

Signal Corps Liaison Officer
RADC (RAOL, ATTN: Maj Norton)
Griffiss AFB N Y

AUL (3T)
Maxwell AFB Ala

ASD (ASAPRD)
Wright-Patterson AFB Ohio

U S Strike Command
ATTN: STRJ5-OR
Mac Dill AFB Fla

AFSC (SCFRE)
Andrews AFB
Wash 25 D C

Hq USAF (AFCOA)
Wash 25 D C

AFOSR (SRAS/Dr G R Eber)
Holloman AFB New Mex

Commandant
Armed Forces Staff College (Library)
Norfolk 11 Va

ADC (ADOAC-DL)
Eng AFB Colo

AFFTC (FTOOT)
Edwards AFB Calif

ESD (ESRL)
L G Hanscom Fld
Bedford Mass

ESD (ESAT)
L G Hanscom Fld
Bedford Mass

U S Air Force

AFLC (MCGSAD)
WPAFB Ohio

ADC (ADMLP-D)
Ent AFB Colo

CONAC (OCC-O)
Robins AFB Ga

ADC (ADMME-DC
Eng AFB Colo

Institute of Technology Library
MCLI-LIB, Bldg 125, Area B
Wright-Patterson AFB Ohio

USAFSS (ECD)
San Antonio Tex

ASD (ASROO)
(ASNE)
Wright-Patterson AFB Ohio

Hq TAC (DORQ-S)
(DOC-C)
(OA)
Langley AFB Va

Hq USAF (AFRDC)
(AFRDR-NU)
(AFOAC)
(AFRDP-S)
(AFOCE-EA)
(AFOAC-A)
(AFCOA)
(AFOMO-X-4)
(AFOOP-SV-E)
Wash 25 DC

OIC, FTD Library
Bldg 828 Area "A"
Wright-Patterson AFB Ohio

AFSC STLO
111 E 16th St
New York 3 NY

AFSC STLO
6331 Hollywood Blvd
Los Angeles 28 Calif

AFMDC (MDO)
Holloman AFB New Mex

AFFTC (FTGD)
Edwards AFB Calif

ASTIA (TISIA-2) 10 cys
Arlington Hall
Arlington 12, Va.

Rome Air Development Center 5 cys
Griffiss AFB, NY
ATTN: (H. Webb, RAWE)

AUL (3T)
Maxwell AFB, Alabama

National Aeronautics and Space Admin.
Langley Research Center
Langley Station
Hampton, Virginia
Attn: Librarian

RTD (RTGS)
Bolling AFB
Washington 25, DC

Hq OAR 2 cys
Tempo D. Bldg
4th St. & Independence Ave, S.W.
Washington 25, D.C.
ATTN: Maj. Ernest Davis